PRATT & WHITNEY AIRCRAFT

DIVISION OF UNITED AIRCRAFT CORPORATION

EAST HARTFORD 8, CONNECTICUT, U. S. A.

33

PRATT & WHITNEY AIRCRAFT

Rockets, Motor Case
Titanium Fabrication
Titanium Alloys

Sixth Quarterly Report on Research and Development of Titanium Rocket Motor Case

By

W. E. Helfrich
Robert P. Brody

January 31, 1962

Pratt & Whitney Aircraft Division
United Aircraft Corporation
East Hartford 8, Connecticut

Contract No. DA-19-020-ORD-5230
OCO R&D Branch Project No. TB4-004
Department of the Army Project No. 5B93-32-004

TECHNICAL REPORT NO. WAL 766.2/1-5

TECHNICAL REPORT NO. WAL 766.2/1-5

Qualified requestors may obtain copies of this report from the Armed Services Technical Information Agency, Arlington Hall Station, Arlington 12, Virginia

PRATT & WHITNEY AIRCRAFT
DIVISION OF UNITED AIRCRAFT CORPORATION
EAST HARTFORD • CONNECTICUT

FOREWORD

This interim technical report was prepared by the Pratt & Whitney Aircraft Division of United Aircraft Corporation, East Hartford, Connecticut, in compliance with Contract No. DA-19-020-ORD-5230. It covers the technical accomplishment on the research and development of titanium rocket motor cases for the three-month period from October 1 through December 31, 1961.

TABLE OF CONTENTS

LIST OF FIGURES

LIST OF FIGURES (CONTINUED)

LIST OF FIGURES (CONTINUED)

LIST OF FIGURES (CONTINUED)

LIST OF FIGURES (CONTINUED)

LIST OF FIGURES (CONTINUED)

LIST OF FIGURES (CONTINUED)

LIST OF TABLES

LIST OF TABLES (CONTINUED)

LIST OF TABLES (CONTINUED)

I. INTRODUCTION

A. Purpose and Scope of Project

This program is aimed at the development of a high strength, light-weight, titanium alloy pressure vessel of the type used for solid fuel rocket motor cases. B-120 VCA titanium alloy has been selected for further investigation because of its inherent high strength, its potential of reliably exceeding the yield strength/density ratio of 1,000,000 inches and the possibility of reaching 1,200,000 inches. The main problems involved in its application include the development of fabrication techniques to achieve consistently high strength levels along with the most economical use of material.

B. Background Information

Previous research and feasibility testing conducted by Pratt & Whitney Aircraft Division indicated that B-120 VCA titanium alloy is an excellent material for lightweight rocket motor cases. Evidence was accumulated that its properties could be improved, as well as the techniques used in fabrication. This alloy contains thirteen per cent vanadium, eleven per cent chromium, and three per cent aluminum. In the cold-worked and aged condition it has achieved the highest strength/weight ratio of all metals that have been used for rocket motor cases. Pratt & Whitney Aircraft Division has demonstrated that full scale rocket motor cases can be fabricated from this alloy with 180,000 psi yield strength. At this stress level the material has a strength equivalent to 290,000 psi in low alloy steel at the same strength/density ratio. Small pressure vessels with yield strengths above 180,000 psi have also been fabricated from this material by Pratt & Whitney Aircraft. B-120 VCA titanium alloy has displayed excellent corrosion resistance to salt spray environment at the 160,000 - 170,000 psi yield strength level, an important consideration where long term storage is involved. Specimens tested to date under this program have indicated similar excellent corrosion resistance at the 180,000 - 200,000 psi yield strength level.

C. Subject Matter Covered in this Report

The work planned under the various phases of the program is outlined and the results of current investigations are reported. These results include the following:

1. Tensile and sustained-load properties (70F) of a full scale 40-inch diameter flow-turned cylinder with 240 ppm of hydrogen,

2. Tensile, bend and fracture toughness (G_c) test results on material TIG-welded using an improved copper fixturing technique and TIG-welded using AMS 4951 (commercially pure titanium) filler wire,

3. Cyclic loading test results on TIG-welded and electron beam-welded material,

4. Tensile properties of subscale 14-inch diameter domes press-forged by the dogbone and the pancake and preform techniques,

5. Tensile properties of full scale 40-inch diameter domes press-forged by the dogbone and the pancake and preform techniques,

6. Tensile properties of a hammer-forged pancake,

7. Tensile properties of subscale 14-inch diameter rolled rings before and after flow-turning,

8. Flow-turning results on subscale 9.4-inch diameter rolled and welded blanks, and

9. Electron microscope and microprobe results on press-forged, TIG- and electron beam-welded, and flow-turned material.

The above results are discussed and tentative conclusions drawn.

II PROGRAM PLANNED

The following detailed program is planned at this time but is subject to revision as development progresses. Major emphasis will be directed to study of the metallurgical factors influencing material behavior during forging, flow-turning, heat treatment and welding and the resultant mechanical properties. The results of these studies will be applied to the achievement of reliability in full scale components at the 180,000 psi yield strength level. The most economical use of material (reduced input weight and thinner sections) will be emphasized during the forging phases of the program. The feasibility of extending the reliable yield strength level to 200,000 psi will also be determined. The status of material being used in the program is outlined in Table I.

A. Effects of Interstitials

The effects of hydrogen content on delayed cracking and stress-corrosion are to be studied, with emphasis on the flow-turned material to be used in motor case cylindrical sections. The present Pratt & Whitney Aircraft specification calls for a maximum hydrogen content of 0.015 per cent (150 ppm). A cathodic hydrogenation technique has been developed to yield reproducible hydrogen contents at the 200 ppm level and an evaluation program has been conducted on cold-rolled and aged sheet stock at the 180,000 psi yield strength level. This program showed no detrimental effect of hydrogen on notched (K_t=8) tensile behavior at the standard strain rate (0.005 inch/inch/minute) or under sustained loads over the -35F to 400F temperature range. Higher notched (K_t=8) sustained tensile strengths were observed with 200 ppm hydrogen material as compared with 70 ppm hydrogen material. Additional testing using notched sustained-load specimens with stress concentration factors (K_t) of 3 and 6 and hydrogen contents of 70 and 200 ppm showed that the above behavior was repeated with a stress concentration of 6, but not with a stress concentration factor of 3.

One of the two 40-inch diameter rolled rings transferred from Thiokol contract RM-962 has been flow-turned to provide material for the hydrogen investigation. The resultant cylinder was sectioned in the as-flow-turned condition, stress relief-flattened at 900F and the aging response determined at 800F and 900F. The hydrogen content in the as-flow-turned condition was approximately 240 ppm and the cylinder was therefore evaluated at this hydrogen level only. Smooth and notched (K_t=8) tensile and notched (K_t=8) sustained load specimens were machined in the axial and circumferential directions after aging at 900F to the 180,000 psi minimum yield strength level and tested at room temperature only. Results showed poor notched (K_t=8) tensile strength but no detrimental effect on sustained

notched (K_t=8) tensile strength due to the relatively high hydrogen content (240 ppm). Because of the poor notched (K_t=8) strengths and because this cylinder did not receive optimum processing, no further work will be conducted on this material.

To evaluate two hydrogen levels (approximately 50 and 200 ppm) on satisfactorily processed flow-turned material, two of the ten subscale 14-inch diameter rings recently rolled by Ladish have been vacuum annealed at 1400F. One of these rings will be flow-turned by the current two-pass technique (50 percent reduction per pass) and evaluated at the 50 ppm hydrogen level and after cathodic hydrogenation to the 200 ppm level. Smooth and notched (K_t=8) tensile and notched (K_t=8) sustained-load specimens will be tested over the -35F to 400F temperature range. The other ring will be used for flow-turning development unless required for the hydrogen investigation.

The effect of oxygen on aging response, notch sensitivity and stress-corrosion susceptibility is being evaluated using six press-forged pancakes with nominal oxygen contents of 0.10, 0.15 and 0.20 percent. Exploration of these pancakes has been completed with the exception of smooth and notched (K_t=8) tensile testing at -35F after aging to the 180,000 psi yield strength level. The remaining three pieces of the nine originally intended will be forged at a later date, if desired.

B. Forging Practice

The forging phase of this program is aimed primarily at the improvement of mechanical properties in forged end closures with maximum economy. It is hoped that this economy will result from lower forging input weights and from a less expensive forging and machining sequence. It is anticipated that these objectives will be achieved by closed-die press forging, controlled to retain optimum working for proper aging response.

1. Press Forging

Seven pancakes have been forged in open dies at Wyman-Gordon. These pancakes, upset at high and low strain rates at 1600F, 1700F, 1850F and 2000F, were evaluated for smooth and notched (K_t=8) tensile property uniformity at the 180,000 psi yield strength level. Additional testing showed that none of these pancakes was capable of attaining the 200,000 psi yield strength level by direct aging at 900F. This material contained 0.10 percent oxygen and its aging response was in agreement with data obtained in study of interstitial effects.

Wyman-Gordon has also forged nine subscale 14-inch diameter domes in closed dies. Three domes were press-forged by the dogbone technique at 1650F, 1700F and 1850F and five by the pancake and preform method at the same temperatures. In addition, one piece was upset at 2000F directly from billet stock. These domes, with the exception of one piece forged at 1850F by the pancake and preform method, have been completely evaluated. The excepted piece which did not fill the dies has been restruck at 1750F and is undergoing evaluation. No further subscale dome forging is planned at the present time.

Three full scale 40-inch diameter domes have also been forged in closed dies at Wyman-Gordon. The first of these domes (front) was forged in three operations at 1700F by the pancake and preform method, using the dies normally employed for second stage Pershing steel domes. This dome did not fill the dies in the final upset and was therefore restruck in the same dies at 1900F. Evaluation of this piece has been completed. The two additional domes, one front and one rear, were forged in the closed dies fabricated under this contract. The front dome was forged by the pancake and preform method (three operations), and the rear by the dogbone technique (three operations). All forging operations were performed from 1850F. These two domes have been sectioned and are presently being evaluated. One additional front dome and one rear dome will be forged pending results of the above evaluations and the subscale 14-inch diameter dome recently restruck at 1750F. Additional front and rear domes will be forged at a later date for individual hydrostatic testing and fabrication of a full scale motor case.

2. Hammer Forging

Ladish has hammer-forged the four pancakes intended under this phase. The first two pieces were forged in two upsets in closed dies and the second two in three upsets with an intermediate recrystallization treatment. Evaluation of these pieces has been completed. No further work is anticipated under this phase.

3. Ring Rolling

All sixteen subscale 14-inch diameter rings intended under this phase have been rolled by Ladish. The first three rings were rolled in single operations at 1800F, 1900F and 2000F and the second three in two or three operations at 1800 - 2000F. Based on results from these pieces, the final ten rings for flow-turning development were rolled in a single operation at 1900F and are presently being machined prior to flow-turning.

Based on the subscale results, it was decided that the seven full scale 40-inch diameter rings allocated would be rolled in two operations at 1900F. Rolling in one operation was prohibited by machine capacity. Because of tooling problems, it became necessary to roll in four operations from 1900F rather than the two originally planned. One ring ruptured during the first rolling operation apparently due to defective material. Replacement material has been ordered and will be similarly rolled upon receipt by Ladish. Test rings for annealing treatment determinations are now being processed from the six rings rolled successfully. Rolling of the replacement material mentioned above and subsequent evaluation of these seven rings will constitute completion of the ring rolling phase of this contract.

C. Flow-Turning Development

The flow-turning of subscale 14-inch diameter rolled rings in conjunction with the ring rolling development phase has been completed. Nine subscale 9.4-inch diameter blanks and three 14-inch diameter blanks have been fabricated by rolling and axially TIG welding 0.375-inch thick plate stock. Flow-turning of the 9.4-inch diameter blanks to determine the effect of roller geometry, mandrel speed, reduction and feed rate on radial growth and local bulging has been partially completed. Upon conclusion of this work, one or more of the 14-inch diameter rolled and welded blanks will be flow-turned prior to processing of the 14-inch diameter and 40-inch diameter roll-forged rings.

D. Weld Development

The weld development phase is aimed primarily at the improvement of weld quality, fracture toughness, and resistance to crack initiation at weld porosity. Initial work on establishment of quality and toughess test techniques has been completed with the exception of final analysis of the wide (biaxial stress field) tensile specimen. Toughness evaluation of multiple-pass TIG welding techniques and alternate filler materials has almost been completed. An improved

copper-fixturing technique has been developed which greatly reduces weld porosity, minimizes distortion, and produces more uniform weld penetration. Cyclic testing is presently being employed as the basic weld evaluation method to determine the characteristics of crack initiation and growth at weld porosity. Cracking through porosity has been observed in pressure vessel circumferential welds during repeated pressurization. The cyclic test technique employing a longitudinally-disposed weld is designed to simulate motor case stress and loading conditions with a three-cycle proof test (80,000 psi stress), followed by additional cycles at increasing stresses (5000 psi increase per cycle) until failure. Specimens are radiographically inspected after each cycle to determine the extent and nature of cracking. Multiple-pass TIG welds, welds made with alternate filler materials, welds made by the improved fixturing method, electron beam welds and weld repairs are being evaluated by this technique. The best weld method evolving from these studies will be applied to TIG welding of full scale 40-inch diameter circumferential samples and ultimately a full scale motor case. A weld specification will also be developed to limit permissible porosity to a level not susceptible to crack initiation on loading.

Hamilton Standard electron beam welds of various widths made at various travel speeds have been evaluated for quality and toughness. No further work is anticipated on electron beam welding other than cyclic testing and evaluation as a possible repair technique.

Rolled rings of 6Al-6V-2Sn titanium alloy have been received from Ladish for weldability studies. These pieces have been solution-treated and machined into 20-inch diameter circumferential weld samples. TIG welding studies are soon to be initiated upon completion of fixturing now being fabricated.

E. Metallographic Examination

Battelle Memorial Institute has completed electron microscope and microprobe studies on press-forged, flow-turned and TIG and electron beam-welded material. Intended x-ray diffraction studies could not be completed due to exhaustion of funds. Additional samples will be analyzed using these techniques when such action is indicated.

F. Full Scale Components

Six of the seven roll-forged rings have been forged. The seventh ring is tentatively scheduled to be forged in January 1962. These rings are to be annealed and rough-machined for delivery in February 1962. Subsequently, the rings will be machined into flow-turning blanks and flow-turned into cylindrical center sections. One front and one rear dome have been forged. The second front and rear domes are to be forged when evaluation of the first domes has been completed.

III TEST RESULTS

A. Effects of Interstitials

Evaluation of the full scale 40-inch diameter flow-turned cylinder has been completed. As reported previously (Technical Report No. 766.2/1-4), this cylinder had been sectioned in the as-flow-turned condition, stress relief-flattened at 900F for one hour and the aging response determined at 800F and 900F. An aging treatment of 900F for two hours was selected to achieve the 180,000 psi minimum yield strength level (axial direction). This cylinder had a high hydrogen content (240 ppm), apparently due to excessive annealing and subsequent pickling during processing and for this reason was evaluated at this hydrogen level only. Vacuum annealing to reduce the hydrogen content after flow-turning would destroy the cold work necessary for optimum aging response and ductility.

Smooth and notched (K_t=8) tensile and notched (K_t=8) sustained-load specimens were machined from the cylinder in the axial and circumferential directions after aging at 900F and were tested at room temperature only. Results of these tests, tabulated in Table II, showed low notched (K_t=8) tensile strengths (90,900 - 125,400 psi) and sustained notched (K_t=8) tensile strengths (100,000 - 110,000 psi). These strengths are considerably lower than those normally obtained on flow-turned material (approximately 140,000 - 160,000 pis), apparently due to a smaller reduction (33 per cent) in the final flow-turn pass. No detrimental effect was attributed to the high hydrogen content (240 ppm) since the notched (K_t=8) tensile and sustained-load strengths were equivalent. Because this cylinder was not processed by the normal procedure and because this processing apparently resulted in increased notch sensitivity, no further work is intended on this material.

To obtain normally processed flow-turned material for the hydrogen investigation, two of the ten subscale 14-inch diameter rings recently rolled by Ladish have been semifinish-machined and vacuum-annealed at 1400F. Hydrogen analyses after vacuum annealing are currently in process. After finish machining, one of these rings will be flow-turned and then evaluated at two hydrogen levels (approximately 50 and 200 ppm).

Evaluation of the effect of oxygen on smooth and notched (K_t=8) tensile ductility at -35F is being conducted using the three pancakes (0.10, 0.15 and 0.20 per cent nominal oxygen) most recently press-

forged by Wyman-Gordon in three upsets at 1700F. Similar testing at room temperature has shown a trend towards decreasing ductility with increasing oxygen content (Technical Report No. WAL 766.2/1-4). Samples from these pancakes have been aged at 900F to the 180,000 psi yield strength level and are presently being machined into smooth and notched (K_t=8) tensile specimens for testing at -35F. These tests will complete the presently intended oxygen investigation.

B. X-Ray Diffraction Studies

No further x-ray diffraction studies of preferred orientation were conducted during this quarter. Additional studies may be undertaken during the more advanced stages of the flow-turning development phase.

C. Weld Development

Stress analysis is continuing on the wide (4.5-inch) biaxial tensile specimen configuration being evaluated for the testing of longitudinally-disposed weld beads. As reported in Technical Report No. WAL 766.2/1-3, preliminary analysis had shown maximum biaxiality (elastic range) midway between the edge notches of an unwelded specimen. A similar analysis in the plastic region on the same specimen has shown approximately equivalent biaxiality. The resulting biaxial ratios at three locations (at the notches and at intervals between the notches) are illustrated in Figure 1. Further evaluation in the elastic and plastic regions is presently being conducted on a specimen containing a longitudinal TIG weld.

Fracture toughness (G_c) specimens (ASTM standard 3 x 12 inch internally-notched) have been tested from panels TIG-welded using AMS 4951 (commercially pure titanium) filler wire. Specimens were machined and tested with prefatigue-cracked notches located at the weld centers. The test results on single-pass (straight butt joint) and three-pass (U-type prepared joint) welds showed poor toughness, G_c* values of 71 and 100 in-lbs/in^2 respectively. G_c^* is defined as the critical crack extension force corrected for plastic strain at the notches. Because of the high oxygen contents of the welds as reported previously (0.160 - 0.293 per cent, Technical Report No. WAL 766.2/1-4), additional specimens are presently being prepared from panels TIG-welded in a single pass and with lower oxygen contents (approximately 0.10 per cent).

Bend, smooth and notched (K_t=8) tensile, and fracture toughness (G_c) tests, have been conducted on TIG welds made using the improved copper-fixturing technique. Bend specimens were machined with transversely-disposed weld beads ground flush prior to testing. Smooth and notched (K_t=8) tensile and fracture toughness (G_c) specimens also contained transversely-centered beads. Smooth specimens were tested with the weld beads both intact and ground flush. Notched (K_t=8) tensile and fracture toughness (G_c) specimens were prepared with notches at the weld centers and left intact for testing. The results of these tests, tabulated in Table III, showed slightly improved tensile ductility but similar toughness as compared with TIG welds made by the previously employed method (steel fixturing). Macro- and microstructures and hardness data on these welds, presented in Figures 2-5, showed no significant changes over previous welds. A comparison of the improved and previously employed weld schedules is shown in Table IV. The essentially porosity-free nature of the improved welds is apparently a result of decreased weld travel speed, increased current input and most significant, the type of weld fixturing. It is felt that the higher resultant heat input (8100 BTU/hr) for the improved technique produces higher temperatures at the edges of the weld puddle thus allowing evolution of otherwise entrapped gases. Previously, the vast majority of weld porosity occurred at the weld edges. Because of the advantages accrued by this improved method, all future TIG welding will employ the above described technique.

Bend tests have been carried out on panels manually TIG-welded using commercially pure vanadium and columbium-3.5 titanium filler materials. These materials were being evaluated to determine applicability for repair welding. Bend test data (weld beads transversely-disposed and ground flush), tabulated in Table V, showed satisfactory ductility. Macrostructures along with hardness data are shown in Figures 6-8. Additional TIG-welded panels are presently being repaired using vanadium filler rod since this material showed greater compatibility with the parent metal. The higher melting point of the columbium alloy necessitated higher welding heat inputs and resulted in locally unfused areas and severe distortion.

The analysis of crack initiation and growth from porosity in TIG welds by the cyclic test method described in Technical Report No. WAL 766.2/1-3 is continuing. The latest specimen configuration being used is shown in Figure 9. This test method involves initial loading three times to a stress of 80,000 psi for three-minute durations and then increasing the stress level in 5000 psi increments on succeeding three-minute cycles until failure. The three cycles at 80,000 psi are intended to simulate a motor case proof test. This stress is also the operating level for the Pershing motor case design formulated under this contract. The specimens are radiographically inspected after each cycle to determine crack initiation and growth. Testing has now been expanded to include specimens

TIG-welded with various joint configurations, filler materials, repair procedures, and weld overlap, and also electron beam-welded specimens.

From past experience it was known that TIG weld porosity in this alloy was of a relatively random nature and existing weld porosity specifications would not suffice. A porosity rating scheme was therefore devised which would be more closely adaptable to the characteristics of this alloy and the specimen configuration being employed. This scheme includes the total number of porosity pores in the cyclic test specimen gage length (4 inches) and the number of pores in the worst 1 inch of length to indicate porosity distribution along the bead length. Also included is the distance of closest approach for pores in the worst 1 inch of bead length, for pores outside of the worst 1 inch, and the maximum pore diameter in the specimen gage area. The resultant porosity ratings for all specimens tested to destruction or presently being tested are presented in Table VI. Of the 35 specimens prepared and tested to date, 17 have been cycled to destruction. The incidence of cracking through weld porosity at each stress level for these specimens is tabulated in Table VII and graphically illustrated in Figure 10. A summary of the conditions present immediately prior to and after failure along with gas analyses is shown in Table VIII. Specimens containing little or no weld porosity fractured at stresses of 170,000-185,000 psi with failures not occurring through weld porosity or prior cracks. In one instance (specimen No. 5), failure occurred at 125,000 psi and was not associated with weld porosity. Two specimens (Nos. 4 and 16) failed at low stresses (27,000 and 68,200 psi respectively) through transverse weld cracks which occurred during specimen machining. Schematic representations of the weld cracking during cycling and after failure are illustrated in Figures 11-20. Fracture surfaces and gage areas after failure are depicted in Figures 21-38. Binocular examination of these fracture surfaces revealed similar failures to those obtained after fracture toughness (G_c) testing. Microexamination has indicated all weld cracking to be partially transgranular and partially intergranular in nature (Figure 39).

From the data obtained thus far it appears that the TIG weld failure stresses are inversely proportional to the numerical incidence of porosity above a certain porosity level (Figure 40). The weld technique itself apparently does not influence the crack initiation characteristics. Only the actual amount of porosity governs susceptibility to this cracking. The tests currently in process on TIG welds made using the improved copper-fixturing technique have verified this indication. These specimens including welds with overlap and manual repairs (parent metal filler wire) have been cycled to approximately 110,000 psi with no cracking observed except in one of several repaired areas. These welds, characteristic of the improved technique, contain

essentially no porosity with the exception of the manual repairs (Table VI). The incidence of cracking at each stress level for these specimens is tabulated in Table IX.

Analyses of the electron beam weld results has been hampered by difficulties encountered in interpreting the radiographs. The narrow weld beads and small porosity and crack lengths characteristic of this welding process preclude the use of standard radiographic techniques. To circumvent this problem, equipment capable of producing higher magnification radiographs would be necessary. In addition and in contrast to the TIG-welded specimens, all of the electron beam-welded samples tested to date have failed with origins outside of the weld beads. For this reason the resultant failure stresses (130,000 - 160,000 psi) are not representative. This type of failure is apparently due to the narrow bead widths (approximately 0.150 inch) which produce a condition more favorable for parent metal failure. Apparently, electron beam welds are less sensitive than TIG welds to an equivalent amount of porosity. This indication may be attributable to the slightly greater ductility and toughness of electron beam welds as reported in Technical Report No. WAL 766.2/1-4.

Additional specimens for cyclic test evaluation have been prepared from panels with various hydrogen contents TIG-welded using the improved copper fixturing technique. Nominal parent material hydrogen levels of 50 ppm(vacuum annealed), 100 ppm (as-received) and 300, 700 and 1000 ppm (cathodically hydrogenated) are being evaluated. All panels were welded with vacuum-annealed filler wire except the vacuum-annealed and as-received material which was welded with both vacuum-annealed and high hydrogen (approximately 250 ppm) filler wire. Gas analyses (hydrogen and oxygen) of the parent metal, filler wire and resultant weld beads are tabulated in Table X. Radiographic inspection of these panels showed moderate to severe weld porosity (Table VI). This incidence of porosity using the improved copper-fixturing technique cannot be explained at this time. No correlation was evident between the amount of weld porosity and the parent metal or weld bead hydrogen content.

For comparison with the results obtained to date on B-120 VCA titanium alloy, cyclic testing will be conducted on TIG-welded AISI H-11 steel and 6Al-4V titanium alloy. These two materials are presently being used in production motor case fabrication. Specimens of AISI H-11 steel (0.077-inch thick) have been machined and are presently being heat treated to the 200,000 psi yield strength level prior to cyclic testing. These specimens are being austenitized at 1850F for 30 minutes, air-cooled and triple-tempered at 1050F for two hours. A purchase order has been initiated for 6Al-4V titanium alloy sheet stock for similar testing. Upon receipt, this material will be TIG-welded in the solution-treated and half-aged condition using AMS 4951 (commercially pure titanium) filler wire and then half-aged prior to machining.

To evaluate the effects of cold working on the toughness of TIG-welded material, panels prepared with double longitudinally-disposed welds were reduced 30, 40 and 50 per cent by cold rolling parallel to the weld bead axes. These panels were subsequently machined into fracture toughness (G_c) specimens with notches positioned to produce cracking transversely through the cold-rolled beads. Concurrent with these tests, cold-rolled and aged parent metal specimens were machined to thicknesses corresponding to those of the roll-reduced specimens to determine the effect of thickness alone on toughness (G_c) values. Table XI and Figure 41 present the results obtained on both the parent metal and welded specimens. The fracture surfaces of the parent metal specimens are shown in Figure 42. From these data, it appears that there is a decrease in weld toughness with increasing cold reduction and the usual effect of thickness (G_c increasing with decreasing thickness) on toughness is concealed. Additional specimens are being prepared to confirm these data and investigate the effect of lower reduction (10 - 20 per cent).

To study the effect of roller geometry, angle and other parameters on radial growth and bulging during flow-turning (See Section E on flow-turning development) a series of 9.4-inch and 14-inch diameter rolled and welded blanks has been prepared. Prior to preparation of these blanks, a series of experimental plate stock panels (0.375-inch thick) were TIG-welded to determine the optimum weld schedules to be employed. Both manual (four pass) and automatic (two pass) welding methods were evaluated concurrently with different joint configurations. Although both methods produced reasonably good ductility (105° bend angle with bend diameter of 8.0 - 11.0 times the thickness) the automatic method (double pass) was selected because of improved uniformity and relative freedom-from porosity. Figures 43 - 46 illustrate the macrostructures and fracture surfaces obtained from the two methods described. A V-type prepared joint configuration with an included angle of 80° and 0.100-inch land was utilized.

D. Forging Practice

1. Press-Forging

Evaluation of subscale 14-inch diameter dome forgings EFM-8 and EFM-10 has been concluded. Dome EFM-8 had been forged by the pancake and preform technique in three operations at 2000F (pancake), 2000F (preform) and 1850F (closed die).

Dome EFM-10 had been forged by the dogbone method in two operations at 1850F. In addition, limited data has been obtained on dome EFM-9 forged by the pancake and preform method in three operations at 1850F. This dome did not fill the dies during the final closed-die operation and has been restruck at 1750F (approximately 30 per cent reduction). Results after this restrike are expected to aid in determining the feasibility of full scale dome forging at temperatures lower than 1850F with lower reductions.

Wyman-Gordon has determined the aging response of domes EFM-8 and EFM-10 at 900F and at 900F after an interim 1450F treatment. The data for EFM-8 tabulated in Table XII showed higher strengths toward the skirt areas and generally lower ductility than experienced with domes forged at lower temperatures (1650 - 1700F). Dome EFM-10 forged by the dogbone method showed better ductility than dome EFM-8 forged by the pancake and preform technique (Table XIII). In both instances, aging at 900F after a 1450F treatment produced improved uniformity of properties and ductility as compared with direct aging at 900F. Macroexamination of these domes showing uniformly coarse grain structures throughout (Figures 47 and 48). Specimens were also machined from samples trepanned from the pole and sectioned from the skirt locations of dome EFM-9 prior to restrike. These specimens were aged at 900F for 24 hours following an intermediate solution treatment at 1450F for 30 minutes. These data also showed poor ductility (2.0-4.0 per cent elongation) with higher strengths at the skirt location (Table XIV).

Pratt & Whitney Aircraft has further evaluated the uniformity of tensile properties in domes EFM-8 and EFM-10. Smooth and notched (K_t=8) tensile specimens have been machined from various locations after aging to the 180,000 psi yield strength level. Aging treatments at 900F and at 900F following an interim 1450F treatment were evaluated. The resultant data, shown in Tables XV and XVI, again indicated poor ductility for pancake and preform dome EFM-8. The ductility of dogbone dome EFM-10 was superior, but erratic elongation values as low as 2.5 per cent were evident. In both cases, the interim 1450F treatment improved property uniformity and in the case of dogbone dome EFM-10 also increased the ductility. The interim solution treatment decreased the aged ductility of pancake and preform dome EFM-8. Plots illustrating property uniformity for these domes are shown in Figures 49 and 50. Microexamination of both domes showed a relatively coarse grain size, little working and a coarse and nonuniform aging constituent (Figure 51).

The poor ductility of these subscale domes relative to those previously forged at lower temperatures (1650-1700F) is probably attributable to the higher forging temperature (1850F) but analysis is complicated by the long 1850F furnace soaking times received by these pieces. As reported in Technical Report No. 766.2/1-4, these domes were heated for 3.7-4.0 hours at 1850F prior to the final forging operation. It is impossible at this time to determine the relative effects of 1) furnace temperature and 2) heating time at furnace temperature, although the latter is believed to play a minor role.

Evaluation of the first full scale 40-inch diameter dome EJO-1 has been completed. This dome had been forged in three operations at 1700F by the pancake and preform method and then restruck at 1900F due to incomplete die closure during the final 1700F operation. Wyman-Gordon aging response determinations and preliminary Pratt & Whitney Aircraft testing had shown poor ductility after both direct aging at 900F and aging at 900F following 1400F and 1450F treatments. Additional testing has been conducted to better establish the response using the above aging heat treatments and determine the uniformity of tensile properties in the polar and offset (thrust reverser) boss locations. Specimen blanks were cut in the radial direction from the mid-radius location and machined into smooth tensile specimens after direct aging for various times at 900F and at 900F following 1400F and 1450F solution treatments. These data showed poor tensile ductility (0.5-3.5 per cent elongation) for all aging times (16-32 hours) including those resulting in yield strengths as low as 165,000-170,000 psi (Table XVII). Additional blanks were cut from various locations in the polar boss and one of the offset (thrust reverser) bosses and machined into smooth tensile specimens after aging at 900F for 24 hours following solution treatment at 1450F for 30 minutes. These results also showed poor ductility but satisfactory yield strength uniformity within the bosses and as compared with other dome locations. Tensile properties and specimen locations are shown in Tables XVIII and XIX. Microexamination of this dome revealed a coarse and equi-axed grain structure with no evidence of working and nonuniform distribution of aging precipitate (Figures 52 and 53).

In an attempt to improve the unsatisfactory ductility discussed above, axial blanks were cut from the skirt area of the full scale dome (EJO-1), heat treated at 1800F for 5 minutes and

aged at 900F for 24 hours. Additional blanks were similarly heated at 1800F, solution-treated at 1400F and 1450F for 15-30 minutes and aged at 900F for 24 hours. These and similar heat treatments had indicated improved ductility on aging of full scale 40-inch diameter rolled ring samples evaluated previously (Technical Report No. WAL 766.2/1-4, Figure 59). The above blanks were machined into smooth tensile specimens and tested to yield the results presented in Table XX. These data showed some improvement in ductility as compared with direct aging at 900F or solution treating at 1400-1450F and aging at 900F. These tests conclude the evaluation of this dome.

Wyman-Gordon has press-forged two additional full scale 40-inch diameter domes, one front dome (ELA-3) by the pancake and preform technique and one rear (ELA-2) by the dogbone technique. Each dome was forged in three operations at 1850F with the final operation in closed dies fabricated under this contract. Handling and scheduling difficulties encountered during the processing of these pieces necessitated relatively long furnace heating times (3.8-4.0 hours). Motion pictures were taken of the press gages during the final closed-die operations to accurately determine strain rates and peak pressures. Detailed forging sequences for both pieces are outlined in Table XXI. Metal flow during the forging of front dome ELA-3 was satisfactory but the desired reduction to approximately 1.25 inches was not accomplished, especially towards the polar boss. Wyman-Gordon is presently redesigning the die configuration to permit increased flow into the skirt region. A plug is also being trepanned from the polar region of the preform to allow increased metal flow towards the polar boss. The rear dome (ELA-2) did not fill the dies satisfactorily in the skirt area due to excessive metal movement toward the pole. To alleviate this problem, the dogbone preform configuration is being revised to seat lower on the dies and produce more flow toward the skirt.

In addition to these two pieces, Wyman-Gordon has completed the first two forging operations at 1850F on an additional pair of domes, one front (ELA-4) and one rear (ELA-1). These pieces are to be final-forged by practices incorporating such revisions as are shown desirable by the results of subscale and full scale dome evaluations now in process.

Wyman-Gordon has sectioned both completed domes (ELA-2 and ELA-3) and conducted aging response determinations. Macro-examination of radial sections has shown a relatively fine grain structure throughout with evidences of working in all locations except the polar and offset bosses of the front dome (Figures

54-57). Aging response tensile data, tabulated in Tables XXII and XXIII showed results quite similar to those obtained on subscale 14-inch diameter domes EFM-8 (pancake and preform) and EFM-10 (dogbone), also finish-forged at 1850F. Rear dome ELA-2 forged by the dogbone technique showed slightly faster aging response than front dome ELA-3 forged by the pancake and preform method (Figures 58 and 59). Results after direct aging at 900F showed poor ductility in both instances and lower strengths in the polar and offset bosses of the front dome. Both domes also showed higher strengths at the skirt or rim location,as is generally observed with forgings of this type. Solution treatment at 1450F for 30 minutes prior to 900F aging showed strength and ductility increases for both parts as compared with direct aging for similar times at 900F. In addition, increased yield strength uniformity, especially in the front dome boss locations,resulted on aging after solution treatment. Plots illustrating tensile property uniformity after the above heat treatments are shown in Figures 60 and 61. After solution treatment and aging to the 180, 000 psi yield strength level, both front dome ELA-3 and rear dome ELA-2 showed unsatisfactory ductility (2.0-7.0 per cent elongation).

Pratt & Whitney Aircraft has received half-sections of the above two full scale domes and specimens are presently being processed to determine the uniformity of smooth and notched (K_t=8) tensile properties at the 180, 000 psi yield strength level. Extensive tests are being conducted from the front dome boss locations to determine uniformity,and the feasibility of using boss cutouts for aging response testing of future dome forgings for hydrostatic testing and full scale motor case fabrication. Microexamination to date in the as-forged condition has shown a worked and partially recrystallized structure (Figure 62). The boss locations have not as yet been examined.

As discussed previously under subscale domes EFM-8 and EFM-10, the low ductility of these full scale domes may again be attributed to the relatively high forging temperature (1850F) and/or the long furnace heating time (3.8-4.0 hours) at 1850F prior to the final closed-die operation. As mentioned before, however, the heating time is considered a minor factor. It is believed that a forging temperature of 1850F could be employed to produce satisfactory aged ductility if a large enough reduction could be accomplished during the final forging operation.

To complete the microstructure study reported in Technical Report WAL 766.2/1-4, radial samples from the skirt location of the first full scale dome forging EJO-1 have been tensile tested after heat treatment at 1800F for 5 and 15 minutes and either water or brine quenching. The previous study was conducted using full scale 40-inch diameter rolled ring sections and had shown optimum solution-treated smooth and notched (K_t=8) tensile ductility after water quenching from 1800F. Material from this ring was expended during the previous study and dome EJO-1 was therefore utilized for these tests. Smooth and notched (K_t=8) tensile properties after the above heat treatments are tabulated in Table XXIV. These results show excellent ductility after both water and brine quenching from 1800F with optimum ductility after heating at 1800F for 5 minutes and brine quenching.

2. Hammer Forging

Additional tensile tests have been conducted on pancake No. 4 hammer-forged by Ladish in closed dies in three operations, with an intermediate recrystallization treatment (Technical Report No. WAL 766.2/1-3). Previous testing of this pancake had shown considerably lower yield strength at the pancake center after direct aging at 900F for 60 hours (Technical Report No. WAL 766.2/1-4, Figure 51). Results of these latest tests showed that the lower strength center condition is restricted to an area approximately 3.0 inches in diameter. Completed data from this pancake are tabulated in Table XXV and the uniformity illustrated by Figure 63. This work completes the hammer forging phase of this program.

3. Ring Rolling

Additional smooth tensile specimens have been tested from flow-turned subscale 14-inch diameter cylinders No's 1-3 after solution treatment at 1400F for 30 minutes and after subsequent aging at 900F for 48-96 hours. These cylinders had been flow-turned by the current two-pass technique (50 per cent reduction per pass) using rings rolled in one operation at 2000F, 1900F, and 1800F, respectively. The cylinders were stress-relieved at 900F for one hour prior to sectioning. Tensile properties (axial direction) after the above heat treatments are tabulated in Table XXVI and aging curves shown in Figure 64. These data showed very sluggish aging response for all three cylinders (approximately 180,000 psi yield strength after 96 hours at 900F) with more rapid response with decreasing ring rolling tempera-

ture. Despite the long aging times require to achieve 170,000-180,000 psi yield strength, ductilities were excellent (7.0-10.0 per cent elongation).

Smooth tensile tests have also been conducted on subscale 14-inch diameter rolled ring No. 4 after similar flow-turning. This ring had been rolled by Ladish in three operations at 2000F, 1900F, and 1800F, respectively. Circumferential smooth tensile specimens were machined and tested after aging at 900F for 3 and 5 hours. These data, tabulated in Table XXVII, showed excellent yield strengths (194,000-214,000 psi) and ductility (4.0-5.0 per cent elongation) similar to those observed on the first three rings. Based on these results, rings No's 5 and 6 were allocated to the flow-turning development phase. The above described testing on rings No's 1-4 after flow-turning concludes the subscale portion of the ring rolling development phase.

Ladish has rolled the ten subscale 14-inch diameter rings to be utilized for flow-turning development. Based on previous work,it had been decided to roll these pieces in one operation at 1900F. Seven of these pieces were successfully rolled in one operation and water-quenched. The other three rings required two operations at 1900F due to tooling difficulties which resulted in "finning" during the first operation. Complete forging sequences are outlined in Table XXVIII. The rings were then sized at 1450F and test rings cut from each for annealing determinations. Tensile specimens were machined from the test rings after solution treatment at 1450F and 1800F. Results of these specimens showed satisfactory ductility after solution treatment at 1450F for 30 minutes and the rings were therefore given this treatment (Table XXIX). Test ring samples heat treated with the parts were also machined into smooth tensile specimens and tested to yield the results presented in Table XXX. These data also showed adequate ductility. These rings have been received by Pratt & Whitney Aircraft and are presently being machined into blanks for the flow-turning development phase.

Ladish has completed the rolling of six of the seven intended full scale 40-inch diameter rings in four operations at 1900F. The seventh ring failed during the first rolling operation apparently due to defective material. Ladish is presently awaiting replacement material from the supplier for this ring. Microexamination is in process to determine the cause of failure.

It was originally intended to roll these pieces in two operations at 1900F based on the results of subscale work. However, tooling difficulties during the preliminary operations necessitated a total of four passes to achieve the desired diameter. A detailed outline of the forging sequences for these pieces is presented in Table XXXI. After rolling, the rings were sized at 1450F and a test ring cut from one end of each piece. Microexamination and tensile testing is now in process on the test ring material to determine the optimum solution treatment prior to flow-turning.

E. Flow-Turning Development

The fourth subscale 14-inch diameter ring flow-turned by the current practice (50 per cent reduction per pass) has been evaluated for residual stress, aging response, and notched (K_t=8) toughness after various stress-relief and aging heat treatments. Initially, the cylinder was strain-gaged in the as-flow-turned condition and sectioned for residual stress determination. The resultant strain gage data indicated average residual stresses of 188,200 psi tension in the axial direction and 146,200 psi tension in the circumferential direction. Axial smooth tensile specimens were then machined and tested after stress-relieving at 850-900F for 30 minutes to one hour and aging for various times at 700-900F. A 30-minute treatment at 850F (60 per cent stress relief) which had been standard practice was evaluated for comparison with one-hour treatments at 850-950F which yield more complete stress relief (70-95 per cent). These data, presented in Table XXXII, showed most rapid response after stress-relief at 850F for 30 minutes and subsequent aging at 900F. Most sluggish response was observed after stress relief at 900F for one hour and aging at 700F. Aging curves representing these data are depicted in Figures 72-74. Smooth tensile ductility was essentially equivalent regardless of the heat treatment sequence employed.

To determine the stress-relief and aging combination producing optimum notched toughness, additional axial smooth and notched (K_t=8) tensile specimens were machined and tested after aging to the 190,000 psi yield strength level. The resultant data, tabulated in Table XXXIII, indicated some trend toward increasing notch sensitivity with increasing stress-relief and aging temperature. This indication, however, was not definite and additional testing is being considered to more firmly establish an optimum heat treatment sequence. It was encouraging to note that these notched (K_t=8) strengths (approximately 160,000 psi) were the highest observed to date for flow-turned material at this yield strength level (190,000 psi).

Eight 9.4-inch diameter blanks fabricated from rolled and welded 0.375-inch thick plate stock have been flow-turned. The flow-turning was accomplished on a single roll 60-inch machine utilizing the parabolic roller. The flow-turning parameters employed are tabulated in Table XXXIV.

The first two blanks were flow-turned in the as-welded condition. One of these blanks failed immediately upon flow-turning. The failure originated in the circumferential flange weld in an area of incomplete penetration. The crack propagated axially to the point of roller contact and continued circumferentially along the roller path. The second blank was flow-turned for approximately 25 per cent of its length with a 42 per cent reduction. At this point flow-turning was intentionally terminated. When flow-turning was resumed, failure occurred at the point of termination. The fracture propagated circumferentially along the roller path. Blanks numbers three and four were flow-turned successfully with first pass reductions of 44 and 42 per cent and second pass reductions of 63 and 50 per cent. Blank number three was annealed at 1825F for 30 minutes prior to flow-turning while cylinder number four was flow-turned in the as-welded condition. Both blanks were annealed (completely recrystallized) at 1600F for 30 minutes in an argon atmosphere and vapor blast-cleaned prior to the second flow-turn pass. Figure 75 shows a 9.4-inch diameter blank as welded, machined and flow-turned after the first and second passes. Blank number five cracked severely on the inside surface after the first flow-turning pass, for approximately three inches of its length, with a reduction of 25 per cent (commensurate with a three-pass method). The cracking is indicative of insufficient plastic deformation on the inside surface which is considered to be the result of the relatively light reduction (25 per cent) during the first pass. Subsequently, all blanks were flow-turned in two passes and treated similarly to blank number three: annealed at 1825F for 30 minutes prior to the first pass, annealed at 1600F in an argon atmosphere, and vapor blast-cleaned prior to the second pass.

The results of this series of flow-turning experiments have indicated that significant reduction in radial growth was achieved with the new roller configuration (parabolic) during both the first and second passes. Also, a definite trend of decreased radial growth was evident with increased roller feed rate for both passes.

The blanks were free of bulging after the first pass and the radial growth (0.035 to 0.022 inch diameter) was less than that experienced during previous work. Metal tearing occurred on the inside surface in the axial weld in most blanks during the first pass. These were generally shallow surface tears within the length of the flow-turned portion and one or two deep tears at the beginning and end of the flow-turned section. These tears did not extend into parent material and did not propagate during subsequent flow-turning. Because of the presence of these tears, the blanks were not sized to correct the loose fit of the blank on the mandrel prior to the second pass. The second flow-turn pass at the higher feeds and reductions produced little or no radial growth. However, because of the loose fit of the blank, local bulging occurred on some blanks. The higher feeds were also effective in reducing the amount of bulging.

Further optimizing of feeds and reductions to reduce radial growth during the first pass and to correct local bulging during the second pass will be done on the 14-inch diameter roll-forged rings.

F. Metallographic Examination

Battelle Memorial Institute has completed electron microscope and microprobe analyses of press-forged, flow-turned and TIG and electron beam-welded material. Results of electron microexamination of press-forged pancake DGT-2, TIG and electron beam welds and full scale 40-inch diameter cylinders which exhibited extremes in flow-turning behavior were reported in Technical Report No. WAL 766.2/1-3. Additional examination has been carried out on the flow-turned material to further substantiate conclusions indicated by the initial studies. The previous examination had suggested that unsatisfactory flow-turnability was associated with a more extensive grain boundary precipitate. More comprehensive study has shown that essentially equivalent amounts of grain boundary precipitate exist in the cylinders which did and did not flow-turn successfully (Figures 65-68). However, the cylinder which failed during flow-turning showed a greater amount of etch pitting along grain boundaries not necessarily associated with a second phase (Figures 65-68). These pits may represent localized regions of segregated alloying elements or interstitials but this of course has not been substantiated.

Microprobe analyses have been completed on samples from press-forged pancake DGT-2 which had exhibited various tensile properties dependent on pancake location. These specimens included the following:

1) Location A which showed low yield strength (175,500 psi) and low elongation (2.5 per cent) after aging at 900F for 96 hours, and

2) Location A-1 which showed low yield strength (177,000 psi) and high elongation (8.0 per cent) after aging at 900F for 96 hours.

Light and electron microscopy of these specimens had shown that lower strength in samples A and A-1 was associated with less dense aging constituent as compared with higher strength regions. In addition, the low ductility of sample A (2.5 per cent elongation) had been attributed to dense grain boundary precipitate and adjacent areas with a very low concentration of constituent. (Technical Report No. WAL 766.2/1-3). Analyses for chromium, vanadium and aluminum were made on these samples at two-micron intervals in a traverse across grain boundaries. These traverses, depicted in Figures 69-71 showed no evidence of grain boundary segregation. In addition, no composition variations were evident upon traversing from a grain exhibiting dense constituent to one showing less dense constituent. Fluctuations in element concentration did occur but these appeared to be quite random and not associated with grain boundary locations. The absolute magnitudes of the concentrations are not significant because the probe was not calibrated since only concentration variations were of interest.

G. <u>Full Scale Components</u>

The first front and rear domes forged on the new dies have been sectioned and are being evaluated. The second front and rear domes have been processed through the preform operation concurrently with and similar to the first domes, but the finish forging operations are being held until the evaluation of the first domes and of the sub-scale dome EFM-9 has been completed.

IV CONCLUSIONS

A. Based on limited data (notched and sustained notched tensile strengths) on a full scale 40-inch diameter cylinder, a hydrogen content of 240 ppm has no detrimental effect at room temperature on flow-turned material aged to the 180,000 psi yield strength level.

B. TIG welding using an improved copper-fixturing technique produces more uniform weld bead geometry, substantially less weld porosity but no significant improvement in tensile ductility or fracture toughness (G_c) as compared with present method (steel fixturing).

C. Using the cyclic test method described, the failure stress for TIG-welded material is inversely proportional to the numerical incidence of porosity, regardless of the weld technique. Limited data have indicated that electron beam welds are less susceptible than TIG welds to crack initiation and growth at weld porosity.

D. Closed-die press forging of subscale 14-inch diameter and full scale 40-inch diameter domes at 1850F with the reductions employed and using the present die configuration has produced low tensile ductility after aging to the 180,000 psi yield strength level.

E. For subscale 14-inch diameter and full scale 40-inch diameter domes press-forged in closed dies at 1850F, a 1450F solution treatment prior to 900F aging produces improved tensile ductility and property uniformity as compared with direct aging at 900F.

APPENDIX A

Tables

TABLE I

Status of Program Material and Investigations

A. Laboratory Investigations

Program	Work Location	Material Composition	Type of Material	Status: Material	Status: Investigation
Effect of Interstitials (hydrogen)	PWA	PWA 1200 and 1230	Sheet stock and flow-turned cylinders (14-inch and 40-inch diameter)	Received by PWA *, **	Sheet stock phase and evaluation of 40-inch diameter flow-turned cylinder with 240 ppm of hydrogen completed. Rolled rings (14-inch diameter) now being processed for evaluation.
Effects of Interstitials (oxygen)	Wyman-Gordon (forging) and PWA (evaluation)	Modified PWA 1200	Open die pancakes (9 pieces)	Received by Wyman-Gordon	Seven pieces forged and evaluation being completed. Three final pieces will not be forged at this time.
Metallographic (electron microscope, diffraction and microprobe techniques) examination.	Battelle Memorial Institute	PWA 1200	Press-forged, flow-turned and TIG and electron beam welded material	Received by Battelle Memorial Institute	Evaluation of eight samples completed and final report received by PWA. No further studies in process at this time.
X-ray Diffraction studies	Manufacturing Laboratories	PWA 1200	Flow-turned material	No material being evaluated at this time.	No additional work in process at this time.
Weld Improvement	PWA	PWA 1230	Sheet and plate stock	Received by PWA**	Investigation continuing

Table I (Cont.)

B. Subscale Components

Program	Work Location	Material Composition	Component	No. of Pieces Allocated	Status: Material	Status: Fabrication
Press forging (high and low strain rates)	Wyman-Gordon (forging) and PWA (evaluation)	PWA 1200	Open die pancakes	8	Received by Wyman-Gordon	Seven pieces forged and evaluated. Final piece will not be forged at this time.
Press forging (dogbone technique)	Wyman-Gordon (forging) and PWA (evaluation)	PWA 1200	14-inch diameter domes	3	Received by Wyman-Gordon	3 pieces forged and evaluated.
Press forging (pancake and preform technique)	Wyman-Gordon (forging) and PWA (evaluation)	PWA 1200	14-inch diameter domes	6	Received by Wyman-Gordon	Five pieces forged and evaluated. One piece forged at 1850F, restruck at 1750F and being evaluated.
Hammer forging	Ladish (forging) and PWA (evaluation)	PWA 1200	Closed die pancake with offset bosses	4	Received by Ladish	Four pieces forged and evaluated.
Ring rolling	Ladish (rolling) and PWA (evaluation)	PWA 1200	14-inch diameter rings	6	Received by Ladish	Four pieces rolled, flow-turned and evaluated. Final two pieces rolled and diverted to flow-turning development phase.

Table I (cont.)

B. Subscale Components (Cont.)

Program	Work Location	Material Composition	Component	No. of Pieces Allocated	Status: Material	Status: Fabrication
Flow-Turning	PWA	PWA 1200 (rolled rings) and PWA 1230 (rolled and welded blanks)	9.4-inch and 14-inch diameter rings and blanks	1) Two 9.4-inch diameter rolled rings 2) Nine 9.4-inch diameter rolled and welded blanks 3) Three 14-inch diameter rolled and welded blanks 4) Twelve 14-inch diameter rolled rings	9.4-inch and 14-inch diameter rings and material for 9.4-inch and 14-inch diameter rolled and welded blanks received by PWA	1) Two 9.4-inch diameter rolled rings flow-turned and evaluated 2) Eight of nine 9.4-inch diameter rolled and welded blanks flow-turned and evaluated. 3) Three 14-inch diameter rolled and welded blanks being machined prior to flow-turning. 4) Two of twelve 14-inch diameter rolled rings ready for flow-turning. Two additional rings diverted to hydrogen investigation. Three rings being machined prior to flow-turning.

C. Full Scale Components

Program	Work Location	Material Composition	Component	No. of Pieces Allocated	Status: Material	Status: Fabrication
Press-forging (pancake and preform technique)	Wyman-Gordon (forging) and PWA (evaluation)	First piece PWA 1200, Remaining four pieces modified PWA 1200	Full scale 40-inch diameter front domes	5	Material received by Wyman-Gordon	First piece forged at 1700F, restruck at 1900F in Pershing steel dies and evaluated. Second pieces forged at 1850F and

Table I (Cont.)

Program	Work Location	Material Composition	Component	No. of Pieces Allocated	Status: Material	Status: Fabrication
						being evaluated. Third piece pancaked and preformed at 1850F prior to final closed die forging. Final two pieces to be forged in OMRO dies at a later date.
Press-forging (dogbone technique)	Wyman-Gordon (forging) and PWA (evaluation)	Modified PWA 1200	Full scale 40-inch diameter rear domes	4	Material received by Wyman-Gordon	One piece forged in OMRO dies at 1850F and being evaluated. Three pieces to be forged at a later date.
Ring rolling	Ladish (forging) and PWA (evaluation)	Modified PWA 1200	Full scale 40-inch diameter rings	7	Material received by Ladish	Seven pieces rolled at 1900F.
Flow-turning	PWA	PWA 1200 (two pieces) and modified PWA 1200 (seven pieces)	Full scale 40-inch diameter cylinders	9	Two pieces received by PWA*. Material for seven pieces received by Ladish	Two pieces flow-turned, one cylinder being used for hydrogen investigation. Final seven pieces to be flow-turned based on results of subscale work.

* Two 40-inch diameter rings transferred from Thiokol contract RM-962.

** 0.125, 0.250 and 0.375-inch thick sheet and plate stock transferred from Thiokol contract RM-962.

TABLE II

Tensile and Sustained Notched (K_t=8) Tensile Properties (70F) of Full Scale 40-Inch Diameter Flow-Turned Cylinder No. 1 (240 ppm of Hydrogen) After Aging at 900F for Three Hours

A. Tensile Properties

Direction	T.S.	Y.S. (0.2%)	Elong (1")	N.T.S. (K_t=8)
Circ.	208.5 ksi	197.9 ksi	4.0%	90.9 ksi
Circ.	205.3 ksi	195.1	5.0	113.8
Axial	194.7	181.2	7.0	115.6
Axial	196.6	186.4	7.0	125.4

B. Sustained Notched (K_t=8) Tensile Properties

Specimen No.	Direction	Load	Time at Load	Remarks
1	Circ.	80 ksi	7.2 hours	Load increased to 85.0 ksi
1	Circ.	85	5.0	Load increased to 90.0 ksi
1	Circ.	90	53.3	Load increased to 95.0 ksi
1	Circ.	95	6.5	Load increased to 100.0 ksi
1	Circ.	100	5.0	Load increased to 110.0 ksi
1	Circ.	105	5.0	Load increased to 115.0 ksi
1	Circ.	110	0.0	Failed on loading
2	Circ.	100	166.0	Test discontinued
3	Axial	100	5.0	Load increased to 105.0 ksi
3	Axial	105	53.4	Load increased to 110.0 ksi
3	Axial	115	5.0	Load increased to 120 ksi
3	Axial	120	0.0	Failed on loading
4	Axial	105	0.0	Failed on loading
5	Axial	110	150.0	Test discontinued

TABLE III

Bend, Smooth and Notched (K_t=8) Tensile and Fracture Toughness (G_c) Test Results on TIG Welds Made By The Improved Copper-Fixturing Technique

A. Tensile and Notched Tensile (K_t=8) Tests

Specimen and Condition	T.S.	Y.S. (0.2%)	Elong(1")	Elong(1/2")	Elong(1/4")	Remarks
1. Bead Intact	140.3 ksi	138.2 ksi	6.0%	8.0%	12.0%	Heat-affected zone failure
2. Bead ground flush	140.5	---	8.0	15.0	20.0	Weld failure
3. Notched (K_t=8) bead intact	144.8	---	---	---	---	---
4. Notched (K_t=8) bead intact	156.4	---	---	---	---	---

B. Bend Tests

Specimen and Condition	Bend Diameter	Bend Angle	Remarks
1. Bead ground flush.face in tension	5.97 T	27°	Weld failure
2. Bead ground flush.face in tension	6.70	18	Weld failure
3. Bead ground flush.face in tension	9.8	80	Weld failure

C. Fracture Toughness (G_c) Tests

	σ_y	2a	$2a_o$	σ_n	G_c	G_c^*
1. Bead intact - notch at weld center	138.0 ksi	1.187"	1.187"	27.2	38 ipsi	-
2. Bead intact - notch at weld center	138.0	1.156	1.156	25.6	34	-

TABLE IV

Comparison of TIG Welding Schedules Employed For Previous Method And Improved Copper-Fixturing Technique

	Travel Speed	Rod Speed	Current	Arc Voltage	Gas to Torch	Gas to Trailer	Gas to Backup
Previous Technique(1)	5 IPM	30 IPM*	115-120 amps	10 volts	35cfh He	35cfh He	30cfh A
Improved Technique(2)	3 1/2	16 1/2**	160-170	14 volts	35cfh He	35cfh He	10cfh A

(1) Steel holddown and backup. Hold down of "finger" variety. Gas (He) quench applied to surface of weld bead. Backup plate square-cornered.

(2) Copper holddown and backup. Holddown, single-piece variety. No gas quench employed. Backup plate semicircular.

* 30 IPM wire speed with 1/32-inch diameter filler wire.
** 16 1/2 IPM wire speed with 3/64-inch diameter filler wire.

TABLE V

Bend Test Results on Panels Manually TIG-Welded
With Pure Vanadium and With Columbium-3.5
Titanium Filler Material

Specimen No.	Filler Material	Torch Gas Atmosphere	Bend Diameter	Bend Angle	Remarks
1	Columbium-3.5 Titanium	Argon	10.2 T	>105°	Parent metal Filler
2	Columbium-3.5 Titanium	Argon	8.35	>105	Parent metal filler
3	Vanadium	Helium	8.35	>105	Parent metal filler
4	Vanadium	Helium	8.35	26	Weld failure
5	Vanadium	Helium	7.2	20	Weld failure
6	Vanadium	Argon	10.2	>105	Intact
7	Vanadium	Argon	10.2	>105	Intact
8	Vanadium	Argon	8.35	40	Weld failure

TABLE VI

Porosity Rating of TIG and Electron Beam-Welded Cyclic Test Specimens

Specimen No.	Weld Technique	Weld Rating: No. of Pores (4")	No. of Pores (Worst 1")	Max. Pore Size	Closest Approach (Worst 1")	Closest Approach (Outside Worst 1")
1	Single-pass TIG weld present technique	64	18	0.025"	0.015"	0.035"
2	Single-pass TIG weld with overlap	70	23	0.030	0.010	0.015
3	Single-pass TIG weld made with 100 ppm of hydrogen in parent metal	2	2	0.010	0.938	N/A
4	Single-pass TIG weld made with 200 ppm of hydrogen in parent metal	18	6	0.025	0.020	0.010
5	Single-pass TIG weld made with 300 ppm of hydrogen in parent metal	20	10	0.025	0.005	0.010
6	Two-pass TIG weld (V type prepared joint)	27	14	0.020	0.030	0.045
7	Three-pass TIG weld (V type prepared joint)	35	12	0.035	0.015	0.050
8	Three-pass TIG weld (V type prepared joint)	106	33	0.055	0.015	0.030
9	Single-pass TIG weld with AMS 4951 filler wire	18	7	0.085	0.005	0.015
10	Single-pass TIG weld made with copper fixturing	0	N/A	N/A	N/A	N/A

Table VI (Cont.)

Specimen No.	Weld Technique	Weld Rating				
		No. of Pores (4")	No. of Pores (Worst 1")	Max. Pore Size	Closest Approach (Worst 1")	Closest Approach (Outside Worst 1")
11	Single-pass TIG weld made with copper fixturing	2	2	0.015	0.375	N/A
12	Single-pass TIG weld made with copper fixturing	0	N/A	N/A	N/A	N/A
13	Single-pass TIG weld made with copper fixturing	0	N/A	N/A	N/A	N/A
14	Single-pass TIG weld made with copper fixturing and with overlap	0	N/A	N/A	N/A	N/A
15	Single-pass TIG weld made with copper fixturing and with overlap	0	N/A	N/A	N/A	N/A
16	Single-pass TIG weld made without filler wire	36	12	0.010	0.010	0.010
19	Electron beam weld made without filler material	65	25	0.010	0.005	0.010
20	Electron beam weld made without filler material	8	4	0.010	0.010	0.050
21	Electron beam weld made without filler material	14	9	0.010	0.015	0.005
22	Electron beam weld with pre-placed filler wire	11	4	0.010	0.100	0.230

Table VI (Cont.)

Specimen No.	Weld Technique	Weld Rating No. of Pores (4")	No. of Pores (Worst 1")	Max. Pore Size	Closest Approach (Worst 1")	Closest Approach (Outside Worst 1")
23	Electron beam weld with pre-placed filler wire	6	3	0.005	0.110	0.075
24	Single-pass TIG weld with manual repair	23	19	0.015	0.015	0.875
25	Single-pass TIG weld with manual repair	20	16	0.020	0.010	0.075
26	Single-pass TIG weld made with vacuum annealed parent metal and filler wire	95	28	0.040	0.001	0.005
27	Single-pass TIG weld made with vacuum annealed parent metal and high hydrogen filler wire	234	78	0.030	0.001	0.0015
28	Single-pass TIG weld made with as-received parent metal and vacuum annealed filler wire	36	18	0.020	0.015	0.020
29	Single-pass TIG weld made with cathodically hydrogenated parent metal (approx. 300 ppm) and vacuum annealed filler wire	49	22	0.020	0.010	0.015
30	Single-pass TIG weld made with cathodically hydrogenated parent metal (approx. 700 ppm) and vacuum annealed filler wire	246	70	0.060	0.002	0.005

Table VI (Cont.)

Specimen No.	Weld Technique	Weld Rating: No. of Pores (4")	No. of Pores (Worst 1")	Max. Pore Size	Closest Approach (Worst 1")	Closest Approach (Outside Worst 1")
31	Single-pass TIG weld made with cathodically hydrogenated parent metal (approx. 1000 ppm) and vacuum annealed filler wire	40	13	0.015	0.010	0.015
32	Single-pass TIG weld (copper fixturing) made with AMS 4951 filler wire	100	37	0.020	0.005	0.010
33	Single-pass TIG weld made with as-received parent metal and filler wire	31	12	0.020	0.020	0.025
34	Single-pass TIG weld made with as-received parent metal and high hydrogen filler wire	27	15	0.010	0.015	0.020

TABLE VII

Cyclic Test Results of TIG and Electron Beam Welds Showing
Number of Crack Indications At Each Stress Level With Failure

Specimen No.	Weld Technique	As Welded	As Machined	Number of Crack Indications 80 KSI	80 KSI	80 KSI	85 KSI	90 KSI	95 KSI	100 KSI	105 KSI	110 KSI	115 KSI	12[illegible]
1	Single pass TIG weld, present technique	0	0	--	--	--	--	14	15	16	18	18	18	18
2	Single pass TIG weld, present technique with overlap	0	0	--	--	--	--	14	14	14	14	14	17	20
3	Single pass TIG weld, present technique 100 ppm hydrogen	0	0	0	0	0	0	0	0	0	0	0	0	0
4	Single pass TIG weld, present technique 200 ppm hydrogen	0	(1)	(1)(4)*										
5	Single pass TIG weld, present technique 300 ppm hydrogen	0	0	2	3	3	4	4	4	4	4	5	7	7
6	Two pass TIG weld, V type joint	0	1	1	1	1	1	1	1	1	1	1	1	2
7	Three pass TIG weld, V type joint	0	0	0	0	0	0	0	1	1	1	1	2	2
8	Three pass TIG weld, V type joint	0	8	15	23	23	35	35	35	35	41	41*		
9	Single pass TIG weld, AMS 4951 filler wire	0	0	0	0	0	0	0	0	1	1	3	3	6
10	Improved copper fixturing technique	0	0	0	0	0	0	0	0	0	0	0	0	[illegible]
11	Improved copper fixturing technique	0	0	0	0	0	0	0	0	0	0	0	0	[illegible]
16	Single pass TIG weld, no filler wire	0	1	1(16)*										
19	Electron beam weld, no filler wire	0(19)	0	0	0	0	0	0	0	0	0	0	0	[illegible]
20	Electron beam weld, no filler wire	0(20)	0	0	0	0	0	0	0	0	2	2	2	[illegible]

1

SI	105 KSI	110 KSI	115 KSI	120 KSI	125 KSI	130 KSI	135 KSI	140 KSI	145 KSI	150 KSI	155 KSI	160 KSI	165 KSI	170 KSI	175 KSI	180 KSI	185 KSI
	18	18	18	18*													
	14	14	17	20	20*												
	0	0	0	0	0	0	0	0	0	0	0	0	0	0	(1)	(2)	(2)*
	4	5	7	7	7*												
	1	1	1	2	5	5	5*										
	1	1	2	2	2	2	2	7	9	9	9	9	9	9*			
	41	41*															
	1	3	3	6	6	6	6	6	6	8	8	9	10	10	10	10*	
	0	0	0	0	0	0	0	0	0	0	0	0	0	0	0*		
	0	0	0	0	0	0	0	0	0	0	0	0	0	(1)	(1)*		
	0	0	0	0	1	1	2	3	--	-	--	--	*				
1	2	2	2	2	2	--	--	--	--	--	--	*					

Table VII (Cont.)

Specimen No.	Weld Technique	As Welded	As Machined	80 KSI	80 KSI	80 KSI	85 KSI	90 KSI	95 KSI	100 KSI	105 KSI	110 KSI	115 KSI	120 KSI	125
			Number of Crack Indications												
21	Electron beam weld, no filler wire	0(21)	0	0	0	0	0	0	0	0	0	0	0	0	0
22	Electron beam weld, preplaced filler wire	0(22)	0	0	0	0	0	0	0	0	0	0	0	0*	
23	Electron beam weld, preplaced filler wire	0(23)	0	0	0	0	0	0	0	0	0	0	0	--	--

*Denotes fracture
() Numbers in parenthesis denote cracks not associated with porosity

(4) Failed at 26.8 KSI through prior crack not associated with porosity
(16) Failed at 68.2 KSI through prior crack not associated with porosity
(19), (20), (21), (22), (23) Crack indications uncertain due to difficulty in radiograph interpretation; readings discontinued as shown

00 KSI	105 KSI	110 KSI	115 KSI	120 KSI	125 KSI	130 KSI	135 KSI	140 KSI	145 KSI	150 KSI	155 KSI	160 KSI	165 KSI	170 KSI	175 KSI	180 KSI	185 KSI
0	0	0	0	0	0	*											
0	0	0	0	0*													
0	0	0	0	--	--	--	--	--	--	--	--	--	*				

2

TABLE VIII

Conditions Prior to and After Failure and Gas Analyses for TIG-Welded Cyclic Test Specimens

Specimen No.	Weld Technique	Gas Analyses: Hydrogen, Weld Metal	Gas Analyses: Hydrogen, Parent Metal	Gas Analyses: Oxygen, Parent Metal	Gas Analyses: Oxygen, Weld Metal	No. of Porosity Holes	No. Cracks Through Porosity	Stress at Failure	Crack Length Just Prior to Failure	Mode of Failure
1	Single-pass TIG weld, present technique	50 ppm 90	108*ppm	.107%*	.119% .113	64	18	120.0 KSI	0.216"	Through porosity
2	Single-pass TIG weld, present technique with overlap	70 80	108*ppm	.107%*	.133 .136	70	20	125.0	0.080	Through porosity
3	Single-pass TIG weld, present technique 100 ppm hydrogen	130 140	108	.107	.120 .104	2	1	185.0	0.100	Failure not associated with porosity
4	Single-pass TIG weld, present technique 200 ppm hydrogen	320 320	250-310	.107	.102 .093	18	1	27.0	0.475	Through prior machining crack
5	Single-pass TIG weld, present technique 300 ppm hydrogen	400 440	330-400	.107	.091 .100	20	7	125.0	N/A	No porosity or prior crack observed
6	Two-pass TIG weld, V type joint	140 140	108*	.107	.120 .119	27	5	135.0	0.110	Through porosity
7	Three-pass TIG weld, V type joint	120 110	108	.107	.116 .132	35	9	170.0	0.175	Failure not associated with porosity
8	Three-pass TIG weld, V type joint	140 130	108	.107	.122 .127	106	41	110.0	0.080 0.090	Through porosity
9	Single-pass TIG weld, AMS 4951 filler wire	160 170	108	.107	[illegible] .131	18	10	180.0	0.125	Failure not associated with porosity
10	Improved copper fixturing technique	160 170	130	.107	.119 .127	0	0	175.0	0.350	Failure not associated with porosity

Table VIII (Cont.)

Specimen No.	Weld Technique	Gas Analyses: Hydrogen, Weld Metal	Gas Analyses: Hydrogen, Parent Metal	Gas Analyses: Oxygen, Parent Metal	Gas Analyses: Oxygen, Weld Metal	No. of Porosity Holes	No. Cracks Through Porosity	Stress at Failure	Crack Length Just Prior to Failure	Mode of Failure
11	Improved copper fixturing technique	160 170	130	.107%*	.119 .127	0	0	175.0	N/A	Failure not associated with porosity
16	Single-pass TIG weld, no filler wire	110 110	108*	.107	.083 .073	36	1	68.2	0.300	Through prior machining crack
19	Electron beam weld, no filler wire	150 150	108	.107	.140 .140	65	**	165.0	0.100	Parent Metal
20	Electron beam weld, no filler wire	160 180	108	.107	.134 .167	8	**	161.0	0.125	Parent Metal
21	Electron beam weld, no filler wire	120 140	108	.107	.137 .159	14	**	130.0	0.150	Parent Metal
22	Electron beam weld, preplaced filler wire	140 170	108	.107	.121 .122	11	**	---	---	Failure outside gage area
23	Electron beam weld, preplaced filler wire	140 170	108	.107	.121 .122	6	**	170.0	0.150	Failure not associated with porosity

*Average of six analyses

**Not determined due to difficulty in radiograph interpretation

TABLE IX

Cyclic Test Results (Current) On TIG Welds Indicating Number Of Crack Indications At Each Stress Level

Specimen No.	Weld Technique	As-Welded	As-Machined	Number Of Crack Indications											
				80 KSI	80 KSI	80 KSI	85 KSI	90 KSI	95 KSI	100 KSI	105 KSI	110 KSI	115 KSI	120 KSI	125 KSI
12	Improved Copper Fixturing Technique	0	0	0	0	0	0	0	0	0	0	0	0	0	0
13	Improved Copper Fixturing Technique	0	0	0	0	0	0	0	0	0	0	0	0	0	0
14	Improved Copper Fixturing Technique With Overlap	0	0	0	0	0	0	0	0	0	0	0	0	0	0
15	Improved Copper Fixturing Technique With Overlap	0	0	0	0	0	0	0	0	0	0	0	0	0	0
24	Improved Copper Fixturing Technique With Manual Repairs	0	0	0	0	0	0	0	0	0	0				
25	Improved Copper Fixturing Technique With Manual Repairs	0	0	2*	2	2	2	2	2	2	2				

*Crack Indications Through Porosity In One Of Two Manual Repairs.

TABLE X

Gas Analyses Of Cyclic Test Specimens TIG-Welded Using Parent Metal Filler Wire With Various Hydrogen Contents

Specimen No.	Metal Condition	Parent Metal Hydrogen	Parent Metal Oxygen	Gas Analyses Weld Wire Hydrogen	Gas Analyses Weld Wire Oxygen	Weld Metal Hydrogen	Weld Metal Oxygen
26	Vacuum-Annealed Parent Metal And Filler Wire	*	*	60 ppm	.100-.110%	*	*
27	Vacuum-Annealed Parent Metal And High Hydrogen Filler Wire	*	*	240-260 ppm	.100-.110	*	*
28	As-Received Parent Metal And Vacuum-Annealed Filler Wire	*	*	60 ppm	.100-.110	160 170	.119 .127
34	As-Received Parent Metal And High Hydrogen Filler Wire	130 130	.114 .097	240-260 ppm	.100-.110	150	.121
29	Cathodically-Hydrogenated Parent Metal, Vacuum-Annealed Filler Wire	350 360	.115 .108	60 ppm	.100-.110	250 290	.120 .100
30	Cathodically-Hydrogenated Parent Metal, Vacuum-Annealed Filler Wire	570	.100	60 ppm	.100-.110	310 410	.137 .115
31	Cathodically-Hydrogenated Parent Metal, Vacuum-Annealed Filler Wire	1330 1460	.063 NIL	60 ppm	.100-.110	570 710	.088 NIL

*Analyses Not Completed.

TABLE XI

Fracture Toughness (G_c) Test Results On Cold-Rolled TIG Welds And Cold-Rolled And Aged Sheet Stock Of Various Thicknesses

Specimen	Thickness	(1) σ_y	(2) 2a	(3) $2a_o$	G_c	(4) G_c^*	(5) σ_n
Double Longitudinally Disposed Weld Beads, 30% Reduction	0.099"	210.0 KSI	1.40"	1.045"	640 ipsi	640 ipsi	111.5 KSI
Double Longitudinally Disposed Weld Beads, 40% Reduction	0.085		1.40	0.962	590	590	107.2
Double Longitudinally Disposed Weld Beads, 50% Reduction	0.071		1.46	1.002	490	490	98.0
Cold-Rolled And Aged Sheet Stock Machined To Final Thickness	0.142	201.0	1.156	0.8732	72.6	73.0	37.3
Cold-Rolled And Aged Sheet Stock Machined to Final Thickness	0.139	202.0	1.406	0.8660	73.0	73.6	37.8
Cold-Rolled And Aged Sheet Stock Machined To Final Thickness	0.101	203.0	1.156	0.8735	100.0	102.0	43.8
Cold-Rolled And Aged Sheet Stock Machined To Final Thickness	0.102	203.3	1.250	0.8770	93.0	94.0	42.1
Cold-Rolled And Aged Sheet Stock Machined To Final Thickness	0.086	200.0	1.281	0.8688	153.0	155.0	54.1
Cold-Rolled And Aged Sheet Stock Machined To Final Thickness	0.086	203.5	1.312	0.8740	131.0	133.0	50.1
Cold-Rolled And Aged Sheet Stock Machined To Final Thickness	0.070	200.5	1.343	0.8830	249.0	256.0	69.3
Cold-Rolled And Aged Sheet Stock Machined To Final Thickness	0.074	200.0	1.312	0.8770	163.0	167.0	56.1

(1) σ_y - Yield Strength (0.2% Offset)

(2) 2a - Initial Slot Length, Plus Slow Crack Propagation

(3) $2a_o$ - Length Of Initial Slot

(4) G_c^* - G_c With Correction For Plastic Straining At The Root Of Notch

(5) σ_n - Net Section Stress - $\frac{P_{ult}}{(W-2a)t}$

P = Ultimate Load
W = Width
t = Thickness

TABLE XII
Wyman-Gordon Tensile Properties (70F) Of Sub Scale 14-Inch Diameter Dome EFM-8 Press-Forged At 1850F By The Pancake And Preform Technique

Solution Treatment	Age	Radial Location	T.S.	Y.S. (0.2%)	Elong. (1")	R.A.
None	900F(24)AC	1 (RIM)	180.3 KSI	173.8 KSI	1.5%	9.3%
		2 MID RAD	173.4	163.4	4.0	10.1
		3 (POLE)	168.0	160.1	2.0	9.3
None	900F(36)AC	1	194.4	186.2	2.0	7.7
		2	179.1	169.5	3.0	9.3
		3	180.7	169.1	4.0	9.3
None	900F(48)AC	1	197.0	190.1	1.0	7.0
		2	185.6	173.4	4.0	10.1
		3	187.6	175.2	4.0	9.3
1450F (1/2)WQ	900F(24)AC	4 (RIM)	190.5	182.7	2.0	7.7
		5 MID RAD	183.1	171.9	4.5	7.7
		6 (POLE)	179.9	171.3	3.0	8.6
1450F (1/2)WQ	900F(36)AC	4	194.0	186.8	1.0	4.7
		5	188.4	178.5	3.0	7.7
		6	194.4	182.5	2.5	7.5
1450F (1/2)WQ	900F(48)AC	4	196.6	190.5	1.0	4.7
		5	192.5	184.0	2.0	7.0
		6	192.5	182.5	3.0	7.0

TABLE XIII
Wyman-Gordon Tensile Properties (70F) Of Sub Scale 14-Inch Diameter Dome EFM-10 Press-Forged At 1850F By The Dogbone Technique

Solution Treatment	Age	Location	T.S.	Y.S. (0.2%)	Elong. (1")	R.A.
None	900F(24)AC	1 (RIM)	191.7 KSI	181.7 KSI	3.5%	10.9%
		2 MID RAD	189.5	174.0	6.0	7.7
		3 (POLE)	187.6	175.8	6.0	11.7
None	900F(36)AC	1	198.0	184.4	2.0	4.7
		2	191.7	177.6	6.0	12.4
		3	204.0	194.2	4.0	7.7
None	900F(48)AC	1	204.0	194.6	2.0	8.6
		2	198.6	184.2	4.5	10.1
		3	198.4	178.9	6.5	13.1
1450F (1/2)WQ	900F(24)AC	4 (RIM)	185.6	174.0	4.0	15.4
		5 MID RAD	190.5	176.0	7.0	12.4
		6 (POLE)	194.6	182.9	6.0	12.4
1450F (1/2)WQ	900F(36)AC	4	194.8	182.7	2.0*	10.1
		5	195.0	178.7	6.0	13.9
		6	201.1	189.9	1.0*	6.2

TABLE XIII (Cont'd)

Solution Treatment	Age	Radial Location	T.S.	Y.S. (0.2%)	Elong. (1")	R.A.
1450F (1/2)WQ	900F(48)AC	4	201.5	185.2	5.0	11.7
		5	203.7	186.0	6.0	10.9
		6	200.1	190.5	4.5	7.7

*Failed in Outer Third or Outside of Gage Area.

TABLE XIV
Wyman-Gordon Tensile Properties (70F) Of Sub Scale 14-Inch Diameter
Dome EFM-9 Press-Forged At 1850F By The Pancake And Preform Technique

Solution Treatment	Age	Location	T. S.	Y. S. (0.2%)	Elong (1")	R. A.
1450F (1/2) WQ	900F(24)AC	POLE	183.1 KSI	171.1 KSI	3.5%	8.6%
1450F (1/2) WQ	900F(24)AC	POLE	181.5	171.9	4.0	9.3
1450F (1/2) WQ	900F(24)AC	SKIRT	191.3	183.1	2.0	4.7
1450F (1/2) WQ	900F(24)AC	SKIRT	192.1	183.8	2.0	6.2

TABLE XV

Pratt & Whitney Aircraft Tensile Properties (70F) of Subscale 14-Inch Diameter Dome EFM-8 Press-Forged at 1850F by the Pancake and Preform Technique

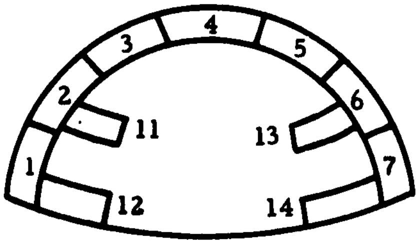

Specimen No.	Direction	Heat Treatment	TS	Y.S. (0.2%)	Y.S. (0.02%)	Elong.	RA	NTS (K_t=8) ksi
5	Radial	900F(70)AC	190.5 ksi	180.0 ksi	171.5 ksi	4.5%	3.3%	103.0 ksi
6	"	"	194.0	179.5	173.5	4.0	4.7	113.2
7	"	"	201.0	193.0	185.5	3.0	2.2	107.6
13	Circ.	"	195.0	180.0	107.0	3.0	3.4	122.2
14	"	"	210.0	205.0	196.0	0.5	1.1	107.2
4	Radial	1450(1/2) WQ+900F(48) AC	188.0	175.7	155.5	2.0	8.0	114.2
3	"	"	193.9	183.8	146.0	2	5.5	122.0
2	"	"	197.3	187.3	177.3	1.5	5.0	126.5
1	"	"	196.0	192.6	180.6	1.0	2.5	124.0
11	Circ.	"	194.7	182.0	142.3	1.0	7.0	119.0
12	"	"	198.8	192.9	175.0	1.0	3.0	105.8

TABLE XVI

Pratt & Whitney Aircraft Tensile Properties (70F) of Subscale 14-Inch Diameter Dome EFM-10 Press-Forged at 1850F by the Dogbone Technique

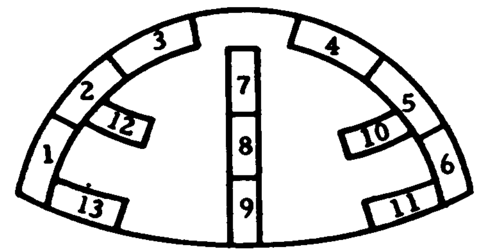

Location	Direction	Heat Treatment	TS	Y.S. (0.2%)	Y.S. (0.02%)	Elong.	RA	NTS K_t=8 ksi
3	Radial	900F(48)AC	195.6 ksi	178.5 ksi	171.4 ksi	5.5%	12.5%	122.0
2	"	"	198.5	179.2	171.3	8.0	12	107.0
1	"	"	209.0	199.0	193.2	1.5	5.5	124
12	Circ.	"	198.3	183.3	172.4	2.5	4.5	132.5
13	"	"	207.0	206.5	194.0	1.0	2.5	127.5
4	Radial	1450F(1/2)WQ + 900F(48)AC	204.0	186.3	176.7	5.0	13	116.0
4	"	"	204.5	187.9	176.8	5.0	11	
5	"	"	205.0	184.0	174.5	6.0	8.5	
5	"	"	199.0	185.0	172.8	2.5	7.5	
6	"	"	204.3	189.5	177.6	4.5	4.0	115.0
6	"	"	202.0	191.9	180.7	2.5	5.5	
10	Circ.	"	203.0	185.0	173.0	4.0	8.0	125.5
11	"	"	207.0	195.2	182.2	3.0	5.0	117.0
7	Radial	1450F(1/2)AC + 900F(48)AC	204.5	187.3	180.2	4.0	9.0	128.5
7	"	"	198.2	186.0	172.3	5.0	12.5	
8	"	"	194.6	181.4	168.4	4.0	10.5	136.0
8	"	"	194.1	183.2	171.7	5.5	12.5	
9	"	"	186.5	175.3	161.5	2.5	8.0	122.0
9	"	"	189.2	177.5	165.2	4.0	12	

TABLE XVII

Pratt & Whitney Aircraft Aging Response Tensile Properties (70F) for Full Scale Front Dome EJO-1 Press-Forged at 1700F and Restruck at 1900F

Heat Treatment	T.S	Y.S. (0.2%)	Elong (1")	R.A.
900F(16)AC	177.6 ksi	165.3 ksi	3.5%	7.0%
900F(24)AC	190.6	186.3	0.5	5.5
900F(32)AC	198.6	185.7	2.5	5.0
1400F (1/2)WQ + 900F (16) AC	188.5	175.3	2.0	5.0
+ 900F (24) AC	186.2	170.1	2.0	7.5
+ 900F (32) AC	196.3	183.3	2.0	5.0
1450F (1/2) WQ + 900F (16) AC	186.0	174.3	2.0	5.5
+ 900F (24) AC	197.4	183.4	3.0	5.0
+ 900F (32) AC	200.0	189.2	2.5	5.5

Note: Specimens machined in radial direcfion from mid-radius location of dome.

TABLE XVIII

Tensile Properties (70F) of Polar Boss From Full Scale 40-inch Diameter Front Dome EJO-1 Press-Forged at 1700F and Restruck at 1900F

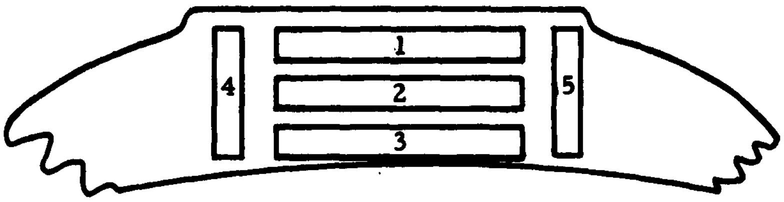

Solution Treatment	Age	Location	TS.	Y.S. (0.2%)	Y.S. (0.02%)	Elong(1")	R.A
1450F(1/2)WQ	900F (24)AC	1	188.6 ksi	182.8 ksi	174.6 ksi	2.0%	5.0%
"	"	1	181.4	175.4	164.8	1.5	3.0
"	"	2	186.8	176.5	157.3	1.5	3.0
"	"	2	186.5	178.5	170.5	2.0	6.0
"	"	3	192.0	185.4	175.2	1.0	4.0
"	"	3	192.3	187.2	171.4	1.0	4.0
"	"	4	192.3	180.3	169.5	2.0	3.5
"	"	5	182.8	176.8	167.5	2.0	4.0

TABLE XIX

Tensile Properties (70F) of One Offset Boss from Full Scale 40-Inch Diameter Front Dome EJO-1 Press-Forged at 1700F and Restruck at 1900F

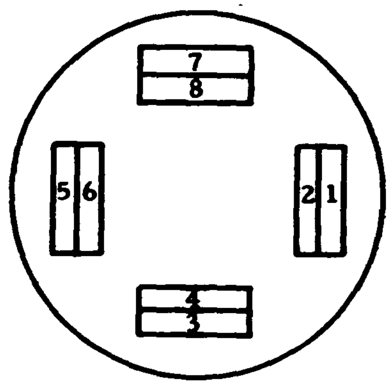

Solution Treatment	Age	Location	T.S.	Y.S. (0.2%)	Y.S (0.02%)	Elong (1")	R.A.
1450F(1/2)WQ	900F(24)AC	1	194.6 ksi	186.3 ksi	174.6 ksi	1.5%	5.8%
"	"	1	193.3	184.5	173.2	1.0	5.3
"	"	2	196.0	187.8	175.0	2.5	4.1
"	"	2	201.8	189.8	179.4	4.0	5.3
"	"	3	196.8	188.7	178.2	3.5	4.1
"	"	3*	180.9	177.3	170.0	1.0	5.2
"	"	4	199.2	187.8	163.3	1.5	5.5
"	"	4	196.0	185.5	159.2	1.5	3.4
"	"	5	196.0	184.6	153.6	.5	5.2
"	"	5	188.8	186.2	155.4	2.0	4.9
"	"	6	199.4	186.4	158.7	2.5	3.4
"	"	6	192.0	185.9	158.1	0.5	4.1
"	"	7	196.7	184.7	157.7	5.5	5.3
"	"	7	197.0	185.8	161.5	2.0	5.2
"	"	8	197.7	186.7	155.6	1.0	1.5
"	"	8	196.0	185.7	154.3	1.5	5.1

* Extremely course grained

TABLE XX

Tensile Properties (70F) of Full Scale 40-Inch Diameter Front Dome EJO-1 Aged at 900F After Various Solution Treatments

Solution Treatment	Age	T.S.	Y.S. (0.2%)	Y.S. (0.02%)	(1") Elong.	R.A.
None	24	187.8 ksi	179.3 ksi	170.5 ksi	1.5%	8.2%
1450F(1/2)WQ	24	197.4	185.7	181.0	1.5	6.4
1800F(1/12)WQ + 1400F(1/4)WQ	16	195.8	181.0	166.2	2.5	5.5
	24	199.6	189.0	177.1	1.0	4.0
1800F(1/12)WQ + 1400F(1/2)WQ	16	193.0	179.0	167.0	1.5	5.5
	24	199.6	186.2	174.0	2.0	5.0
1800F(1/12)WQ + 1450F(1/4)WQ	16	197.1	181.7	167.0	3.5	8.0
	24	202.5	182.0	172.5	3.0	7.0
1800F(1/12)WQ + 1450F(1/2)WQ	16	195.4	178.3	163.3	2.5	5.0
	24	199.0	180.2	167.8	2.5	4.0

TABLE XXI

Forging Sequence For Full Scale 40-Inch Diameter Domes

	ELA-1	ELA-2
A. Rear Domes (Dogbone Method)		
Billet (13" diameter x 21 1/2" long Heated to	1700F for 2 hrs + 1850F for 2 1/3 hrs.	1850F for 2 1/3 hrs.
Pancaking operation		
On die	1675 F	1675 F
Paused at 11" thick to add lubrication	1630 F	1630 F
Finished	1635 F	1635 F
Strain Rate	2 ft/min	2 ft/min
Dimensions of pancake	5" thick x 27" dia.	5" thick x 27" dia.
Dogbone preform operation		
In furnace		1850F for 3 hrs
On die		not recorded
Finished		1640F
Strain Rate		2 ft/min
Press pressure		54, 000 tons
Finish Forging operation		
In furnace		1850F for 3 hrs 50"
On die		1600 F
Finished		1530 F

B. Front Domes (Pancake and Preform Method)

	ELA-3	ELA-4
Billet (13" dia. x 23 1/4" long)		
Heated to	1700F for 2 1/2 hrs+ 1850F for 2hrs 10min	
Pancaking operation		
On die	1620 F	1665 F
Paused at 11" thick to add lubrication	1590 F	1630 F
Finished	1610 F	1640 F
Strain rate	2 ft/min	2 ft/min
Pancake dimensions	5.58" x 27" dia.	5.68" x 27" dia.

Table XXI (Cont.)

	ELA-3	ELA-4
Preform forging		
In furnace	1850F for 3 1/4 hrs	1850 for 3 hrs 17"
On die	1610 F	1640 F
Finish	1550 F	1550 F
Strain rate	2 ft/min	2 ft/min
Finish forging operation		
In furnace	1850F for 2 hrs	
On die	1630F	
1st reheat in furnace	1850F for 40 min	
On die	1580F	
2nd reheat in furnace	1850F for 45 min	
On die	1630F	
3rd reheat in furnace	1850F for 35 min	
On die	1620F	
Finish	<1400F	

TABLE XXII

Wyman-Gordon Tensile Properties (70F) of Full Scale 40-Inch Diameter Rear Dome ELA-2 Forged at 1850F by the Dogbone Technique

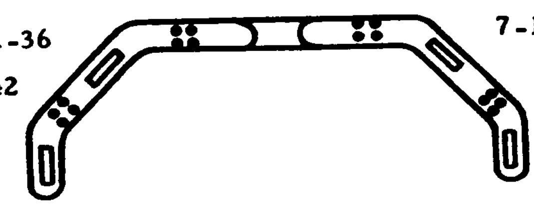

Specimen No.	Solution Treatment	Age	Specimen No.		T.S.	Y.S. (0.2%)	Elong. (1")	R.A.
5	None	900F(16)AC	Pole	Tang.	193.8 ksi	179.5 ksi	2.0%	5.4%
6	None	900F(16)AC	Pole	Tang.	201.9	188.7	2.0	4.7
7	None	900F(16)AC	Mid-radius (top)	radial	192.9	177.2	4.0	7.7
8	None	900F(16)AC	Mid-radius (top)	radial	189.9	180.9	8.0	14.7
13	None	900F(16)AC	Mid-radius (bottom)	tang.	197.0	180.5	2.5	6.2
14	None	900F(16)AC	Mid-radius (bottom)	tang.	194.0	178.2	6.0	8.6
19	None	900F(16)AC	Skirt	Radial	186.8	175.0	4.0	9.3
20	None	900F(16)AC	Skirt	Radial	189.1	178.7	4.0	10.1
1	None	900F(24)AC	Pole	Tang.	202.3	192.9	2.0	4.0
2	None	900F(24)AC	Pole	Tang.	199.5	189.3	2.5	3.2
7	None	900F(24)AC	Mid-radius (top)	radial	197.0	186.2	2.5	4.7
8	None	900F(24)AC	Mid-radius (top)	radial	203.3	185.6	6.5	8.9
13	None	900F(24)AC	Mid-radius (bottom)	tang.	208.2	191.7	3.0	6.6
14	None	900F(24)AC	Mid-radius (bottom)	tang.	196.4	185.4	2.0	4.0
19	None	900F(24)AC	Skirt	Radial	194.2	186.2	2.5	4.3
20	None	900F(24)AC	Skirt	Radial	202.5	194.6	4.5	8.1

Table XXII (Cont.)

Specimen No.	Solution Treatment	Age	Specimen No.		T.S.	(Y.S. (0.2%)	Elong. (1")	R.A.
3	None	900F(36)AC	Pole	Tang.	204.2	193.5	2.0	4.7
4	None	900F(36)AC	Pole	Tang.	203.5	191.9	2.0	3.2
9	None	900F(36)AC	Mid-radius (top) radial		201.9	188.7	4.0	7.0
10	None	900F(36)AC	Mid-radius (top) radial		200.7	190.7	6.5	12.4
15	None	900F(36)AC	Mid-radius (bottom) tang.		209.3	193.8	2.5	4.7
16	None	900F(36)AC	Mid-radius (bottom) tang.		201.5	189.3	2.0	6.2
21	None	900F(36)AC	Skirt	Radial	199.5	190.3	2.0	5.4
22	None	900F(36)AC	Skirt	Radial	204.4	194.0	4.0	7.0
5	None	900F(48)AC	Pole	Tang.	213.5	198.9	2.0	3.8
6	None	900F(48)AC	Pole	Tang.	211.9	201.9	2.0	2.4
11	None	900F(48)AC	Mid-radius (top) radial		209.7	200.7	6.0	11.7
12	None	900F(48)AC	Mid-radius (top) radial		201.3	196.0	4.5	6.8
17	None	900F(48)AC	Mid-radius (bottom) tang.		215.2	199.9	2.5	14.3
18	None	900F(48)AC	Mid-radius (bottom) tang.		202.7	193.8	2.0	4.7
23	None	900F(48)AC	Skirt	Radial	201.5	195.0	2.0	3.8
24	None	900F(48)AC	Skirt	Radial	208.6	199.7	2.0	7.0
5	1450F(1/2)WQ	900F(16)AC	Pole	Tang.	198.9	184.6	2.0	4.0
6	1450F(1/2)WQ	900F(16)AC	Pole	Tang.	204.0	188.2	3.0	2.4
7	1450F(1/2)WQ	900F(16)AC	Mid-radius (top) radial		196.6	185.6	4.0	7.0
8	1450F(1/2)WQ	900F(16)AC	Mid-radius (top) radial		193.1	181.5	7.0	13.1
13	1450F(1/2)WQ	900F(16)AC	Mid-radius (bottom) tang.		201.7	188.0	2.0	6.2
14	1450F(1/2)WQ	900F(16)AC	Mid-radius (bottom) tang.		199.5	183.1	6.0	7.7
19	1450F(1/2)WQ	900F(16)AC	Skirt	Radial	194.6	184.0	3.0	7.0
20	1450F(1/2)WQ	900F(16)AC	Skirt	Radial	194.6	182.5	4.0	4.7
26	1450F(1/2)WQ	900F(24)AC	Pole	Tang.	204.0	190.3	3.0	5.2
31	1450F(1/2)WQ	900F(24)AC	Mid-radius (top) radial		204.4	191.7	6.0	9.0
32	1450F(1/2)WQ	900F(24)AC	Mid-radius (top) radial		197.0	185.6	6.0	10.1
37	1450F(1/2)WQ	900F(24)AC	Mid-radius (bottom) tang.		210.9	195.8	4.0	5.9
43	1450F(1/2)WQ	900F(24)AC	Skirt	Radial	198.2	188.2	3.5	7.7
44	1450F(1/2)WQ	900F(24)AC	Skirt	Radial	207.7	190.9	6.9	8.4

Table XXII (Cont.)

Specimen No.	Solution Treatment	Age	Specimen No.		T.S.	Y.S.(0.2%)	Elong.(1")	R.A.
27	1450F(1/2)WQ	900F(36)AC	Pole	Tang.	212.3	195.8	2.0	4.7
28	1450F(1/2)WQ	900F(36)AC	Pole	Tang.	210.9	197.6	2.0	4.7
33	1450F(1/2)WQ	900F(36)AC	Mid-radius (top)	radial	207.0	194.2	6.0	11.7
34	1450F(1/2)WQ	900F(36)AC	Mid-radius (top)	radial	208.2	190.1	6.0	10.1
39	1450F(1/2)WQ	900F(36)AC	Mid-radius (bottom)	tang.	213.3	199.9	2.0	4.0
40	1450F(1/2)WQ	900F(36)AC	Mid-radius (bottom)	tang.	215.0	198.9	2.0	5.4
45	1450F(1/2)WQ	900F(36)AC	Skirt	Radial	206.2	195.8	2.0	6.2
46	1450F(1/2) WQ	900F(36)AC	Skirt	Radial	207.4	192.3	4.0	10.9
29	1450F(1/2)WQ	900F(48)AC	Pole	Tang.	210.0	201.3	2.0	3.2
30	1450F(1/2)WQ	900F(48)AC	Pole	Tang.	215.6	201.9	1.8	4.7
35	1450F(1/2)WQ	900F(48)AC	Mid-radius (top)	radial	211.7	197.2	6.0	9.0
36	1450F(1/2)WQ	900F(48)AC	Mid-radius (top)	radial	211.7	194.6	6.5	9.0
41	1450F(1/2)WQ	900F(48)AC	Mid-radius (bottom)	tang.	215.8	204.2	2.0	2.9
42	1450F(1/2)WQ	900F(48)AC	Mid-radius (bottom)	tang.	218.2	202.1	2.5	4.3
47	1450F(1/2)WQ	900F(48)AC	Skirt	Radial	210.7	199.7	3.5	2.9
48	1450F(1/2)WQ	900F(48)AC	Skirt	Radial	211.9	196.0	4.5	8.3

TABLE XXIII

Wyman-Gordon Tensile Properties (70F) of Full Scale 40-Inch Diameter Front Dome ELA-3 Press-Forged at 1850F by the Pancake and Preform Method

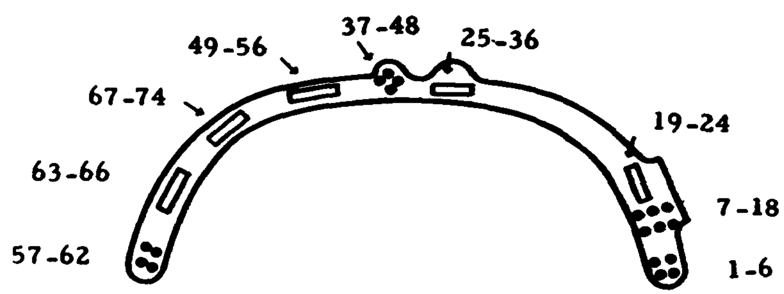

Specimen No.	Solution Treatment	Age	Location	Direction	T.S.	Y.S. (0.2%)	Elong. (1")	R.A.
25	None	900F(24)AC	Polar Boss	Radial	161.9ksi	150.9ksi	3.0%	5.4%
26	None	900F(24)AC	Polar Boss	Radial	155.4	145.4	4.5	13.4
37	None	900F(24)AC	Polar Boss	Tang.	153.8	144.6	4.0	12.4
38	None	900F(24)AC	Polar Boss	Tang.	153.4	143.6	6.0	10.9
49	None	900F(24)AC	Offset Boss	Radial	194.2	183.8	5.0	7.0
50	None	900F(24)AC	Offset Boss	Radial	192.9	181.1	2.0	6.2
7	None	900F(24)AC	Offset Boss	Tang.	182.5	169.1	2.0	7.7
8	None	900F(24)AC	Offset Boss	Tang.	177.6	163.2	4.5	8.6
63	None	900F(24)AC	Mid-radius(bottom)	Radial	186.0	172.3	3.0	7.0
64	None	900F(24)AC	Mid-radius(bottom)	Radial	184.8	170.3	4.5	7.7
1	None	900F(24)AC	Skirt	Tang.	207.8	195.0	2.0	5.4
2	None	900F(24)AC	Skirt	Tang.	206.4	196.2	2.0	5.4
27	None	900F(36)AC	Polar Boss	Radial	155.4	144.8	4.0	12.4
28	None	900F(36)AC	Polar Boss	Radial	165.6	155.0	3.0	5.8
39	None	900F(36)AC	Polar Boss	Tang.	169.3	157.0	2.0	4.7
40	None	900F(36)AC	Polar Boss	Tang.	161.5	149.7	4.0	10.8
9	None	900F(36)AC	Offset Boss	Tang.	188.7	173.4	2.0	5.8
10	None	900F(36)AC	Offset Boss	Tang.	192.5	176.4	3.0	4.7

Table XXIII (Cont.)

Specimen No.	Solution Treatment	Age	Location	Direction	T.S.	Y.S. (0.2%)	Elong. (1")	R.A.
65	None	900F(36)AC	Mid-radius(bottom)	Radial	192.9ksi	177.6ksi	4.0%	7.3%
66	None	900F(36)AC	Mid-radius(bottom)	Radial	192.7	176.4	4.5	8.1
3	None	900F(36)AC	Skirt	Tang.	211.1	199.1	2.0	5.0
4	None	900F(36)AC	Skirt	Tang.	216.2	201.5	2.0	4.7
41	None	900F(48)AC	Polar Boss	Tang.	170.9	156.8	3.0	9.3
42	None	900F(48)AC	Polar Boss	Tang.	170.5	--	2.0	5.0
11	None	900F(48)AC	Offset Boss	Tang.	198.2	183.1	2.0	4.7
12	None	900F(48)AC	Offset Boss	Tang.	193.5	178.2	3.0	7.0
17	None	900F(48)AC	Offset Boss	Tang.	199.3	185.6	2.5	6.6
18	None	900F(48)AC	Offset Boss	Tang.	204.6	191.7	2.0	6.2
23	None	900F(48)AC	Offset Boss	Radial	198.2	185.6	2.0	6.2
24	None	900F(48)AC	Offset Boss	Radial	201.0	190.7	2.5	5.8
55	None	900F(48)AC	Mid-radius(top)	Radial	191.3	174.4	4.0	7.7
56	None	900F(48)AC	Mid-radius(top)	Radial	191.3	174.8	4.0	8.1
5	None	900F(48)AC	Skirt	Tang.	209.3	196.8	3.0	6.6
6	None	900F(48)AC	Skirt	Tang.	213.7	199.9	2.5	4.3
44	1450F(1/2)WQ	900F(24)AC	Polar Boss	Tang.	183.1	169.5	4.0	7.7
46	1450F(1/2)WQ	900F(24)AC	Polar Boss	Tang.	186.1	173.6	3.0	6.2
31	1450F(1/2)WQ	900F(24)AC	Polar Boss	Radial	184.0	173.1	2.0	9.3
32	1450F(1/2)WQ	900F(24)AC	Polar Boss	Radial	182.3	168.4	4.0	8.6
13	1450F(1/2)WQ	900F(24)AC	Offset Boss	Tang.	191.7	179.7	3.0	4.7
14	1450F(1/2)WQ	900F(24)AC	Offset Boss	Tang.	199.1	185.2	2.0	6.2
19	1450F(1/2)WQ	900F(24)AC	Offset Boss	Radial	197.0	184.2	2.0	7.0
20	1450F(1/2)WQ	900F(24)AC	Offset Boss	Radial	189.7	175.4	3.0	6.2
69	1450F(1/2)WQ	900F(24)AC	Mid-radius	Radial	199.1	186.4	4.0	5.4
70	1450F(1/2)WQ	900F(24)AC	Mid-radius	Radial	196.8	185.6	2.5	6.2
57	1450F(1/2)WQ	900F(24)AC	Skirt	Tang.	203.3	189.5	2.0	4.7
58	1450F(1/2)WQ	900F(24)AC	Skirt	Tang.	198.9	187.4	2.0	7.0

Table XXIII (Cont.)

Specimen No.	Solution Treatment	Age	Location	Direction	T.S.	Y.S. (0.2%)	Elong. (1")	R.A.
27	1450F(1/2)WQ	900F(36)AC	Polar Boss	Radial	155.4	144.8	4.0	12.4
28	1450F(1/2)WQ	900F(36)AC	Polar Boss	Radial	165.6	155.0	3.0	5.8
43	1450F(1/2)WQ	900F(36)AC	Polar Boss	Tang.	181.9	166.4	4.0	8.9
44	1450F(1/2)WQ	900F(36)AC	Polar Boss	Tang.	183.8	170.5	4.0	11.3
21	1450F(1/2)WQ	900F(36)AC	Offset Boss	Radial	200.9	188.4	2.0	4.3
22	1450F(1/2)WQ	900F(36)AC	Offset Boss	Radial	199.1	187.6	2.0	4.7
15	1450F(1/2)WQ	900F(36)AC	Offset Boss	Tang.	204.0	190.7	2.0	3.6
16	1450F(1/2)WQ	900F(36)AC	Offset Boss	Tang.	199.1	185.6	2.0	5.8
51	1450F(1/2)WQ	900F(36)AC	Mid-radius (top)	Radial	199.9	184.6	3.0	5.4
52	1450F(1/2)WQ	900F(36)AC	Mid-radius (top)	Radial	200.3	186.0	4.0	6.2
71	1450F(1/2)WQ	900F(36)AC	Mid-radius (bottom)	Radial	202.5	189.5	4.0	7.0
72	1450F(1/2)WQ	900F(36)AC	Mid-radius (bottom)	Radial	202.5	189.7	4.0	5.4
59	1450F(1/2)WQ	900F(36)AC	Skirt	Tang.	206.6	193.3	2.0	3.6
60	1450F(1/2)WQ	900F(36)AC	Skirt	Tang.	206.4	192.9	3.0	4.0
29	1450F(1/2)WQ	900F(48)AC	Polar Boss	Radial	175.4	162.1	4.0	8.5
30	1450F(1/2)WQ	900F(48)AC	Polar Boss	Radial	157.8	148.9	5.0	13.5
35	1450F(1/2)WQ	900F(48)AC	Polar Boss	Radial	193.3	178.5	4.0	8.9
36	1450F(1/2)WQ	900F(48)AC	Polar Boss	Radial	186.2	173.4	4.0	8.4
48	1450F(1/2)WQ	900F(48)AC	Polar Boss	Tang.	196.4	180.5	5.0	9.7
47	1450F(1/2)WQ	900F(48)AC	Polar Boss	Tang.	195.8	181.7	2.0	7.7
53	1450F(1/2)WQ	900F(48)AC	Mid-radius (top)	Radial	201.9	188.7	2.0	3.6
54	1450F(1/2)WQ	900F(48)AC	Mid-radius (top)	Radial	202.5	188.7	2.5	5.5
73	1450F(1/2)WQ	900F(48)AC	Mid-radius (top)	Radial	206.0	193.3	2.5	4.7
74	1450F(1/2)WQ	900F(48)AC	Mid-radius (top)	Radial	205.0	191.5	3.5	7.3
61	1450F(1/2)WQ	900F(48)AC	Skirt	Tang.	209.1	195.6	2.0	4.7
62	1450F(1/2)WQ	900F(48)AC	Skirt	Tang.	211.5	195.4	3.0	4.7

TABLE XXIV

Tensile Properties (70F) of Full Scale 40-Inch Diameter Press-Forged Front Dome EJO-1 After Solution Treatment At 1800F and Either Brine Or Water Quenching

Solution Treatment	T.S.	Y.S. (0.2%)	Y.S. (0.02%)	Elong. 1"	R.A.
1800F (1/12)BQ*	135.4 KSI	128.5 KSI	119.0 KSI	16.5%	43.0%
1800F (1/12)BQ*	134.8	129.7	120.5	20.0	52.5
1800F (1/12)BQ*	194.2	Notched K_t=8			
1800F (1/12)BQ*	196.5	Notched K_t=8			
1800F (1/4)BQ	130.5	129.8	122.4	20.0	44.5
1800F (1/4)BQ	134.1	130.0	119.8	17.0	43.0
1800F (1/4)BQ	159.4	Notched K_t=8			
1800F (1/4)BQ	129.2***	Notched K_t=8			
1800F (1/12)WQ**	137.2	123.6	118.5	17.0	48.5
1800F (1/12)WQ**	138.0	127.5	118.3	14.0	38.0
1800F (1/12)WQ**	203.5	Notched K_t=8			
1800F (1/12)WQ**	205.2	Notched K_t=8			
1800F (1/4)WQ	132.3	129.6	125.3	19.0	47.5
1800F (1/4)WQ	132.5	124.5	122.5	21.0	54.7
1800F (1/4)WQ	180.7	Notched K_t=8			
1800F (1/4)WQ	194.0				

*10 per cent brine quench
**water quench
***specimen was cracked longitudinally prior to test apparently due to severity of quench

TABLE XXV

Pratt & Whitney Aircraft Tensile Properties (70F) of Hammer-Forged Pancake No. 4 Upset In Three Operations With An Intermediate Recrystallization Treatment

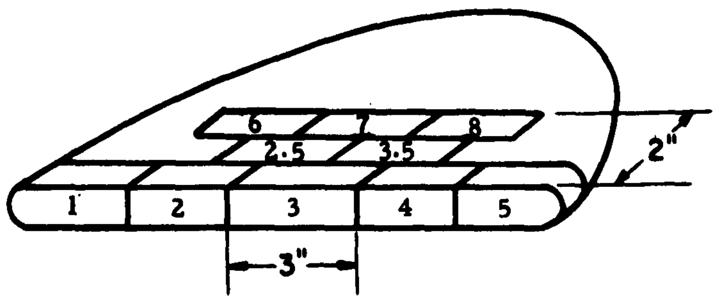

Location	Age	T.S.	Y.S. (0.2%)	Elong.(1")	R.A.
1	900F(60)AC	212.0 ksi	186.8 ksi	2.5%	5.0%
2	900F(60)AC	198.8	184.5	2.5	8.0
3	900F(60)AC	180.7	165.6	2.5	7.0
4	900F(60)AC	201.0	184.5	2.5	6.0
5	900F(60)AC	197.2	181.5	2.2	5.5
2.5	900F(60)AC	199.4	182.0	1.5	6.0
3.5	900F(60)AC	202.5	184	2.5	4.5
6	900F(60)AC	207.5	188.0	1.5	4.0
7	900F(60)AC	203.5	185.8	1.5	6.0
8	900F(60)AC	208.0	189.8	3.5	5.0

TABLE XXVI

Axial Tensile Properties (70F) of Subscale 14-Inch Diameter Flow-Turned Cylinders Nos. 1, 2 and 3 After Solution Treatment at 1400F and Aging at 900F

Solution Treatment	Age	Cylinder No.	T.S.	Y.S.(0.2%)	Y.S. (0.02%)	(1") Elong.
1400F(1/2)WQ	None	1	136.5 ksi	130.8 ksi	123.8 ksi	20.0%
1400F(1/2)WQ	900F(48)AC	1	171.5	155.3	144.0	11.0
1400F(1/2)WQ	900F(72)AC	1	180.0	164.5	156.7	11.0
1400F(1/2)WQ	900F(96)AC	1	193.2	173.8	162.2	8.0
1400F(1/2)WQ	None	2	136.2	131.9	126.2	18.0
1400F(1/2)WQ	900F(48)AC	2	164.0	148.7	140.5	11.0
1400F(1/2)WQ	900F(72)AC	2	189.7	170.0	154.9	10.0
1400F(1/2)WQ	900F(96)AC	2	198.6	180.0	167.3	7.0
1400F(1/2)WQ	None	3	145.5	140.9	134.0	18.0
1400F(1/2)WQ	900F(48)AC	3	180.2	169.5	159.0	11.0
1400F(1/2)WQ	900F(72)AC	3	193.8	174.0	163.9	9.0
1400F(1/2)WQ	900F(96)AC	3	211.5	187.4	174.2	8.0

TABLE XXVII

Circumferential Tensile Properties (70F) of Subscale 14-Inch Diameter Flow-Turned Cylinder No. 4 After Aging At 900F

Age	T.S.	Y.S. (0.2%)	Y.S. (0.02%)	Elong (1")	NTS (K_t=8)
900F(3)AC	215.0 ksi	198.0 ksi	181.0 ksi	4.0%	137.5 ksi
900F(3)AC	204.0	194.0	176.1	4.0	135.8
900F(5)AC	222.0	210.0	142.7	4.5	131.8
900F(5)AC	228.0	214.0	146.5	5.0	118.4

TABLE XXVIII

Rolling Sequence for Ten Subscale 14-Inch Diameter Rings

Ring No.	Pass No.	Temperature Furnace	Temperature Finish	Approximate Reduction
1	1	1900F	1610F	48.0%
2	1	1900	1650	11.0
2	2	1900	--	33.0
3	1	1900	1710	5.0
3	2	1900	--	41.0
4	1	1900	1750	10.0
4	2	1900	--	33.0
5	1	1900	1620	48.0
6	1	1900	1630	48.0
7	1	1900	1650	48.0
8	1	1900	1650	48.0
9	1	1900	1620	48.0
10	1	1900	1660	48.0

TABLE XXIX

Ladish Tensile Properties (70F) of Subscale 14-Inch Diameter Rolled Ring Test Material After Various Solution Treatments

Solution Treatment	Ring No.	T.S.	Y.S. (0.2%)	Elong. (1")	R.A.
1450F(1/4)WQ	1	135.6 ksi	127.4 ksi	11.0%	26.0%
1450F(1/4)WQ	1	134.8	128.0	12.0	24.0
1450F(1/4)WQ	2	136.0	128.6	9.0	20.0
1450F(1/4)WQ	2	136.8	129.6	9.5	21.0
1450F(1/4)WQ	3	135.2	128.4	14.0	29.0
1450F(1/4)WQ	3	135.6	129.8	15.5	27.0
1450F(1/4)WQ	4	133.2	131.6	12.0	26.0
1450F(1/4)WQ	4	131.8	130.4	13.0	29.5
1450F(1/4)WQ	5	134.8	132.5	12.5	27.8
1450F(1/4)WQ	5	136.0	129.8	17.0	30.0
1450F(1/4)WQ	6	134.2	127.6	11.0	23.5
1450F(1/4)WQ	6	133.5	130.2	10.0	25.7
1450F(1/4)WQ	7	135.2	126.4	15.0	23.9
1450F(1/4)WQ	7	134.5	126.3	13.5	25.8
1450F(1/4)WQ	8	132.0	131.2	11.0	24.9
1450F(1/4)WQ	8	134.3	131.9	11.0	24.2
1450F(1/4)WQ	9	135.0	127.2	10.0	26.5
1450F(1/4)WQ	9	135.5	133.0	12.5	26.7
1450F(1/4)WQ	10	134.6	132.4	13.0	32.8
1450F(1/4)WQ	10	136.6	128.5	13.0	32.4
1450F(1/2)WQ	4	136.0	131.6	15.0	33.0
1450F(1/2)WQ	4	136.5	130.8	16.0	32.0
1450F(1/2)WQ	9	134.6	131.4	20.0	42.0
1450F(1/2)WQ	10	136.3	131.2	18.5	40.0
1800F(1/4)WQ	9	136.7	131.8	20.0	50.0
1800F(1/4)WQ	10	136.8	131.0	20.5	52.0

TABLE XXX

Tensile Properties (70F) of Subscale 14-Inch Diameter Rolled Rings After Sizing at 1450F and Solution Treatment at 1450F for 30 Minutes

Ring	T.S.	Y.S. (0.2%)	Elong. (1")	R.A.
1	136.3 ksi	126.1 ksi	20.0%	43.0%
2	135.1	122.2	18.7	33.0
3	136.3	124.1	24.0	41.8
4	135.3	124.8	20.0	34.0
5	135.3	124.5	20.0	41.8
6	135.3	124.8	16.0	31.3
7	130.2	125.1	20.0	37.0
8	135.0	125.0	23.0	42.9
9	134.0	123.1	17.0	37.1
10	135.9	126.1	23.0	39.1

TABLE XXXI

Rolling Sequence for Seven Full Scale 40-Inch Diameter Rings

Ring No.	Pass No.	Mandrel Diameter	Temperature* Start	Temperature* Finish	Finish Dimensions Inside Diameter	Finish Dimensions Wall Thickness	Reduction
1**	1	5"	1850F	1700F	11"	3 3/4"	6.3%
2	1	10	1850	1600	12 1/2	3 5/8	9.4
	2	8	1800	1625	16	3	17.3
	3	8	1860	1610	20	2 3/4	8.4
	4	8	1875	1560	38 3/8	1 1/2	45.5
3	1	5	1850	1300	14	3 1/4	18.8
	2	10	1860	1680	18 3/8	3	7.7
	3	8	1860	1650	21 3/4	2 3/8	20.8
	4	8	1880	1650	38 1/4	1 1/2	36.9
4	1	7	1850	1400	--	3 3/8	15.6
	2	7	1845	1500	--	2 15/32	25.9
	3	7	1845	1650	30 1/4	2	20.0
	4	8	1890	1695	38 1/4	1 1/2	33.3
5	1	7	1845	1530	--	3 3/8	15.6
	2	7	1850	1550	--	2 3/8	29.5
	3	7	1850	1530	30 3/4	2	15.8
	4	8	1890	1620	36 11/16	1 5/16	34.4
6	1	7	1845	1400	--	3 3/8	15.6
	2	7	1880	1500	--	2 5/8	22.2
	3	7	1850	1500	23 1/2	2 7/16	8.2
	4	8	1890	1695	38 1/4	1 1/2	38.5
7	1	7	1840	1510	--	3 3/8	15.6
	2	7	1810	1400	--	3 1/8	7.4
	3	7	1880	1500	20 1/2	2 1/2	20.0
	4	8	1885	1560	38 1/4	1 1/2	40.0

* Furnace temperature of 1900F; all rings water-quenched from rolls after each pass.
** Ruptured axially and circumferentially during first pass.

TABLE XXXII

Tensile Properties (70F) of Subscale 14-Inch Diameter Flow-Turned Cylinder No. 4 (Axial Direction) After Stress-Relieving at 850-900F and Aging at 700-900F

Stress-Relief	Age	T.S.	Y.S.(0.2%)	Y.S.(0.02%)	Elong. (1")
850F(1/2)AC	None	184.8 ksi	172.8 ksi	157.0 ksi	10.0%
	700F(4)AC	196.5	185.0	173.0	6.5
	700F(8)AC	197.8	183.5	163.2	4.5
	700F(12)AC	205.5	191.8	166.4	6.5
	700F(16)AC	209.5	197.8	177.0	5.5
	800F(1)AC	194.3	181.4	164.8	5.5
	800F(2)AC	198.0	186.0	169.8	5.5
	800F(4)AC	216.0	204.5	188.4	5.5
	800F(8)AC	233.5	220.5	203.5	4.5
	900F(1)AC	193.2	181.4	171.0	8.0
	900F(2)AC	207.0	193.3	175.8	6.0
	900F(4)AC	228.0	216.0	200.0	4.0
	900F(8)AC	235.0	223.0	203.5	3.5
850F(1)AC	None	187.0	175.3	158.0	6.5
	700F(4)AC	197.5	188.5	176.3	6.5
	700F(8)AC	200.0	187.8	175.8	8.5
	700F(12)AC	207.0	191.8	180.5	6.5
	700F(16)AC	210.0	195.0	176.8	6.5
	800F(1)AC	194.2	180.5	168.0	6.5
	800F(2)AC	202.5	189.3	177.0	6.5
	800F(4)AC	201.5	190.0	173.6	5.0
	800F(8)AC	224.0	201.0	190.0	2.5
850F(1)AC	900F(1)AC	199.0	189.2	176.0	6.5
	900F(2)AC	208.5	198.0	187.0	6.0
	900F(4)AC	226.5	213.0	193.0	4.0
	900F(8)AC	236.0	222.0	205.0	4.0
900F(1)AC	None	182.0	170.0	158.0	8.5
	700F(4)AC	183.3	173.5	163.3	8.5
	700F(8)AC	186.0	175.6	166.0	8.5
	700(12)AC	189.0	178.8	169.0	8.5
	700F(16)AC	193.8	182.2	167.0	6.0
	800F(1)AC	187.0	171.0	161.0	8.5
	800F(2)AC	189.4	176.0	167.4	8.5
	800F(4)AC	198.8	183.2	171.3	4.5
	800F(8)AC	206.5	190.8	177.4	6.5
	900F(1)AC	194.8	180.5	169.7	6.5
	900F(2)AC	201.5	187.4	177.3	5.0
	900F(4)AC	203.0	189.3	176.0	6.5
	900F(8)AC	218.0	198.5	181.8	6.0

TABLE XXXIII

Smooth and Notched (K_t=8) Tensile Properties (70F) of Subscale 14-Inch Diameter B-120VCA Flow-Turned Cylinder No. 4

Stress-Relief	Age	T.S.	Y.S. (0.2%)	Elong. (1")	N.T.S. (K_t=8)
850F(1/2)AC	700F(11)AC	196.0 ksi	187.3 ksi	8.0%	162.3 ksi
850F(1/2)AC	700F(11)AC	198.0	186.3	8.0	160.0
850F(1/2)AC	800F(2.5)AC	195.7	187.4	6.5	168.1
850F(1/2)AC	800F(2.5)AC	196.0	187.7	7.5	164.5
850F(1/2)AC	900F(1.5)AC	197.4	188.0	9.5	135.6
850F(1/2)AC	900F(1.5)AC	201.0	192.0	6.5	160.8
850F(1)AC	800F(3)AC	197.3	185.3	5.5	153.3
850F(1)AC	800F(3)AC	204.0	185.7	6.5	149.2
900F(1)AC	700F(18)AC	193.8	187.0	8.0	164.2
900F(1)AC	700F(18)AC	194.0	183.5	8.0	136.3
900F(1)AC	800F(7)AC	203.0	193.2	5.5	138.0
900F(1)AC	800F(7)AC	198.0	190.6	5.5	144.5
900F(1)AC	900F(3.5)AC	220.0	207.0	5.5	128.0
900F(1)AC	900F(3.5)AC	221.5	209.0	5.5	122.3

TABLE XXXIV

Flow-Turning Parameters and Dimensions of Subscale 9.4-Inch Diameter Cylinders
(Rolled and Welded 0.375 Plate Stock)

Cylinder No.	Inside Diameter Before Flow-Turning	Wall Thickness Before Flow-Turning	First Flow-Turn Pass: Mandrel Speed	First Flow-Turn Pass: Roller Feed inches/min/roller	First Flow-Turn Pass: Reduction	First Flow-Turn Pass: Wall Thickness	First Flow-Turn Pass: Inside Diameter	Second Flow-Turn Pass: Mandrel Speed	Second Flow-Turn Pass: Roller Feed inches/min/roller	Second Flow-Turn Pass: Reduction	Second Flow-Turn Pass: Wall Thickness	Second Flow-Turn Pass: Inside Diameter
1	9.408	.300"	320 rpm	5	25%	*						
2	9.408	.280	280	3 1/2	38	*						
3	9.406	.232	280	3 1/2	44	.127-.132	9.437	280	3 1/2	63%	048	9.451
4	9.408	.225	280	3 1/2	42	.127-.132	9.443	280	3 1/2	54	.060	9.480
5	9.411	.300	315	4 1/2	25	*						
6	9.408	.267	280	4 1/2	42	.155	9.442	280	4 1/2	60	.062	9.449
7	9.404	.230	300	6	43.5	.127-.130	9.425	300	6	43	.074	9.413
8	9.408	.300	300	6	38.3	.182-.187	9.430	300	4 1/2	69	.057	9.425

*Failed during first pass.

APPENDIX B

Figures

STRESS ANALYSIS FOR VARIOUS LOCATIONS ON WIDE BIAXIAL TENSILE SPECIMEN SHOWING BIAXIAL STRESS RATIOS IN ELASTIC AND PLASTIC REGIONS

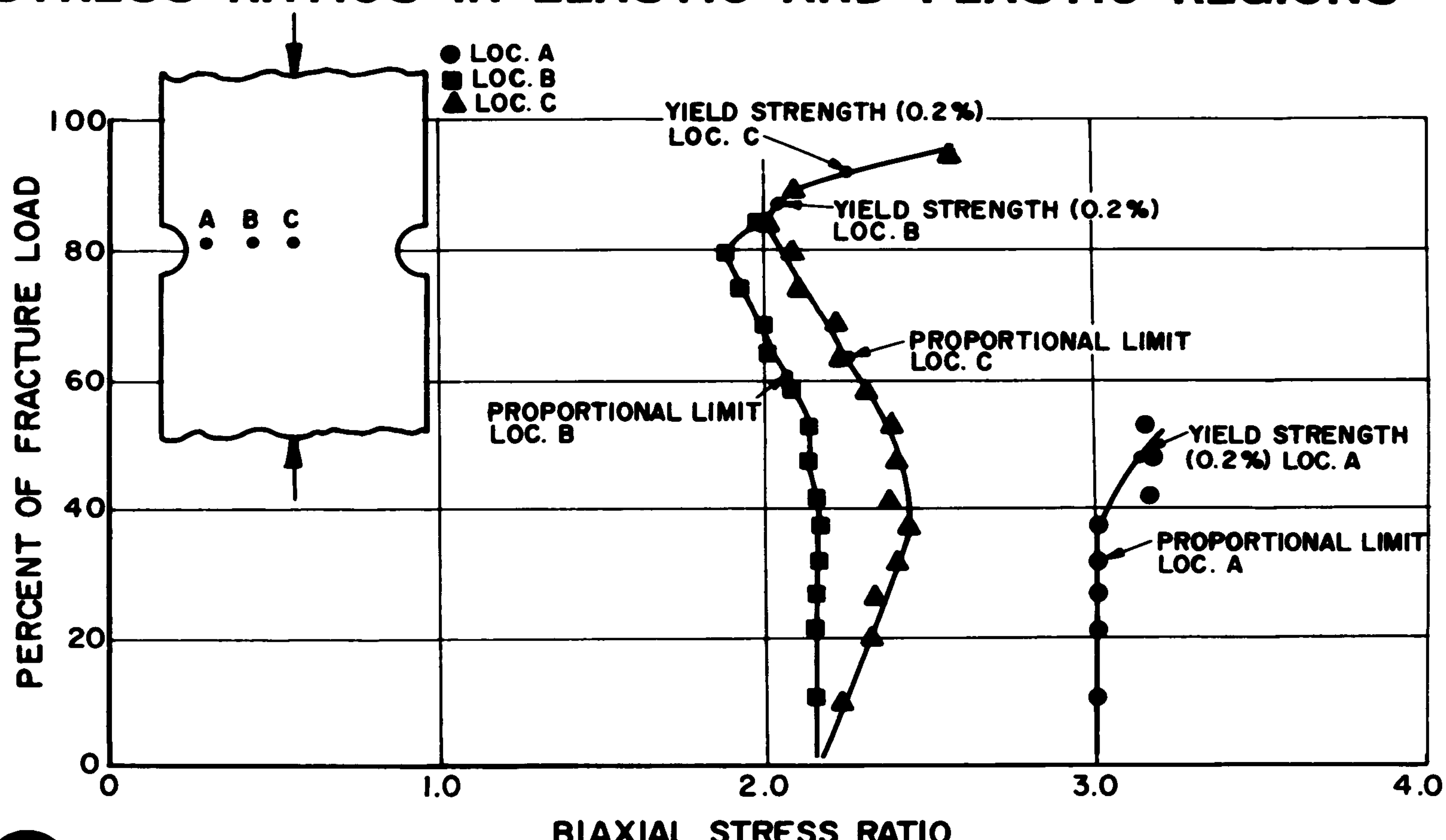

PRATT & WHITNEY AIRCRAFT
DIVISION OF
UNITED AIRCRAFT CORPORATION

Figure 1

ETCHANT: 5% HF, 35% HNO_3 MAG: 10X

MACROSTRUCTURE OF TYPICAL TIG WELD MADE USING THE IMPROVED COPPER FIXTURING TECHNIQUE. HARDNESS DATA (ROCKWELL C SCALE) SHOWN ABOVE

H-23879

Figure 2

ETCHANT: 5% HF, 35% HNO_3 MAG: 100X

TYPICAL MICROSTRUCTURE OF TIG WELD MADE USING THE IMPROVED COPPER FIXTURING TECHNIQUE

H-23949-31

Figure 3

ETCHANT: 5% HF, 35% HNO_3 MAG: 500X
TYPICAL MICROSTRUCTURE OF TIG WELD MADE USING THE IMPROVED
COPPER FIXTURING TECHNIQUE

H-23949-32

Figure 4

HARDNESS TRAVERSE FROM WELD CENTER OF TIG WELD MADE USING THE IMPROVED COPPER-FIXTURING TECHNIQUE

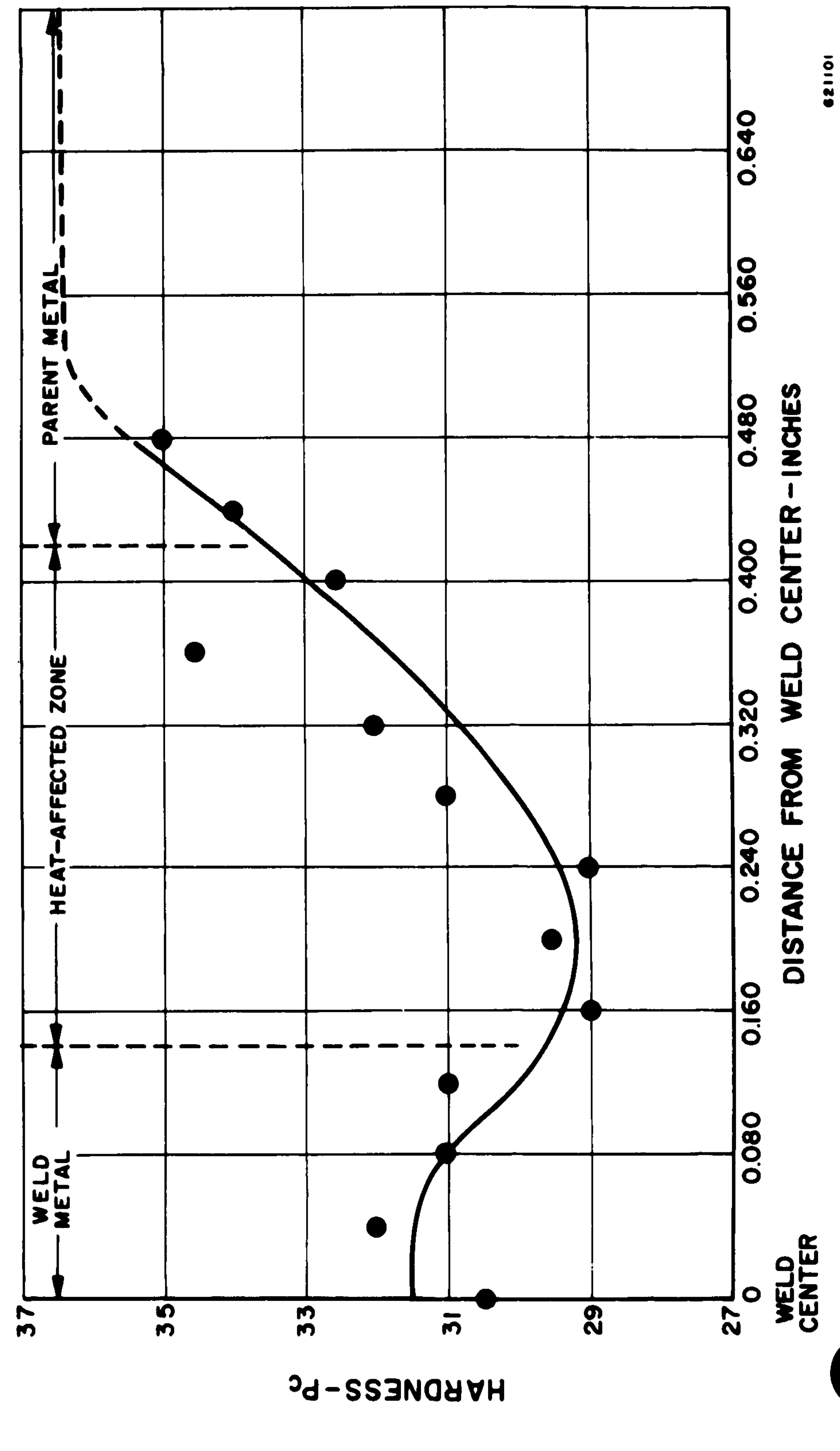

PRATT & WHITNEY AIRCRAFT
DIVISION OF
UNITED AIRCRAFT CORPORATION

Figure 5

ETCHANT: 5% HF, 35% HNO_3 MAG: 10X
MACROSTRUCTURE OF MANUAL TIG WELD MADE WITH PURE VANADIUM FILLER MATERIAL AND ARGON TORCH GAS ATMOSPHERE. HARDNESS DATA (ROCKWELL C SCALE) SHOWN ABOVE

H-23877

Figure 6

ETCHANT: 5% HF, 35% HNO_3 MAG: 10X
MACROSTRUCTURE OF MANUAL TIG WELD MADE WITH PURE VANADIUM FILLER MATERIAL AND HELIUM TORCH GAS ATMOSPHERE. HARDNESS DATA (ROCKWELL C SCALE) SHOWN ABOVE

H-23876

Figure 7

ETCHANT: 5% HF, 35% HNO_3 MAG: 10X
MACROSTRUCTURE OF MANUAL TIG WELD MADE WITH PURE VANADIUM FILLER MATERIAL AND HELIUM TORCH GAS ATMOSPHERE. HARDNESS DATA (ROCKWELL C SCALE) SHOWN ABOVE

H-23878

Figure 8

CYCLIC TEST SPECIMEN EMPLOYED FOR EVALUATION OF TIG AND ELECTRON BEAM WELDS

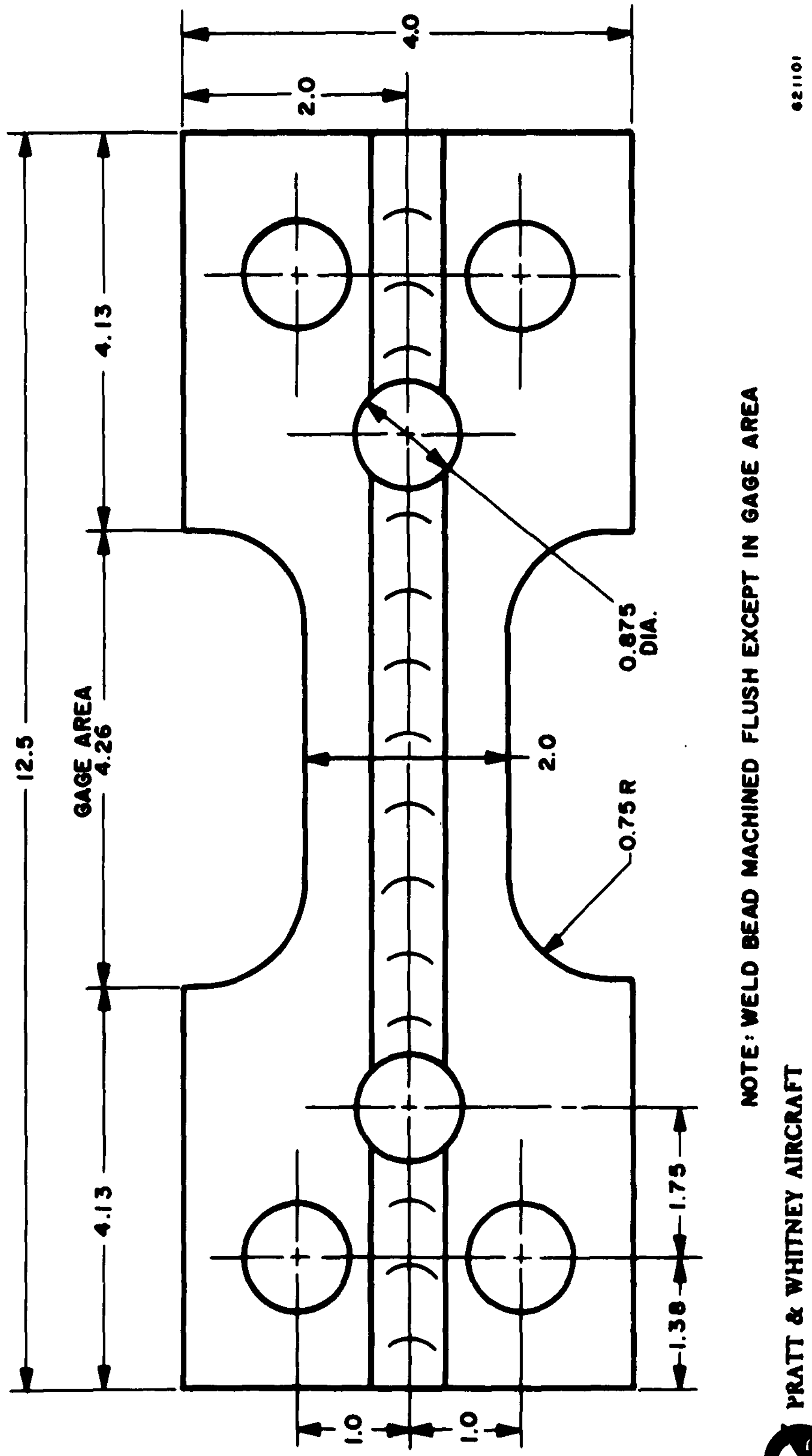

NOTE: WELD BEAD MACHINED FLUSH EXCEPT IN GAGE AREA

PRATT & WHITNEY AIRCRAFT
DIVISION OF
UNITED AIRCRAFT CORPORATION

Figure 9

CRACK INDICATIONS vs STRESS LEVEL FOR CYCLIC TESTS ON TIG - WELDED MATERIAL

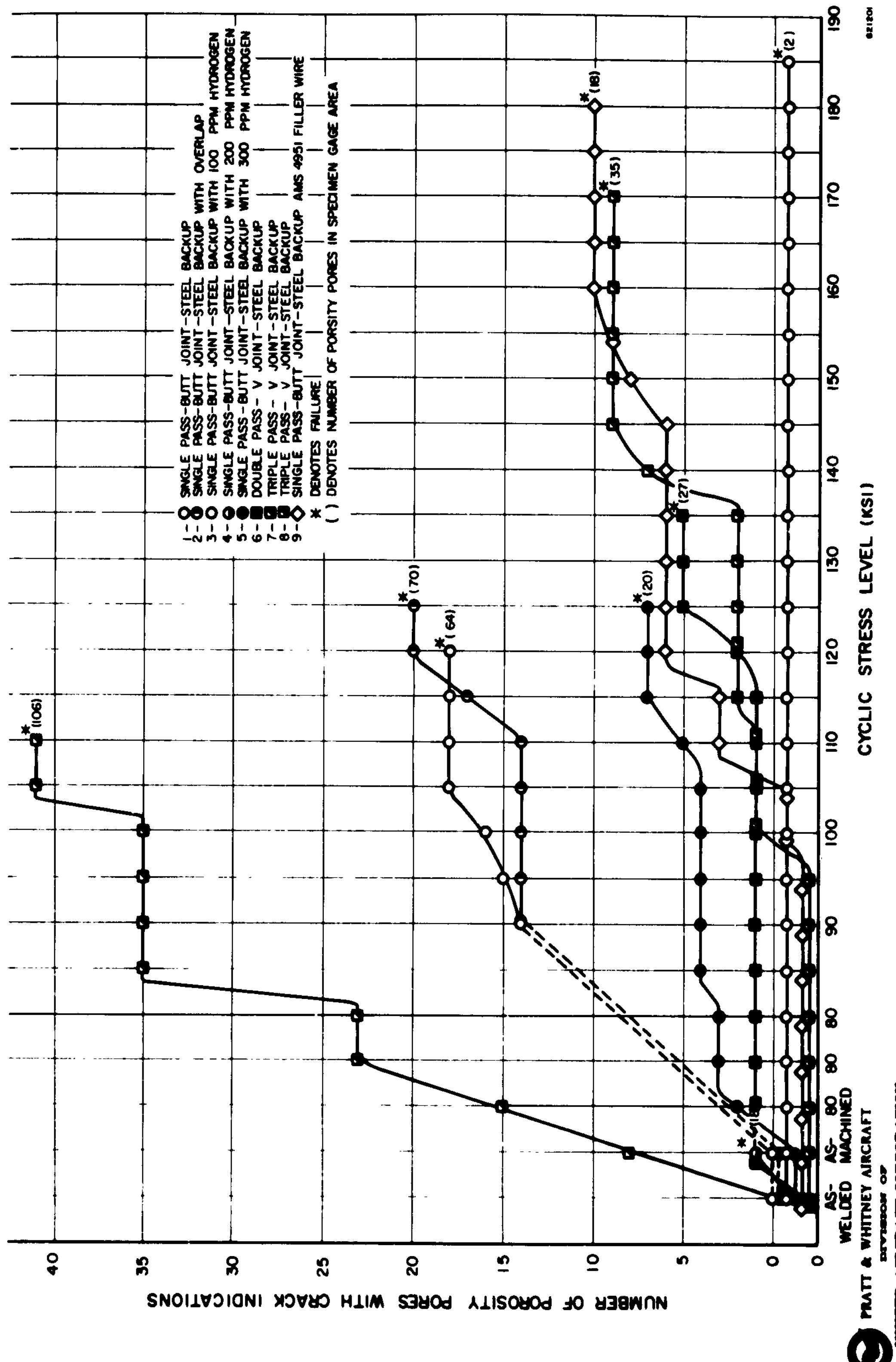

Figure 10

CYCLIC LOAD TEST RESULTS ON SINGLE-PASS TIG WELD (SQUARE BUTT JOINT) 100 PPM HYDROGEN PARENT MATERIAL (SPECIMEN NO. 3)

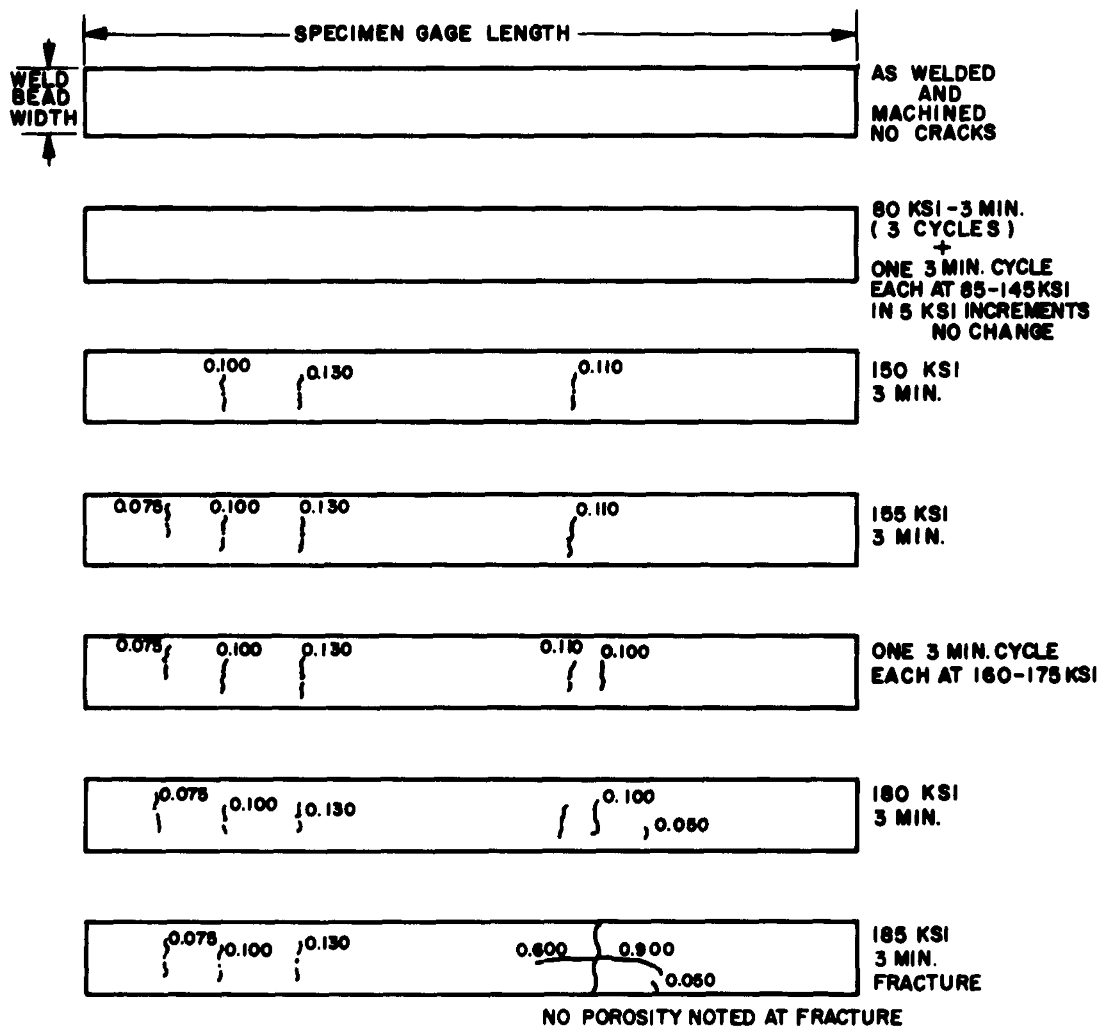

NOTE: CRACKS NOT INDICATED IF LESS THAN 0.050" IN LENGTH.

PRATT & WHITNEY AIRCRAFT
DIVISION OF
UNITED AIRCRAFT CORPORATION

62II01

Figure 11

CYCLIC LOAD TEST RESULTS ON SINGLE - PASS TIG WELD (SQUARE BUTT JOINT) 200 PPM HYDROGEN PARENT MATERIAL (SPECIMEN NO. 4)

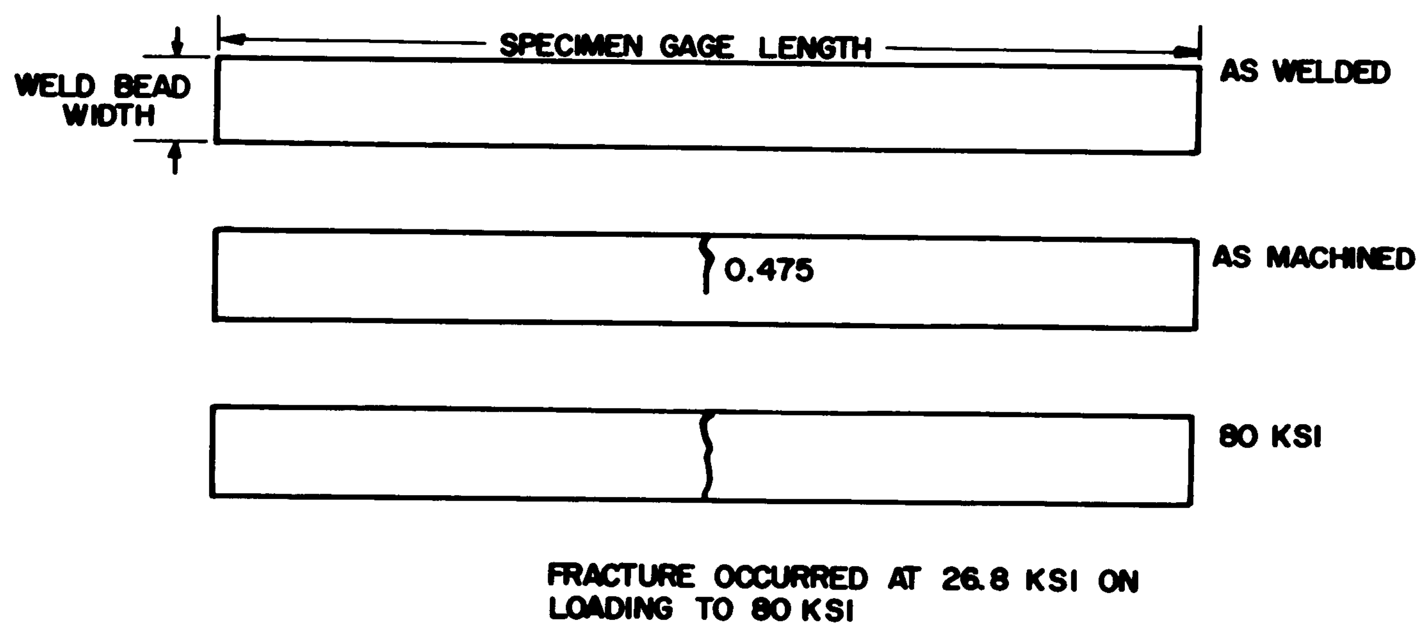

NOTE: CRACKS NOT INDICATED IF LESS THAN 0.050" IN LENGTH

PRATT & WHITNEY AIRCRAFT
DIVISION OF
UNITED AIRCRAFT CORPORATION

621201

Figure 12

CYCLIC LOAD TEST RESULTS ON SINGLE-PASS TIG WELD (SQUARE BUTT JOINT) 300 PPM HYDROGEN PARENT MATERIAL (SPECIMEN NO. 5)

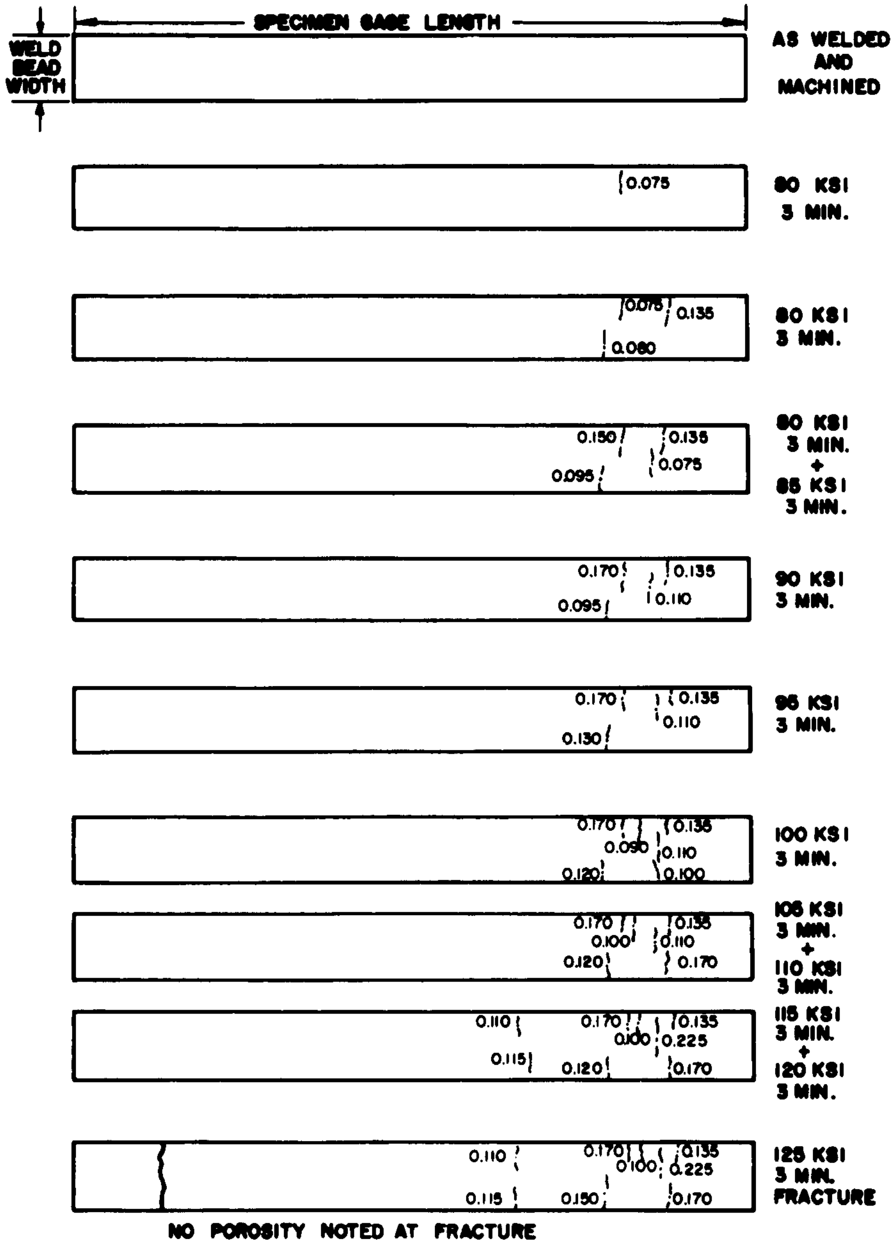

NOTE: CRACKS NOT INDICATED IF LESS THAN 0.050" IN LENGTH

PRATT & WHITNEY AIRCRAFT
DIVISION OF
UNITED AIRCRAFT CORPORATION

621201

CYCLIC LOAD TEST RESULTS ON TWO - PASS (V TYPE JOINT) TIG WELD (SPECIMEN NO. 6)

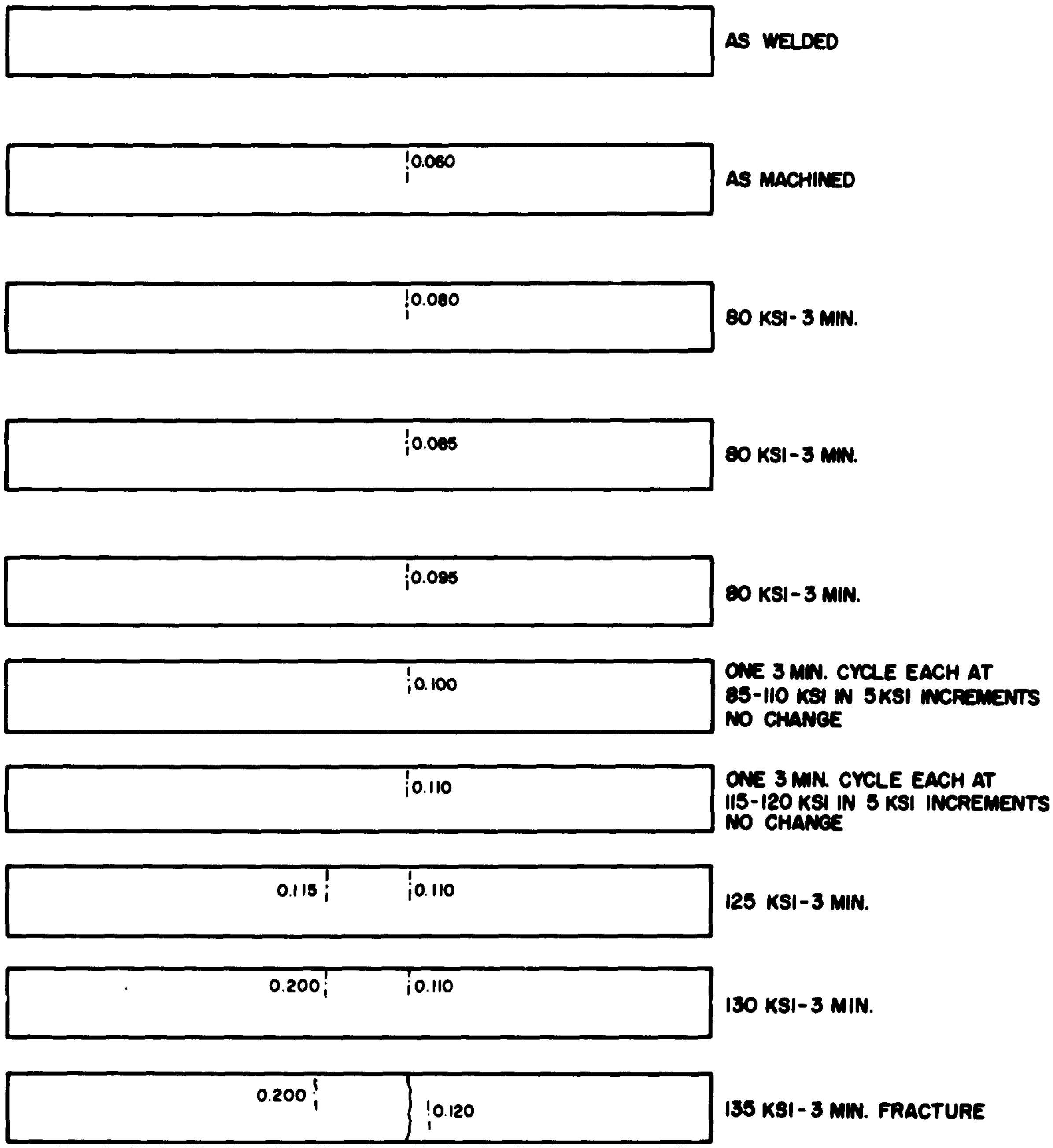

NOTE: CRACKS NOT INDICATED IF LESS THAN 0.050" IN LENGTH

621201

Figure 14

CYCLIC LOAD TEST RESULTS ON THREE - PASS (V TYPE JOINT) TIG WELD (SPECIMEN NO. 7)

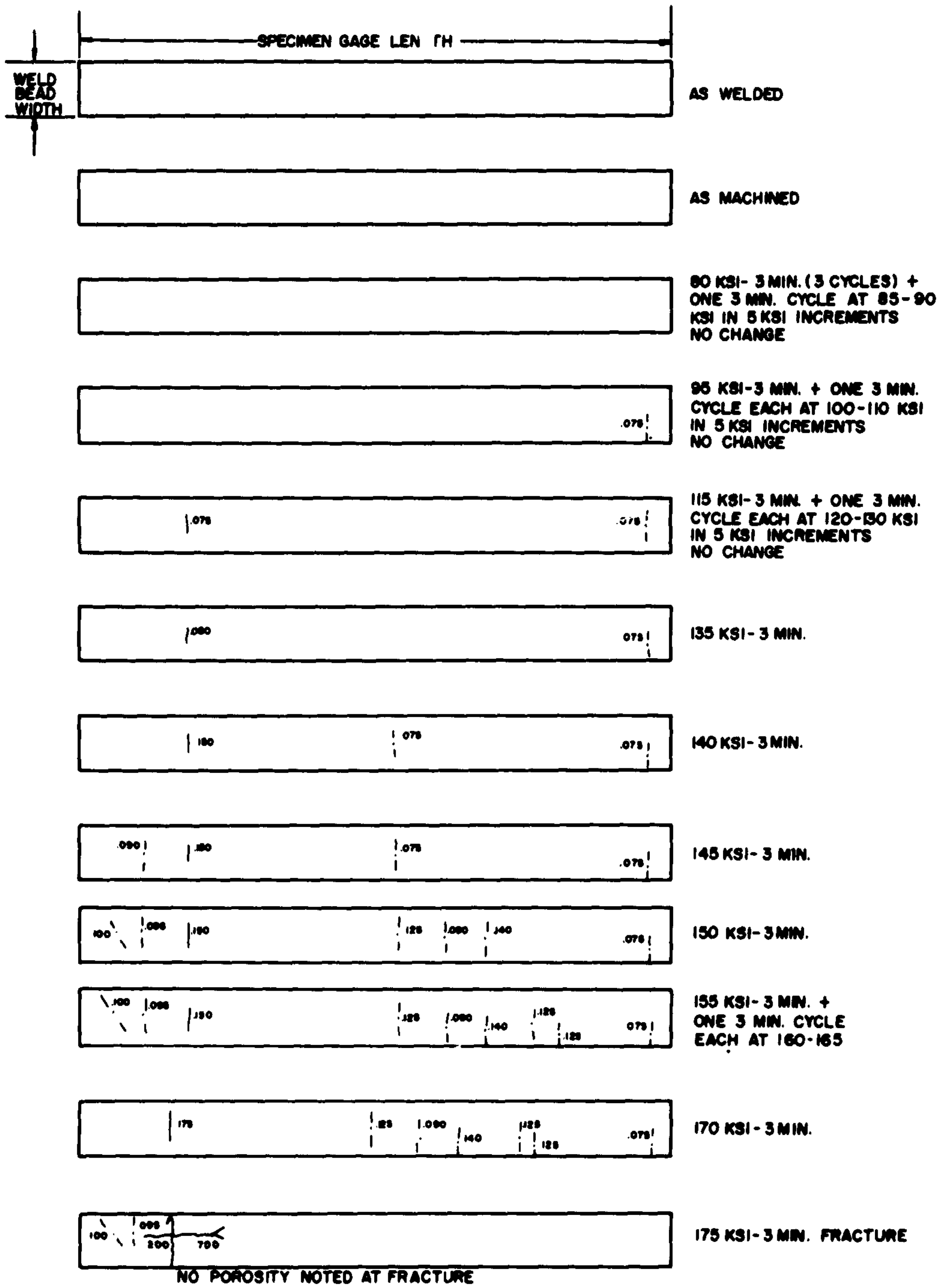

NOTE: CRACKS NOT INDICATED IF LESS THAN 0.050" IN LENGTH

Figure 15

CYCLIC LOAD TEST RESULTS ON THREE - PASS (V TYPE JOINT) TIG WELD (SPECIMEN NO. 8)

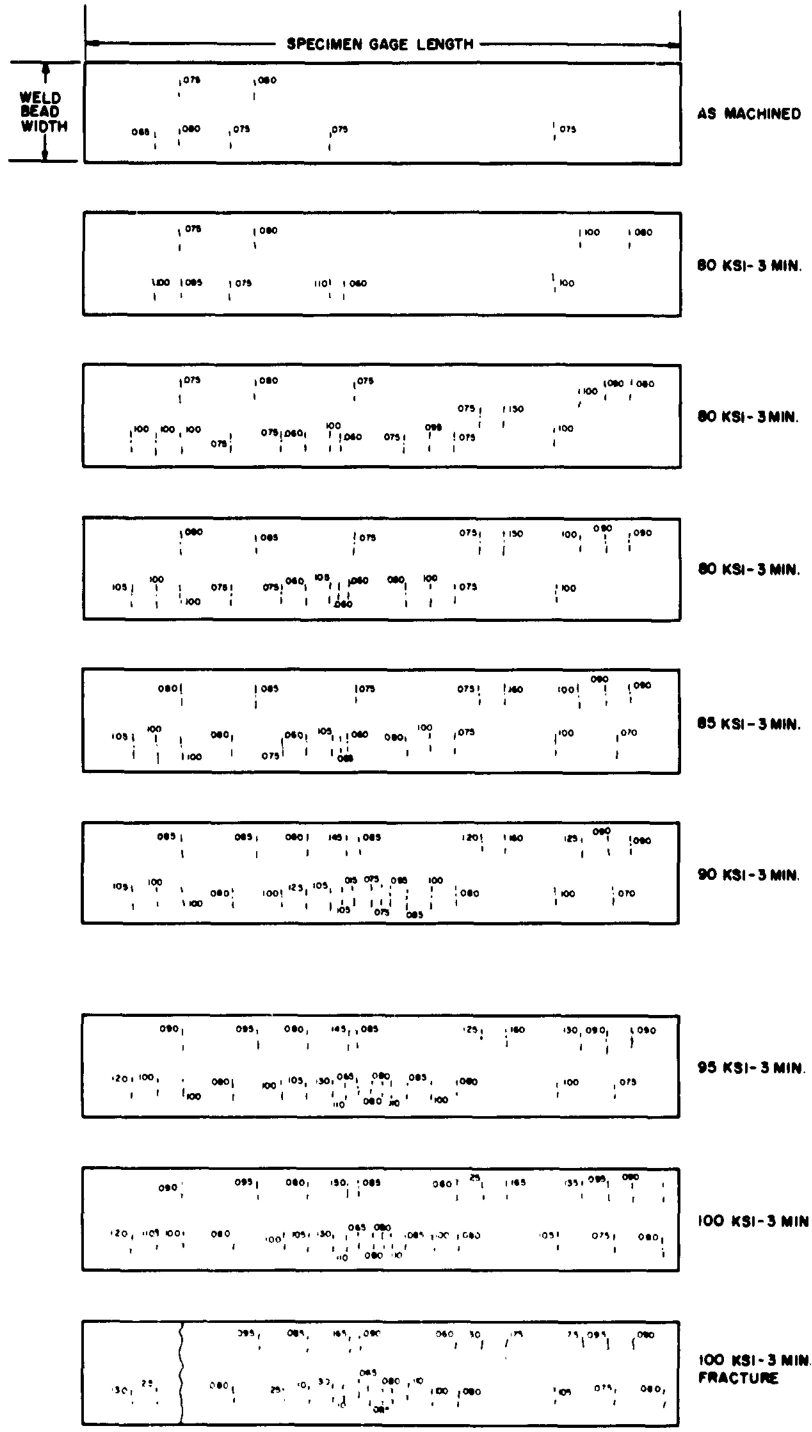

NOTE CRACKS NOT INDICATED IF LESS THAN 0.050" IN LENGTH

CYCLIC LOAD TEST RESULTS ON SINGLE - PASS TIG WELD (SQUARE BUTT JOINT WITH AMS 4951 FILLER WIRE) (SPECIMEN NO. 9)

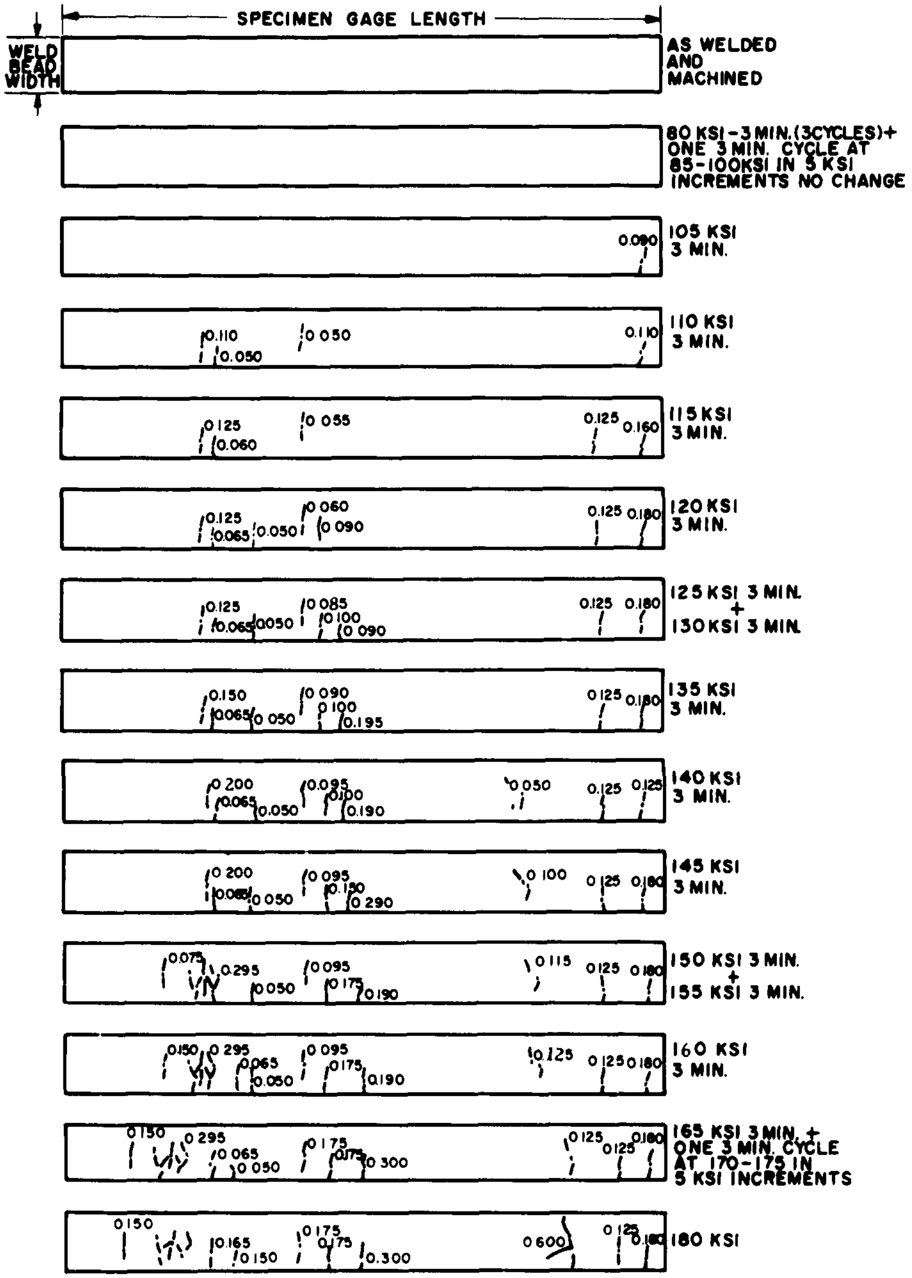

NOTE CRACKS NOT INDICATED IF LESS THAN 0.050" IN LENGTH

PRATT & WHITNEY AIRCRAFT
DIVISION OF
UNITED AIRCRAFT CORPORATION

62120

CYCLIC LOAD TEST RESULTS ON TIG WELD MADE USING IMPROVED COPPER FIXTURE TECHNIQUE (SPECIMEN NO. 10)

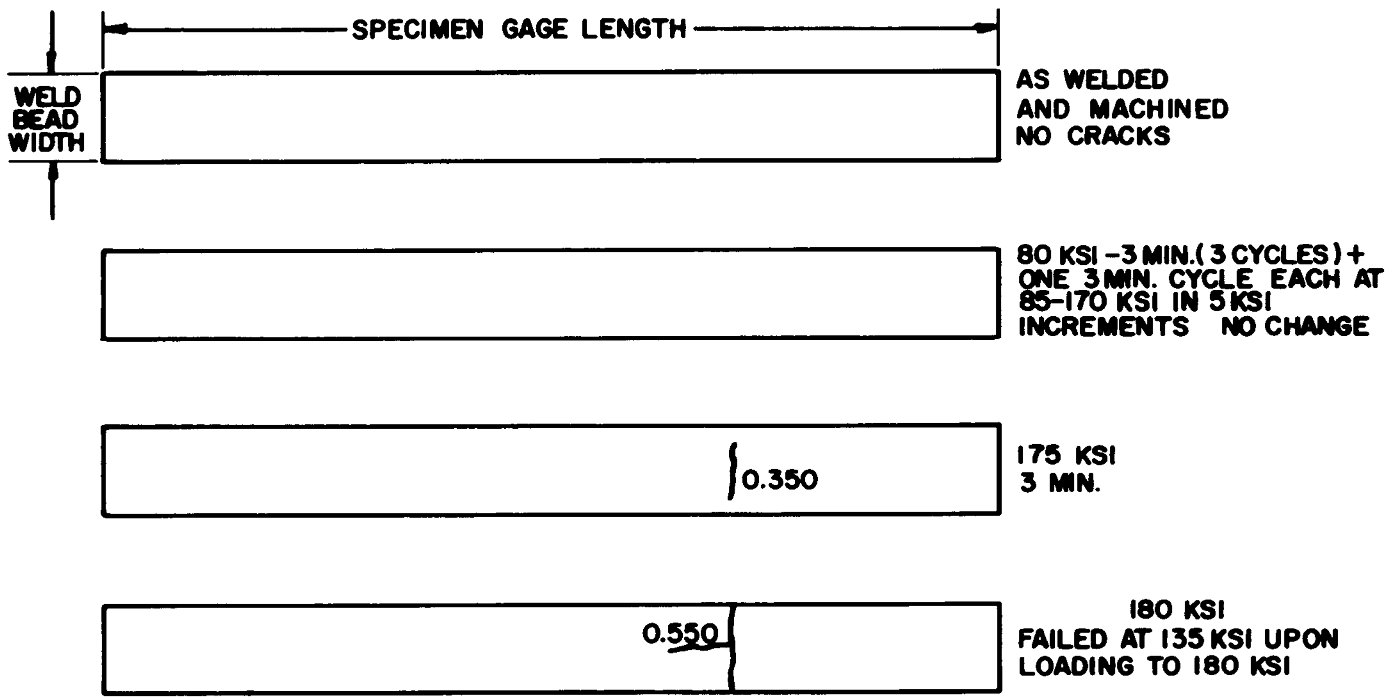

NO POROSITY NOTED AT FRACTURE

NOTE: CRACKS NOT INDICATED IF LESS THAN 0.050" IN LENGTH.

PRATT & WHITNEY AIRCRAFT
DIVISION OF
UNITED AIRCRAFT CORPORATION

621201

Figure 18

CYCLIC LOAD TEST RESULTS ON TIG WELD MADE USING IMPROVED COPPER FIXTURE TECHNIQUE (SPECIMEN NO. 11)

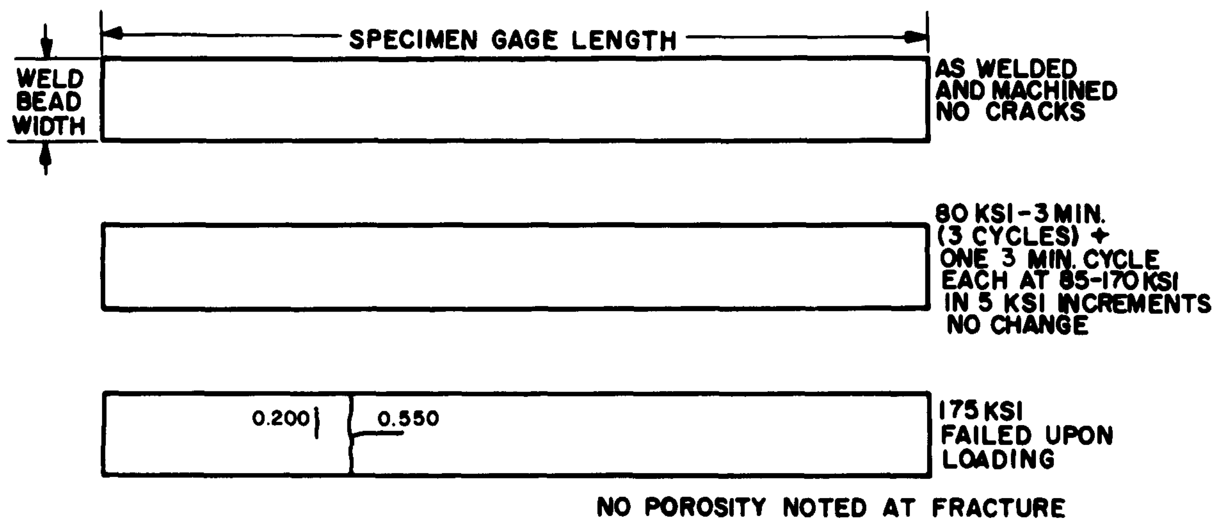

NOTE: CRACKS NOT INDICATED IF LESS THAN 0.050" IN LENGTH

PRATT & WHITNEY AIRCRAFT
DIVISION OF
UNITED AIRCRAFT CORPORATION

621201

Figure 19

CYCLIC LOAD TEST RESULTS ON SINGLE - PASS TIG WELD (NO FILLER MATERIAL, SQUARE BUTT JOINT) (SPECIMEN NO. 16)

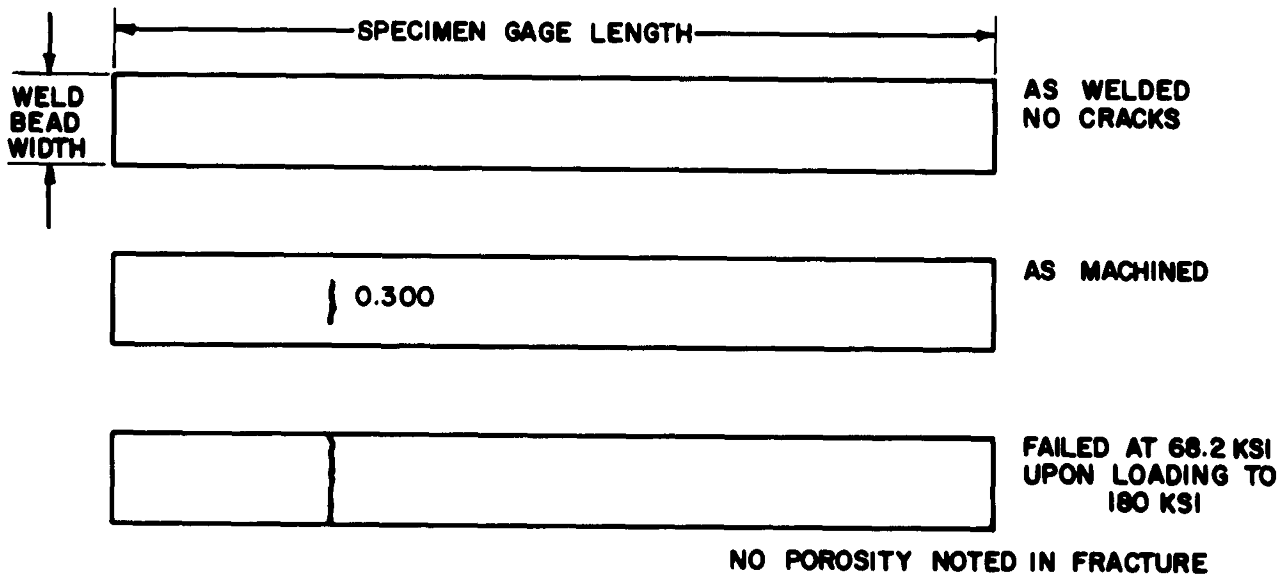

NOTE: CRACKS NOT INDICATED IF LESS THAN 0.050" IN LENGTH.

PRATT & WHITNEY AIRCRAFT
DIVISION OF
UNITED AIRCRAFT CORPORATION

62I201

Figure 20

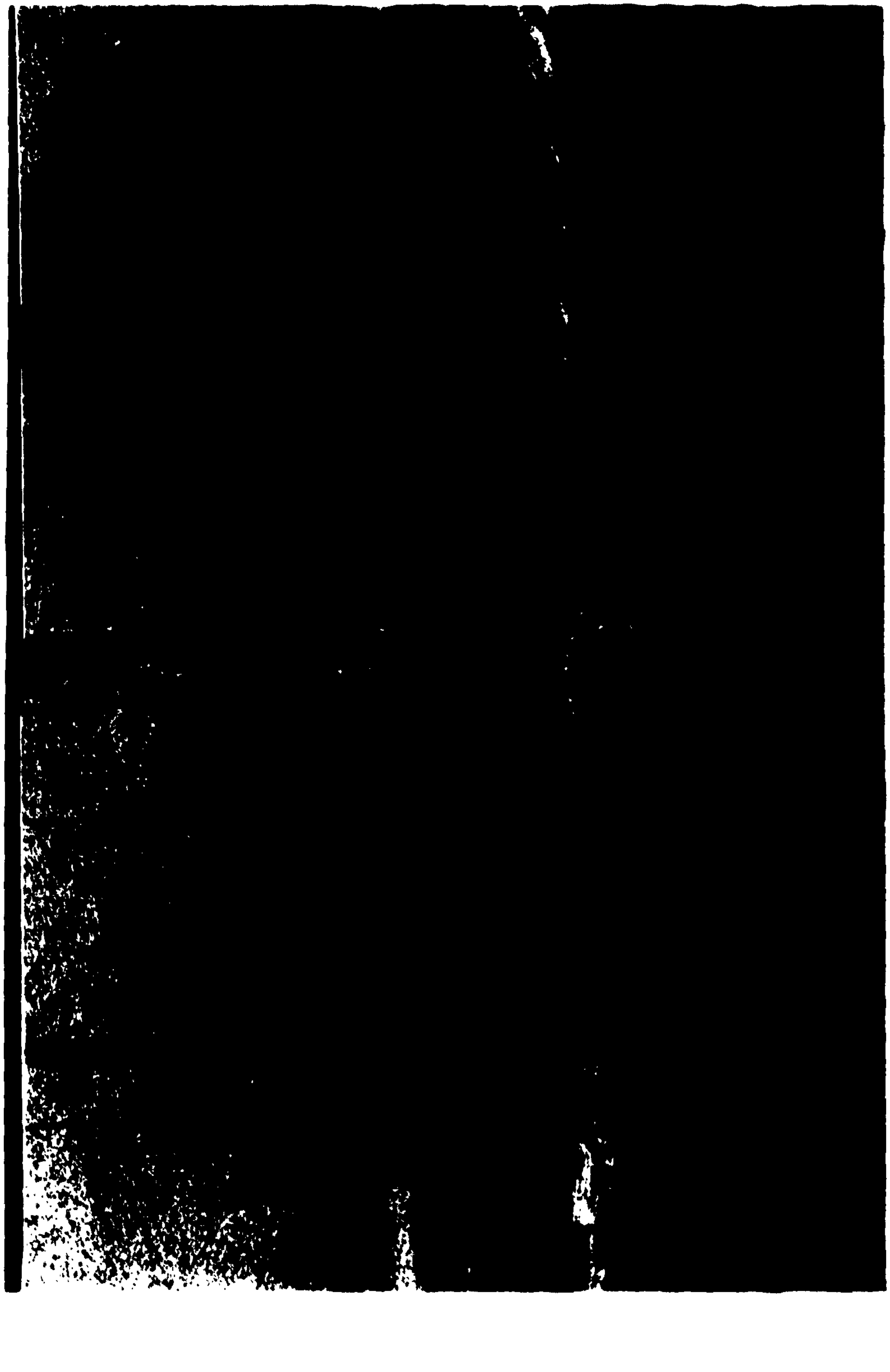

GAGE AREA SURFACE OF FAILED CYCLIC TEST SPECIMEN NO. 3 MAG: 5X
TIG-WELDED USING SHEET STOCK WITH 100 PPM OF HYDROGEN.
SPECIMEN FAILED AT 185,000 PSI THROUGH PRIOR CRACK NOT
ASSOCIATED WITH WELD POROSITY

H-25085

Figure 21

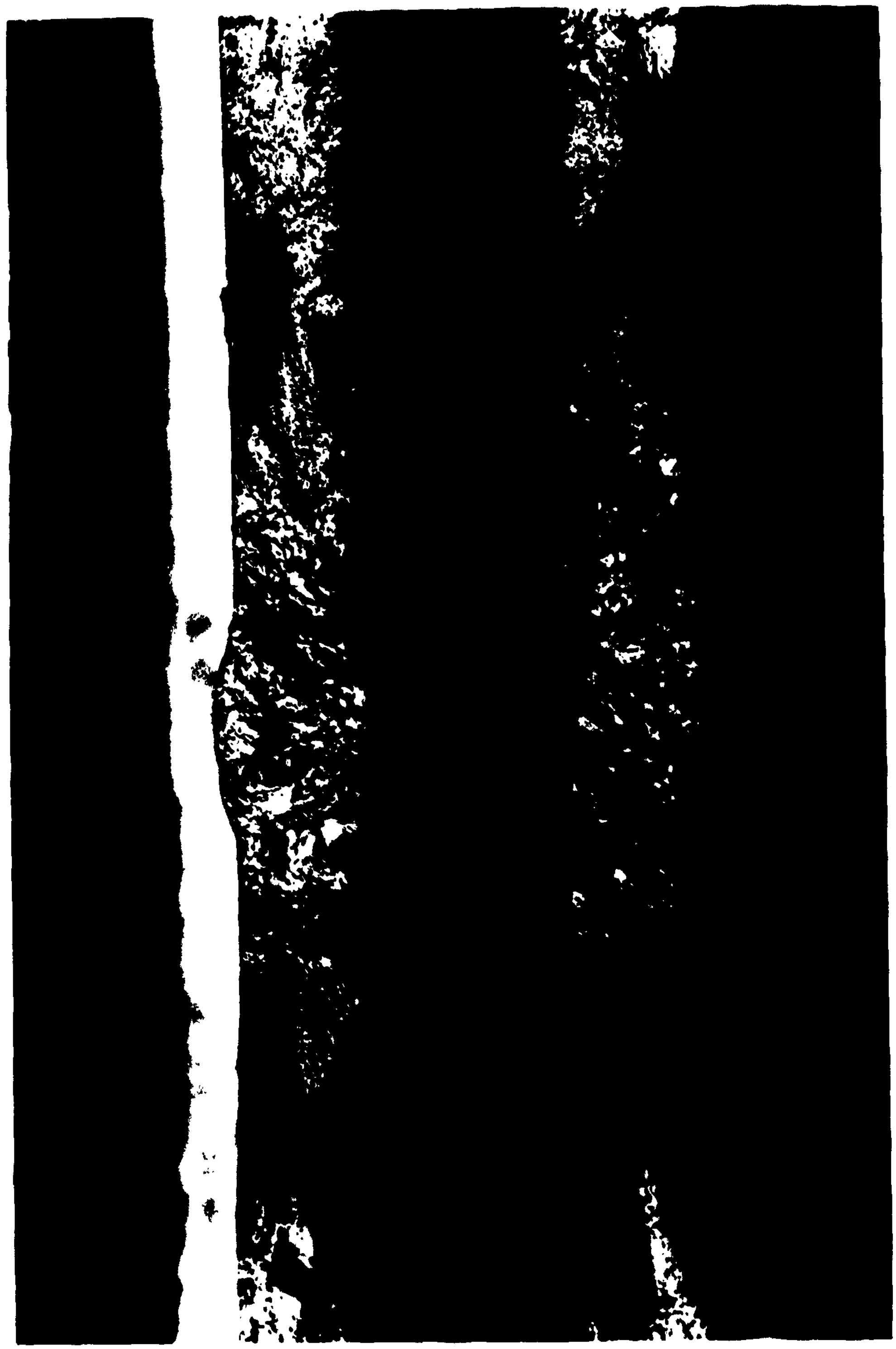

FRACTURE SURFACES OF FAILED CYCLIC TEST SPECIMEN NO. 3
TIG-WELDED USING SHEET STOCK WITH 100 PPM OF HYDROGEN.
SPECIMEN FAILED AT 185,000 PSI THROUGH PRIOR CRACK NOT
ASSOCIATED WITH WELD POROSITY

MAG: 6X

H-25088

Figure 22

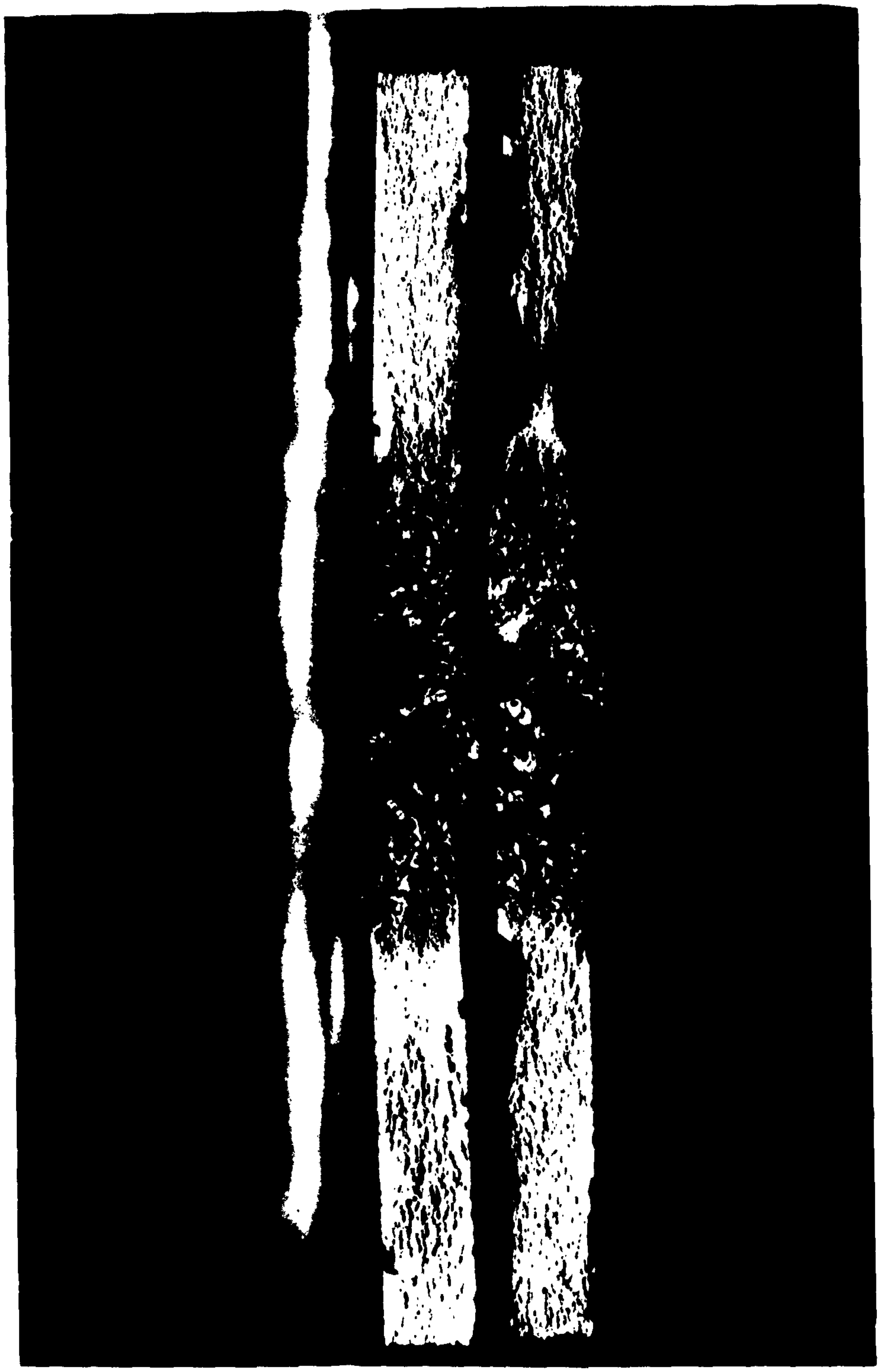

MAG: 5X

FRACTURE SURFACES OF FAILED CYCLIC TEST SPECIMEN NO. 4
TIG-WELDED USING SHEET STOCK WITH 200 PPM OF HYDROGEN.
SPECIMEN FAILED ON LOADING TO 80,000 PSI THROUGH PRIOR
CRACK NOT ASSOCIATED WITH WELD POROSITY

H-23663

Figure 23

MAG: 6X

FRACTURE SURFACES OF FAILED CYCLIC TEST SPECIMEN NO. 5
TIG-WELDED USING SHEET STOCK WITH 300 PPM OF HYDROGEN.
SPECIMEN FAILURE AT 125,000 PSI WAS NOT ASSOCIATED WITH
PRIOR CRACK OR POROSITY

H-25091

Figure 24

MAG: 6X

FRACTURE SURFACES OF FAILED CYCLIC TEST SPECIMEN NO. 6 TIG-WELDED IN TWO PASSES (V-TYPE PREPARED JOINT). SPECIMEN FAILED AT 135,000 PSI THROUGH PRIOR CRACK AT WELD POROSITY PORE (ARROWS)

H-25094

Figure 25

MAG: 5X

GAGE AREA SURFACE OF FAILED CYCLIC TEST SPECIMEN NO. 7
TIG-WELDED IN THREE PASSES (V-TYPE PREPARED JOINT). SPECIMEN
FAILED AT 170,000 PSI THROUGH PRIOR CRACK NOT ASSOCIATED
WITH WELD POROSITY. NOTE DISCONTINUITY IN WELD BEAD AT
FRACTURE

H-25087

Figure 26

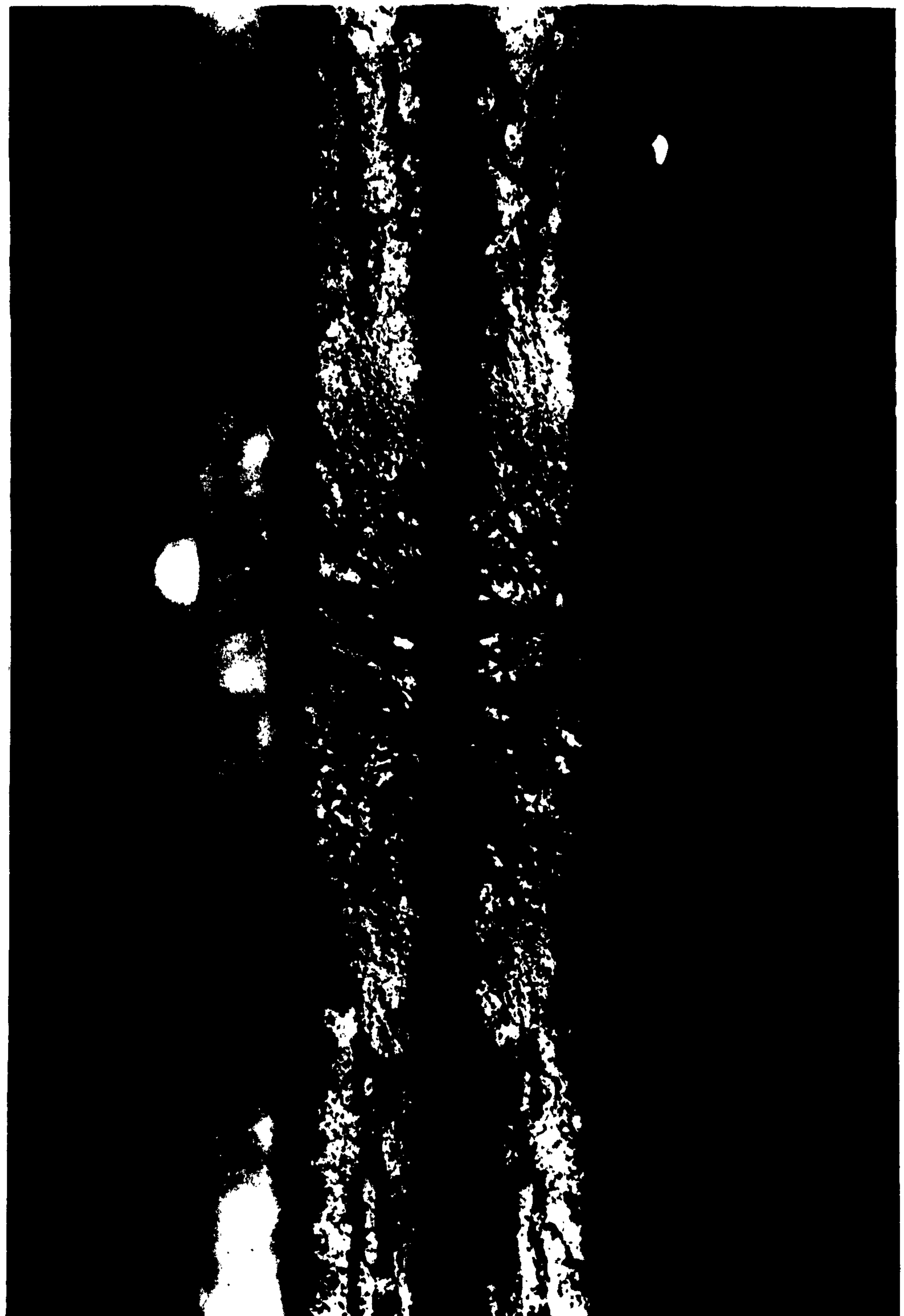

MAG: 6X

FRACTURE SURFACES OF CYCLIC TEST SPECIMEN NO. 7 TIG-WELDED IN THREE PASSES (V-TYPE PREPARED JOINT). SPECIMEN FAILED AT 170,000 PSI THROUGH PRIOR CRACK NOT ASSOCIATED WITH WELD POROSITY

H-25090

Figure 27

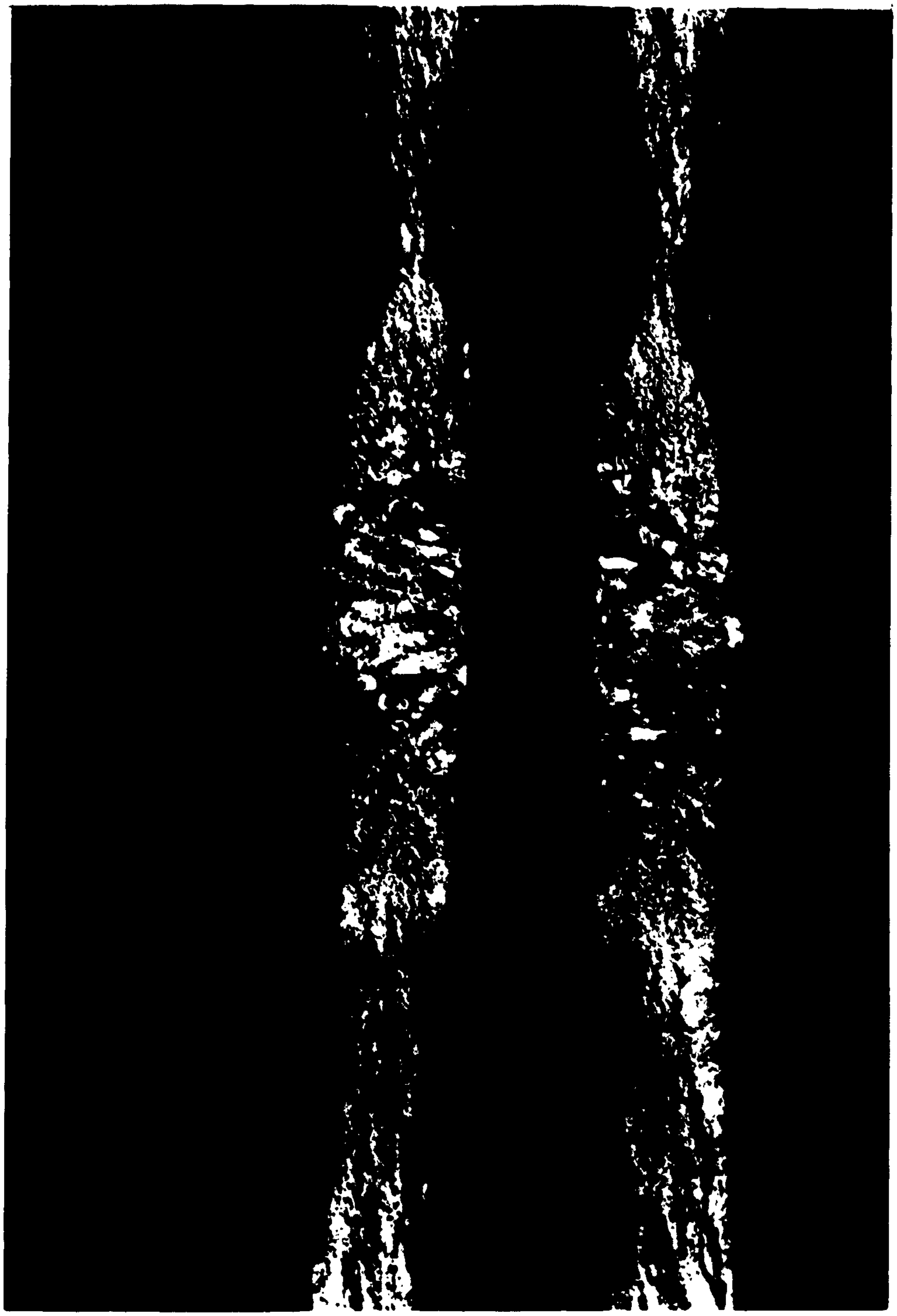

MAG: 6X

FRACTURE SURFACES OF CYCLIC TEST SPECIMEN NO. 8 TIG-WELDED IN THREE PASSES (V-TYPE PREPARED JOINT). SPECIMEN FAILED AT 110,000 PSI THROUGH PRIOR CRACK AT WELD POROSITY PORE (ARROWS)

H-25092

Figure 28

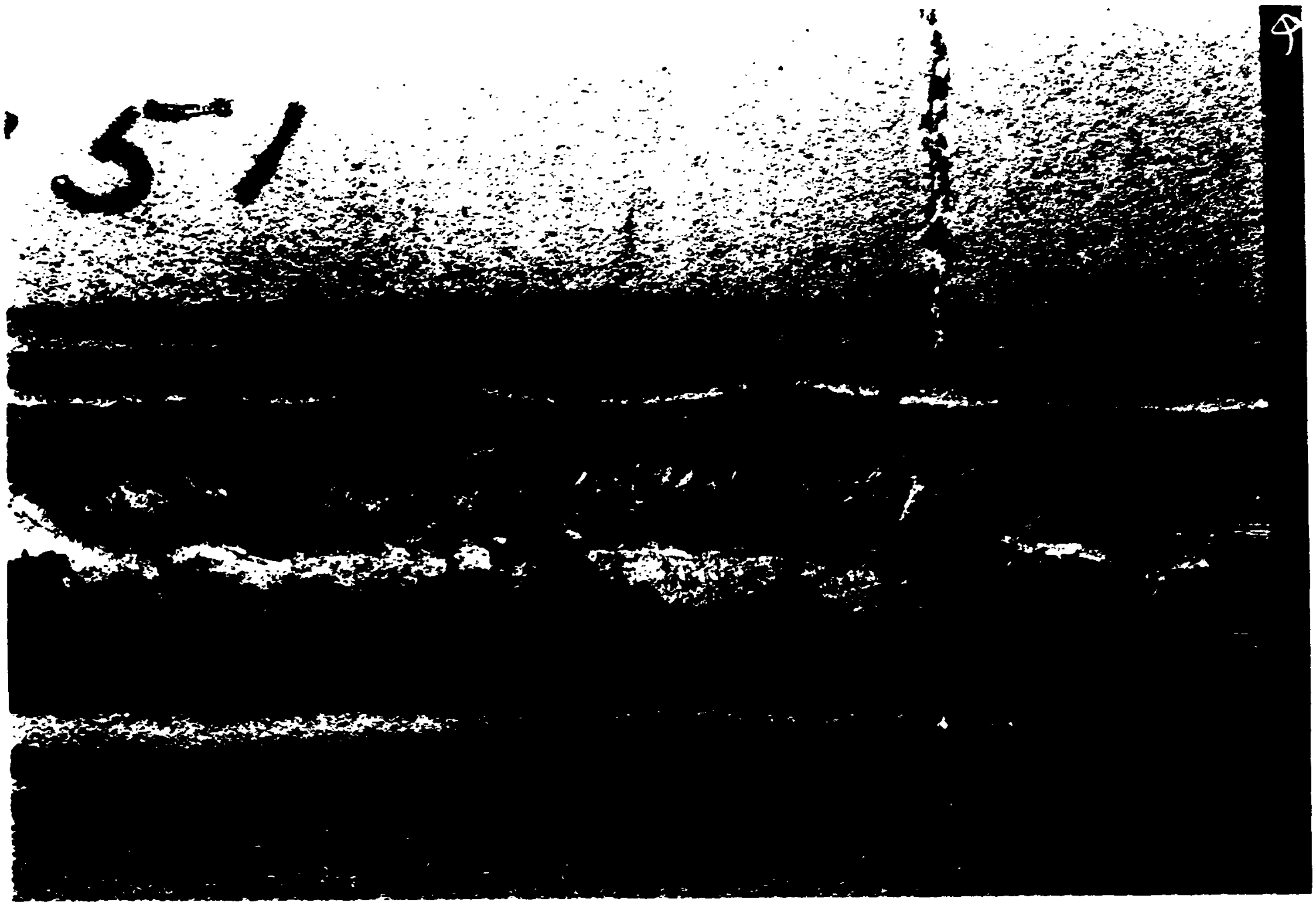

MAG: 4X

GAGE AREA SURFACE OF FAILED CYCLIC TEST SPECIMEN NO. 9 TIG-WELDED USING AMS 4951 (COMMERCIALLY PURE TITANIUM) FILLER WIRE. SPECIMEN FAILED AT 180,000 PSI THROUGH PRIOR CRACK NOT ASSOCIATED WITH WELD POROSITY

H-25086

Figure 29

FRACTURE SURFACES OF FAILED CYCLIC TEST SPECIMEN NO. 9 MAG: 6X
TIG-WELDED USING AMS 4951 (COMMERCIALLY PURE TITANIUM)
FILLER WIRE. SPECIMEN FAILED AT 180,000 PSI THROUGH PRIOR
CRACK NOT ASSOCIATED WITH WELD POROSITY

H-25089

Figure 30

MAG: 5X

GAGE AREA SURFACE OF FAILED CYCLIC TEST SPECIMEN NO. 10
TIG-WELDED USING IMPROVED COPPER FIXTURING TECHNIQUE.
SPECIMEN FAILED AT 175,000 PSI THROUGH PRIOR CRACK NOT
ASSOCIATED WITH WELD POROSITY

H-25597

Figure 31

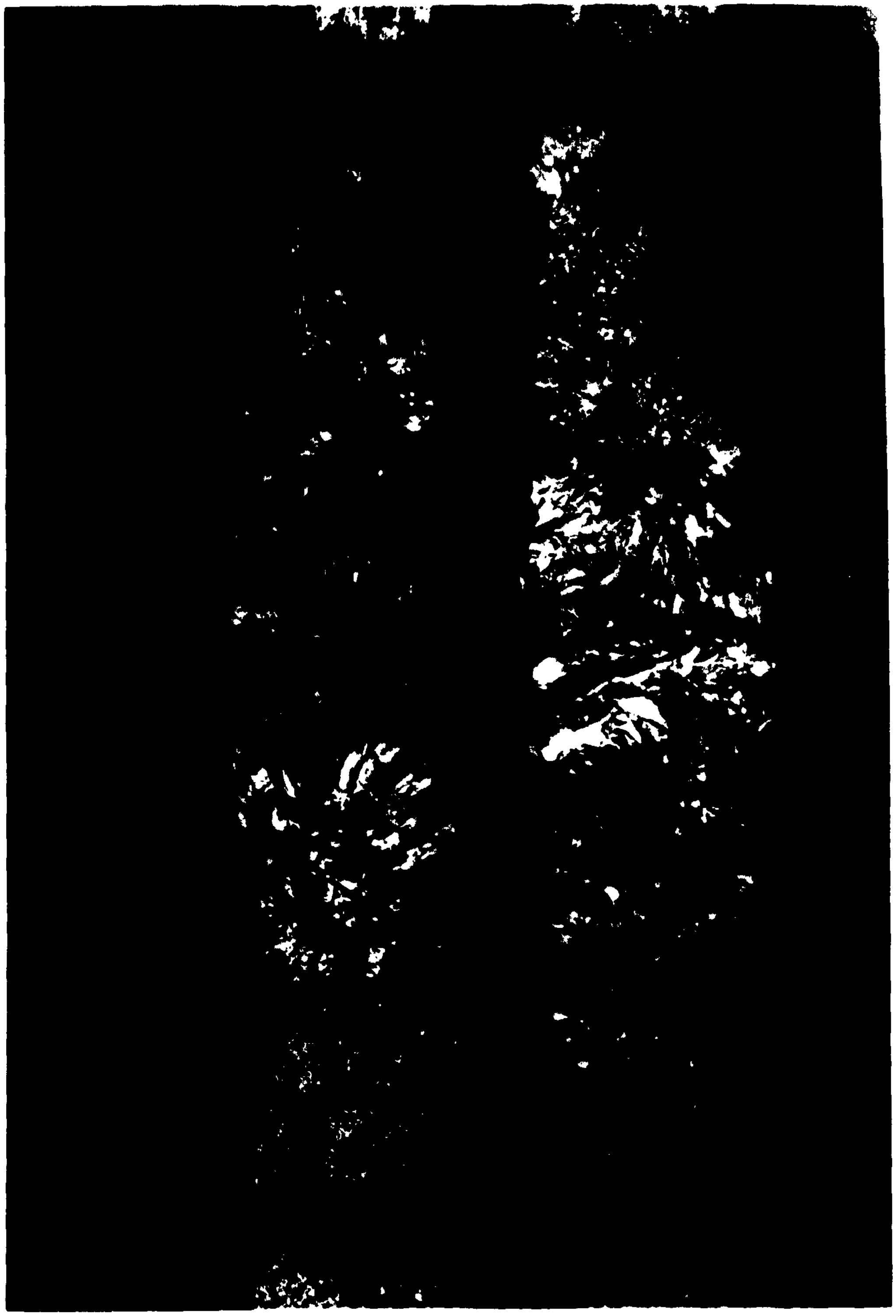

MAG: 10X

FRACTURE SURFACES OF FAILED CYCLIC TEST SPECIMEN NO. 10
TIG-WELDED USING IMPROVED COPPER FIXTURING TECHNIQUE.
SPECIMEN FAILED AT 175,000 PSI THROUGH PRIOR CRACK NOT
ASSOCIATED WITH WELD POROSITY

H-25598

Figure 32

MAG: 2X

GAGE AREA SURFACE OF FAILED CYCLIC TEST SPECIMEN NO. 11
TIG-WELDED USING IMPROVED COPPER FIXTURING TECHNIQUE.
SPECIMEN FAILED AT 175,000 PSI THROUGH PRIOR CRACK NOT
ASSOCIATED WITH WELD POROSITY

H-25537

Figure 33

FRACTURE SURFACES OF FAILED CYCLIC TEST SPECIMEN NO. 11
TIG-WELDED USING IMPROVED COPPER FIXTURING TECHNIQUE.
SPECIMEN FAILED AT 175,000 THROUGH PRIOR CRACK NOT ASSOCIATED
WITH WELD POROSITY

MAG: 10X

H-25538

Figure 34

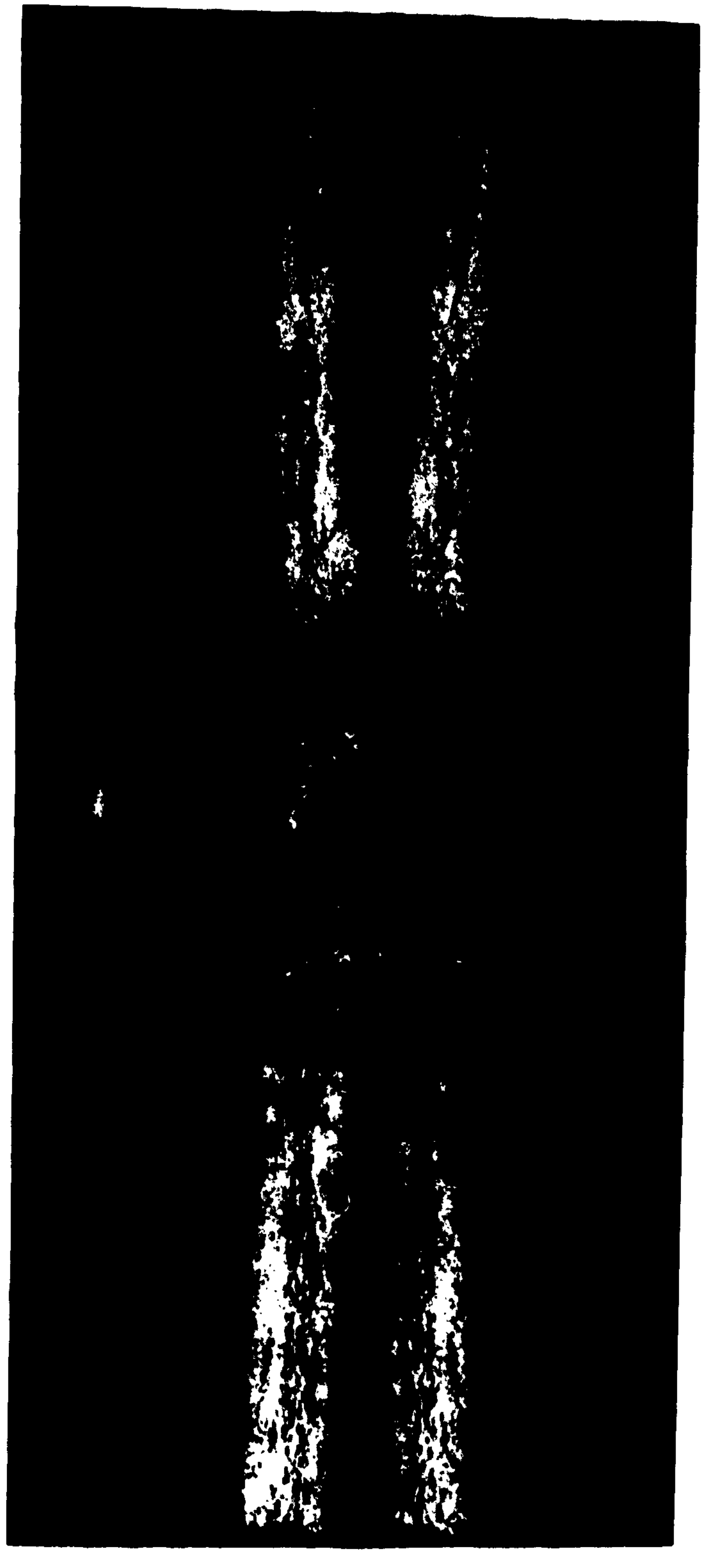

MAG: 4X

FRACTURE SURFACES OF FAILED CYCLIC TEST SPECIMEN NO. 16
TIG-WELDED USING NO FILLER WIRE. SPECIMEN FAILED ON LOADING
TO 80,000 PSI THROUGH PRIOR CRACK NOT ASSOCIATED WITH WELD
POROSITY

H-23664

Figure 35

MAG: 5X

FRACTURE SURFACES OF FAILED CYCLIC TEST SPECIMEN NO. 19
ELECTRON BEAM-WELDED WITHOUT FILLER MATERIAL. SPECIMEN
FAILED AT 165,000 PSI WITH ORIGIN IN PARENT MATERIAL.
(NOT SHOWN).

H-25093

Figure 36

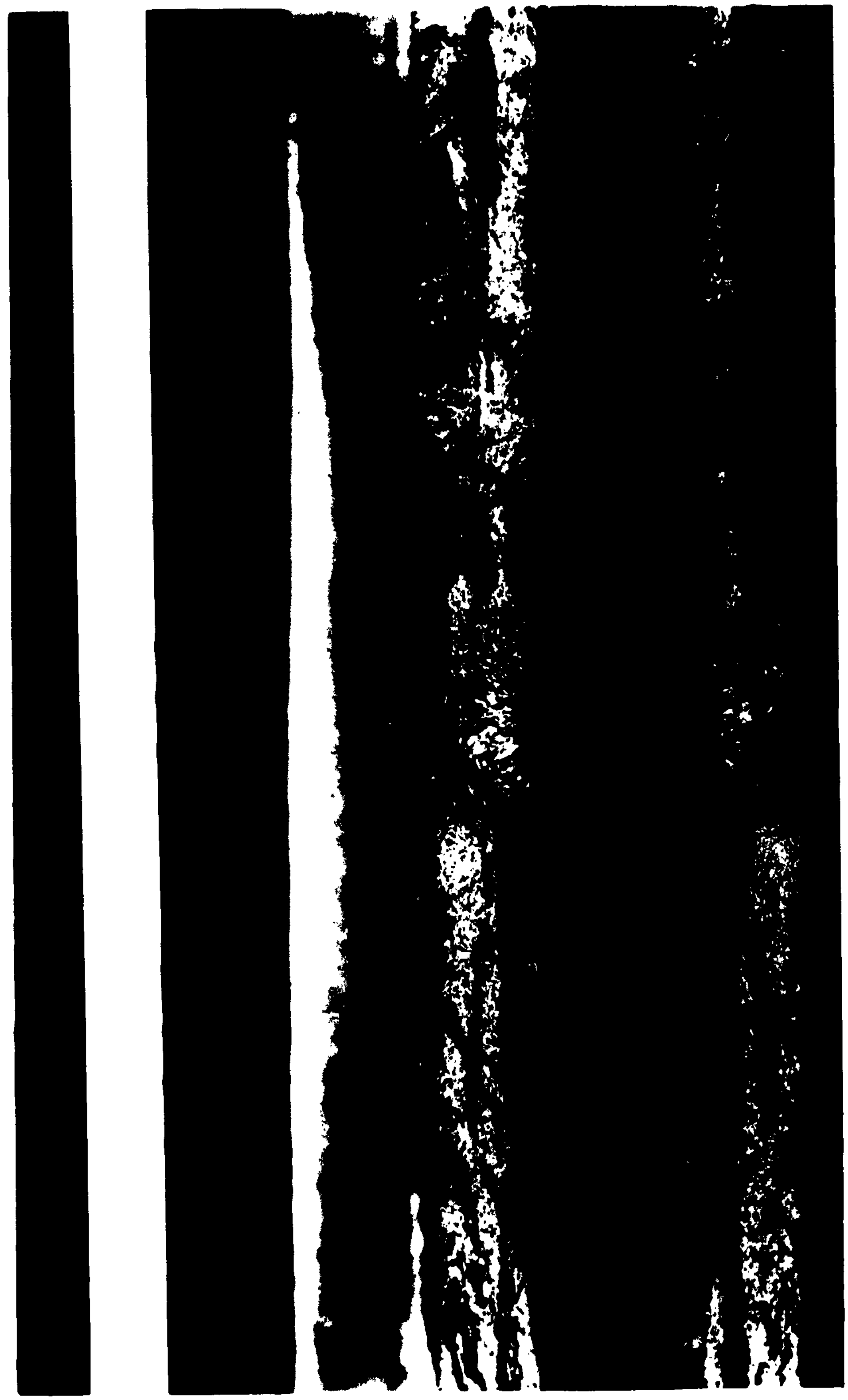

MAG: 5X

FRACTURE SURFACES OF FAILED CYCLIC TEST SPECIMEN NO. 20
ELECTRON BEAM-WELDED WITHOUT FILLER MATERIAL. SPECIMEN FAILED
AT 161,000 PSI WITH ORIGIN IN PARENT MATERIAL (NOT SHOWN)

H-25095

Figure 37

FRACTURE SURFACES OF FAILED CYCLIC TEST SPECIMEN NO. 23 MAG: 10X
ELECTRON BEAM – WELDED WITH PREPLACED FILLER WIRE. SPECIMEN
FAILED AT 170,000 PSI WITH ORIGIN IN PARENT MATERIAL (NOT
SHOWN)

H-25539

Figure 38

ETCHANT: 5% HF, 35% HNO_3 MAG: 100X

MICROSTRUCTURE OF PLANAR SECTION THROUGH TYPICAL FAILED CYCLIC TEST SPECIMEN SHOWING PARTIALLY INTERGRANULAR - PARTIALLY TRANSGRANULAR NATURE OF CRACKING

H-25754-23

Figure 39

FAILURE STRESS vs NUMBER OF POROSITY PORES AND NUMBER OF CRACKS THROUGH PORES FOR CYCLIC TEST SPECIMENS CONTAINING TIG WELDS MADE BY VARIOUS TECHNIQUES.

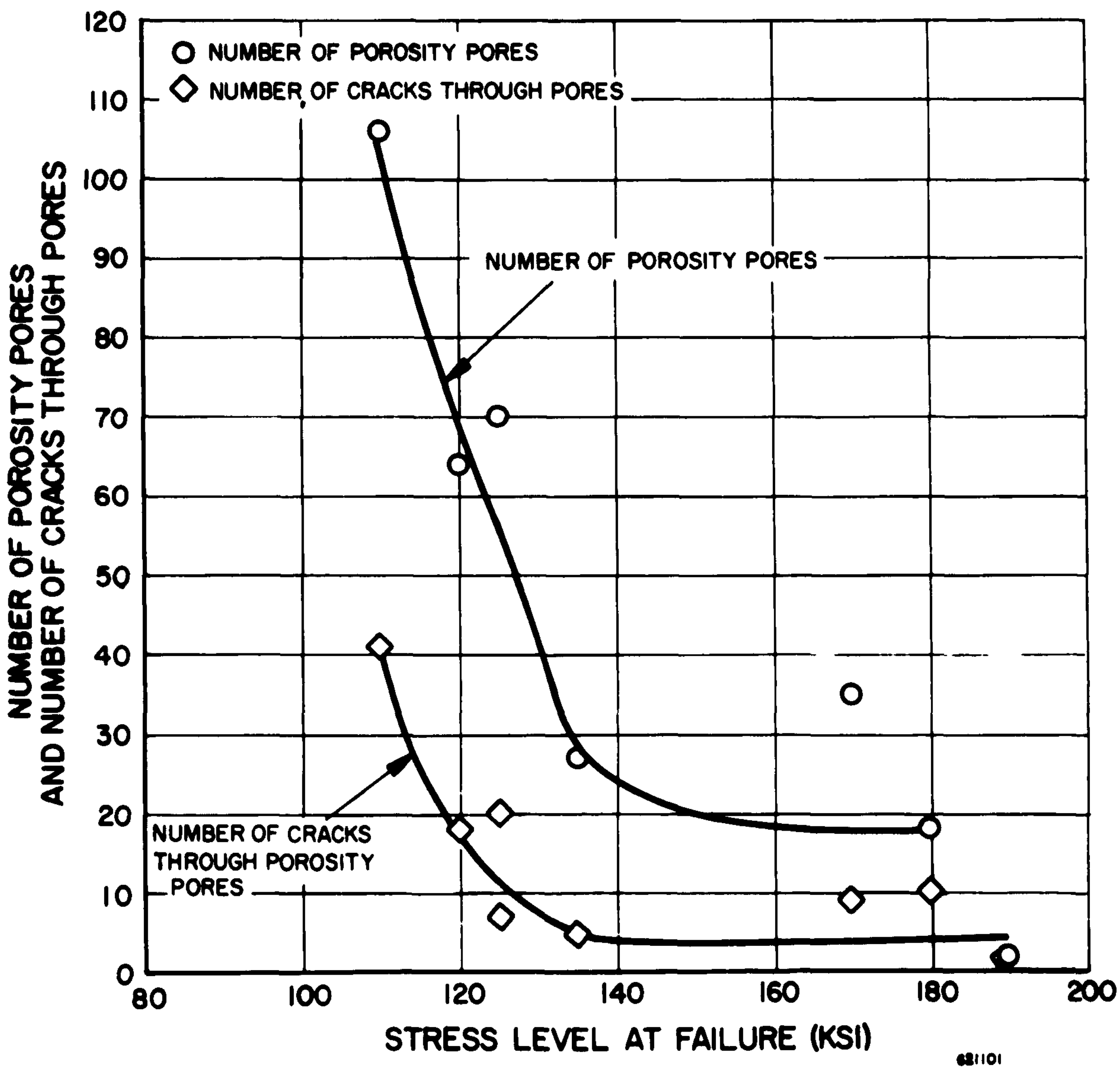

FRACTURE TOUGHNESS RESULTS vs THICKNESS FOR COLD - ROLLED AND AGED SHEET STOCK AND COLD - ROLLED TIG WELDS

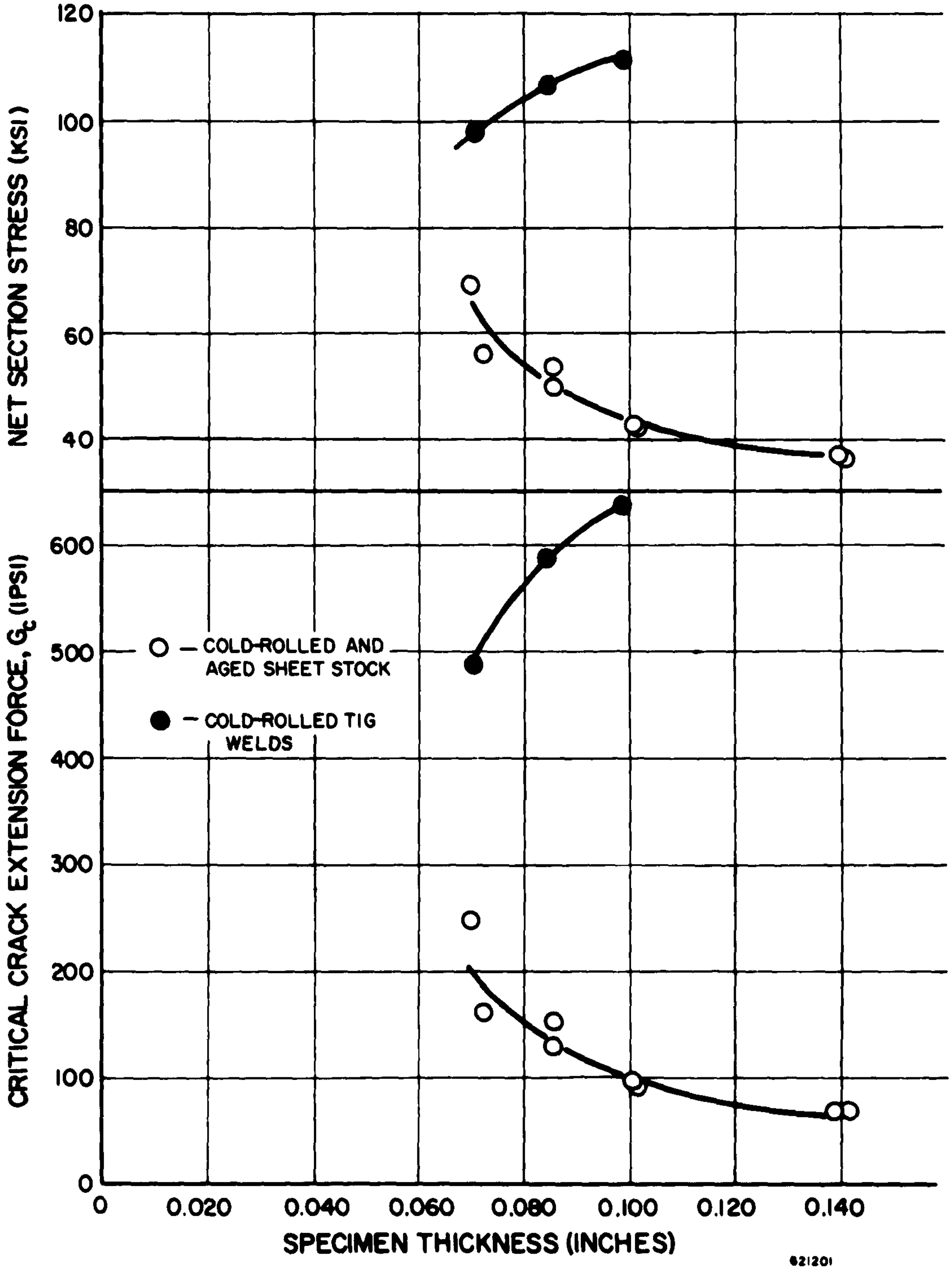

Figure 41

MAG: 2 3/4X

FRACTURE SURFACES OF TOUGHNESS (Gc) SPECIMENS FROM COLD-ROLLED AND AGED SHEET STOCK OF VARIOUS THICKNESSES. NOTE EXTENT OF SLOW CRACK PROPAGATION (INK STAINS)

H-24325

Figure 42

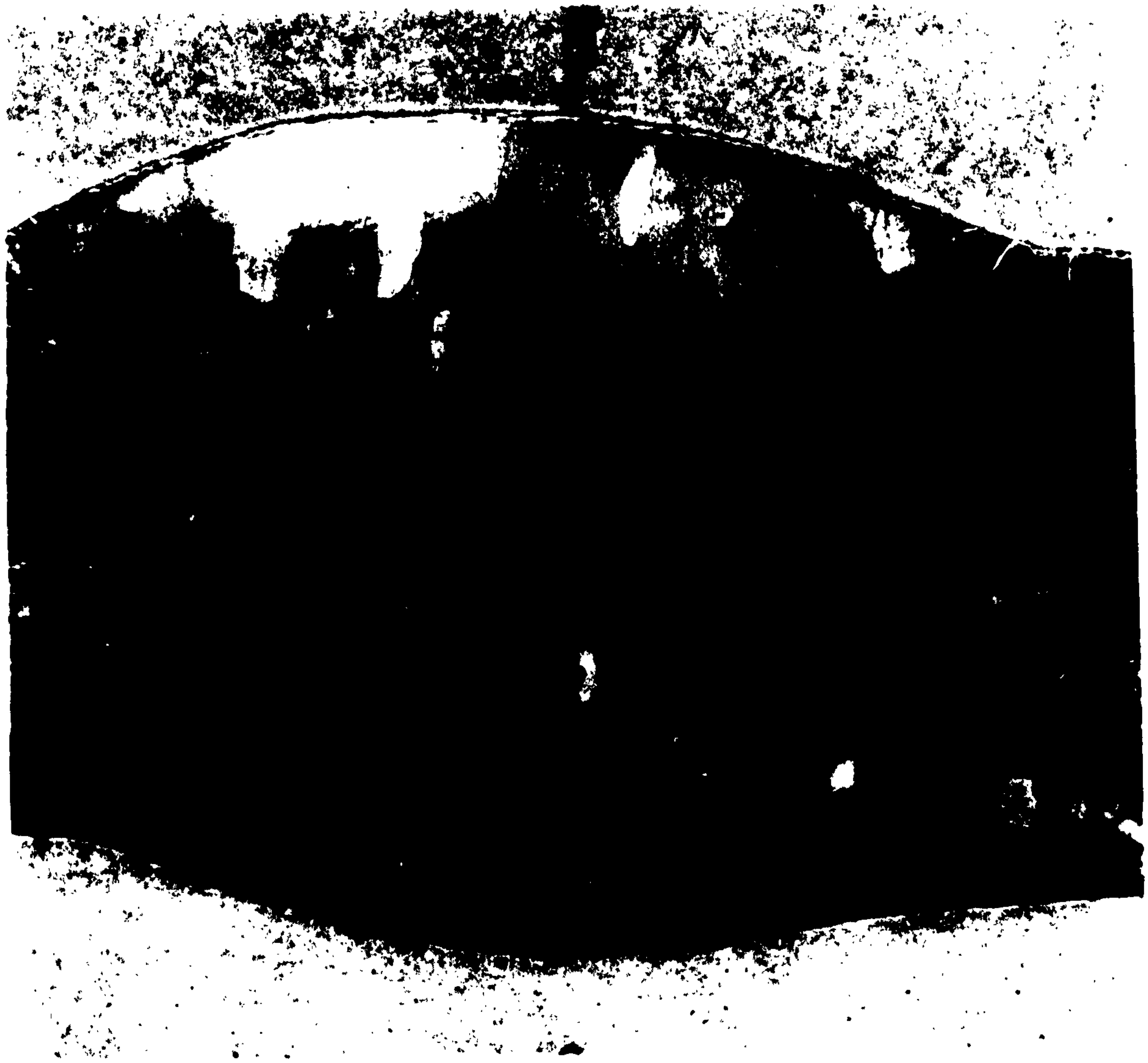

ETCHANT: 5% HF, 35% HNO_3 MAG: 11X
MACROSTRUCTURE OF FOUR-PASS TIG WELD (MANUAL) ON 0.375 INCH THICK PLATE STOCK

H-24010

Figure 43

MAG: 11X

FRACTURE SURFACE OF BEND SPECIMEN CONTAINING FOUR-PASS TIG WELD (MANUAL) ON 0.375 INCH THICK PLATE STOCK

H-24011

Figure 44

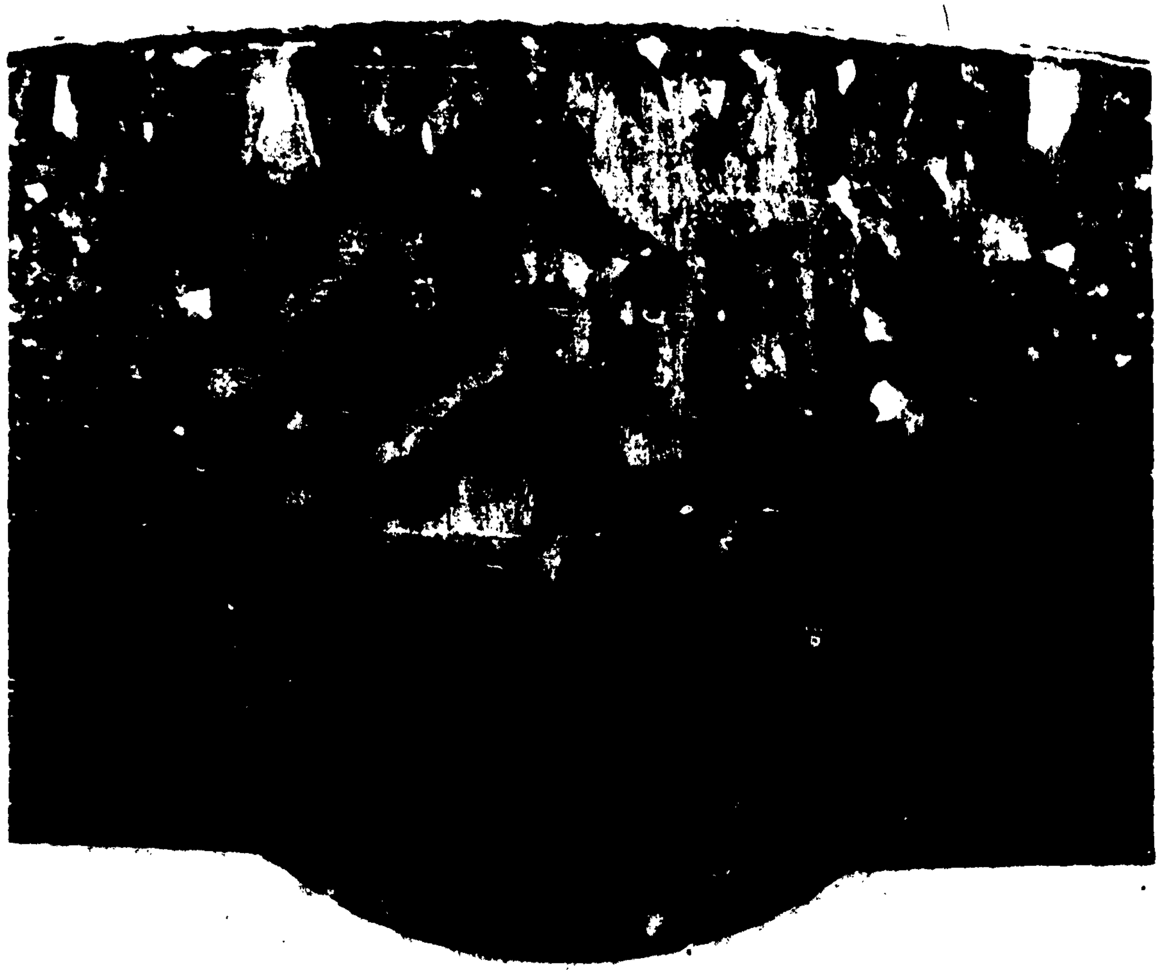

ETCHANT: 5% HF, 35% HNO_3 MAG: 13X
MACROSTRUCTURE OF TWO-PASS TIG WELD (AUTOMATIC) ON 0.375 INCH THICK PLATE STOCK

H-24015

Figure 45

FRACTURE SURFACE OF BEND SPECIMEN CONTAINING TWO-PASS TIG WELD (AUTOMATIC) ON 0.375 INCH THICK PLATE STOCK

MAG: 13X

H-24012

Figure 46

ETCHANT: 5% HF, 35% HNO_3 MAG: 1/2X
MACROSTRUCTURE (RADIAL SECTION) OF SUBSCALE 14-INCH DIAMETER DOME EFM-8 PRESS-FORGED AT 1850F BY THE PANCAKE AND PREFORM METHOD. NOTE UNIFORMLY COARSE GRAIN STRUCTURE

H-23410

Figure 47

ETCHANT: 5% HF, 35% HNO_3 MAG: 1/2X
MACROSTRUCTURE (RADIAL SECTION) OF SUBSCALE 14-INCH DIAMETER DOME EFM-10 PRESS-FORGED AT 1850F BY THE DOGBONE METHOD.
NOTE UNIFORMLY COARSE GRAIN STRUCTURE

H-23409

Figure 48

TENSILE PROPERTY UNIFORMITY FOR SUBSCALE 14 - INCH DIAMETER DOME EFM - 8 PRESS - FORGED AT 1850 F BY THE PANCAKE AND PREFORM TECHNIQUE

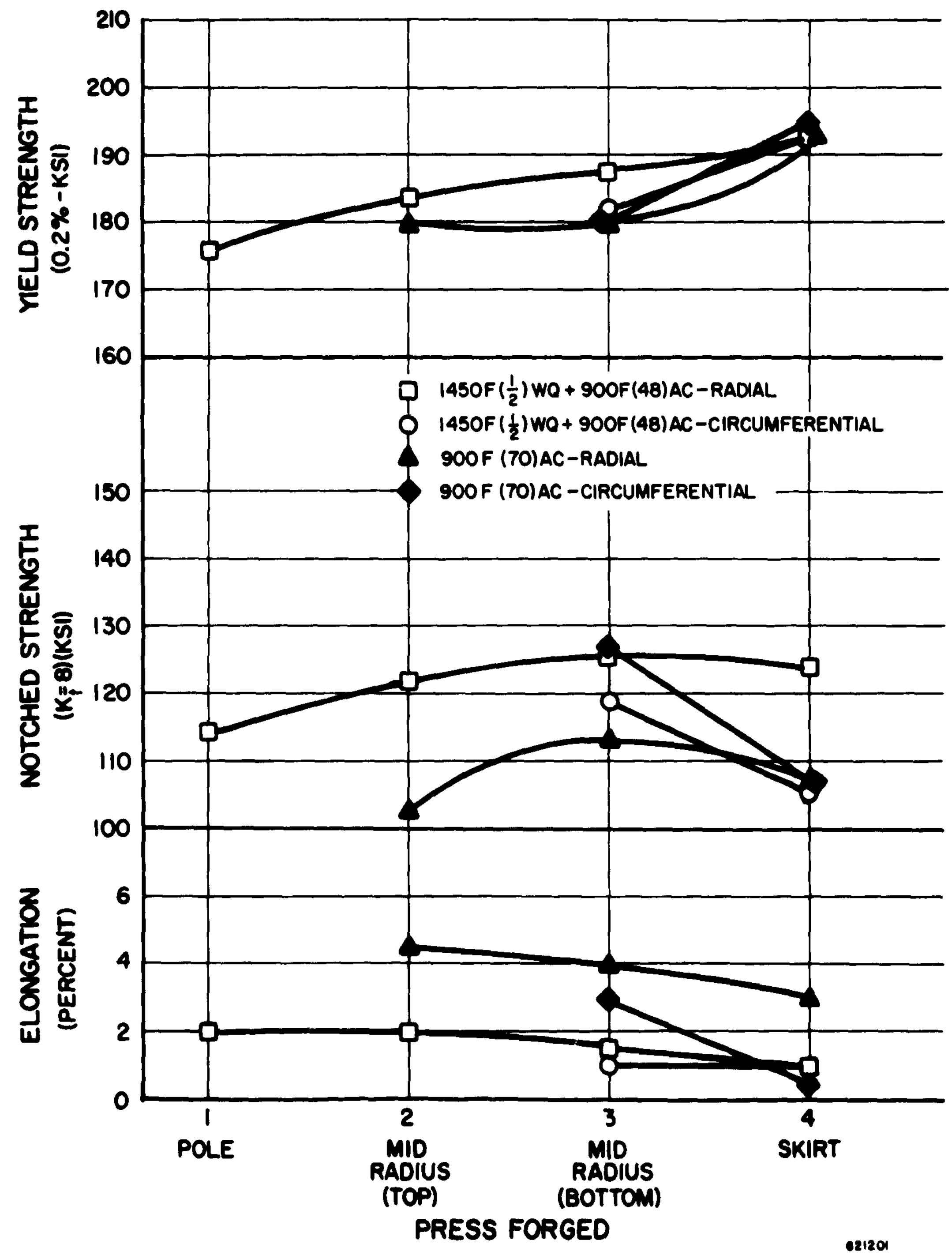

TENSILE PROPERTY UNIFORMITY FOR SUBSCALE 14-INCH DIAMETER DOME EFM-10 PRESS-FORGED AT 1850 F BY THE DOGBONE TECHNIQUE

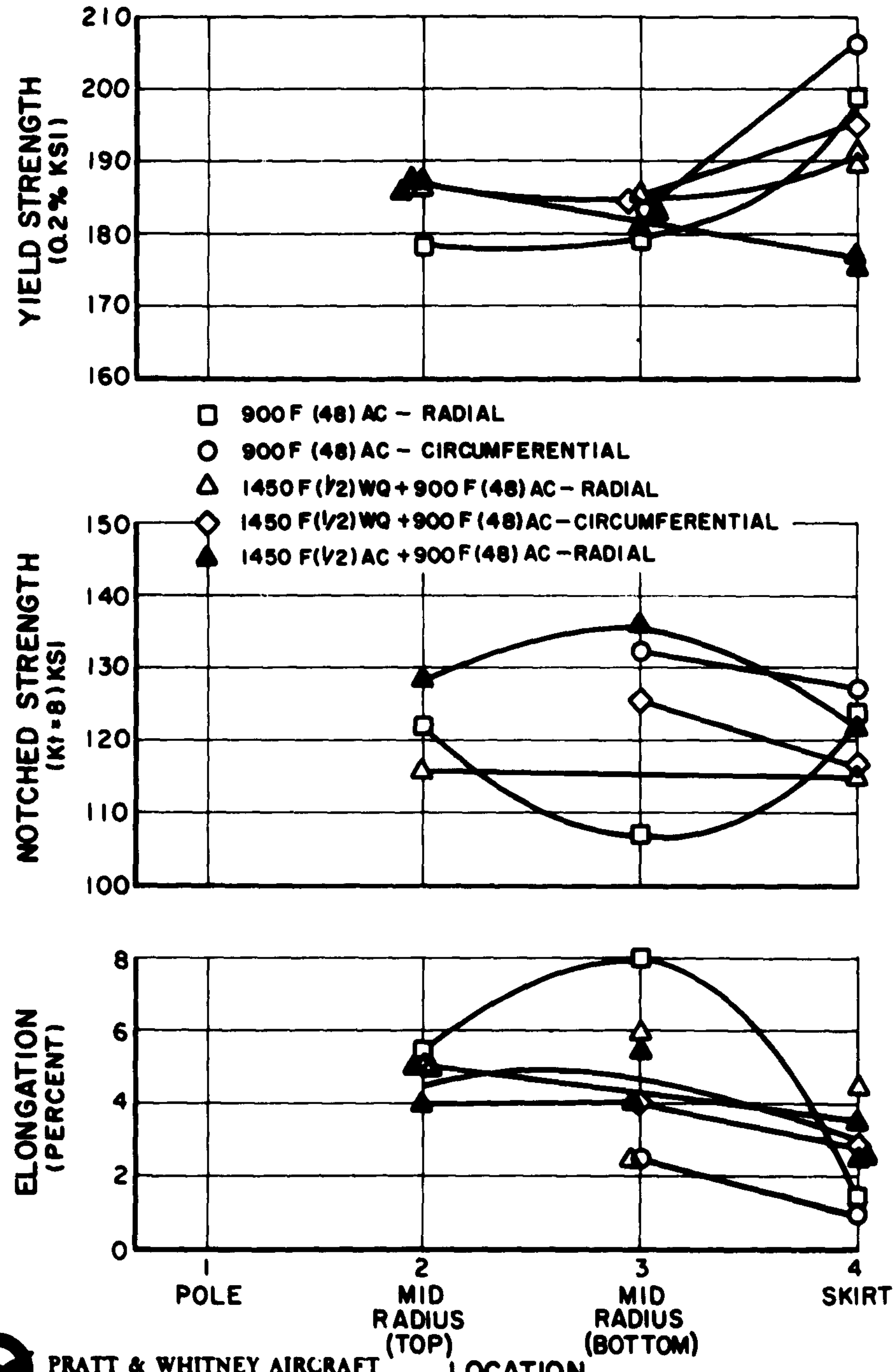

PRATT & WHITNEY AIRCRAFT
DIVISION OF
UNITED AIRCRAFT CORPORATION

Figure 50

ETCHANT: 5% HF, 35% HNO_3 MAG: 500X
TYPICAL MICROSTRUCTURE OF SUBSCALE 14-INCH DIAMETER DOMES EFM-8 AND EFM-10 PRESS-FORGED AT 1850F AFTER SOLUTION TREATMENT AT 1450F AND AGING AT 900F. NOTE RELATIVELY COARSE AND NONUNIFORM AGING CONSTITUENT

H-24618-9

Figure 51

ETCHANT: 5% HF, 35% HNO_3 MAG: 100X
TYPICAL MICROSTRUCTURE OF FULL SCALE FRONT DOME EJO-1 PRESS-FORGED AT 1700F BY THE PANCAKE AND PREFORM METHOD AND RESTRUCK AT 1900F NOTE COARSE EQUI-AXED GRAIN SIZE AND NONUNIFORM AGING

H-22996-36

Figure 52

ETCHANT: 5% HF, 35% HNO_3 MAG: 500X

TYPICAL MICROSTRUCTURE OF FULL SCALE 40-INCH DIAMETER FRONT DOME EJO-1 PRESS-FORGED AT 1700F BY THE PANCAKE AND PREFORM METHOD AND RESTRUCK AT 1900F NOTE RELATIVELY COARSE AND NONUNIFORM AGING CONSTITUENT

H-24619-67

Figure 53

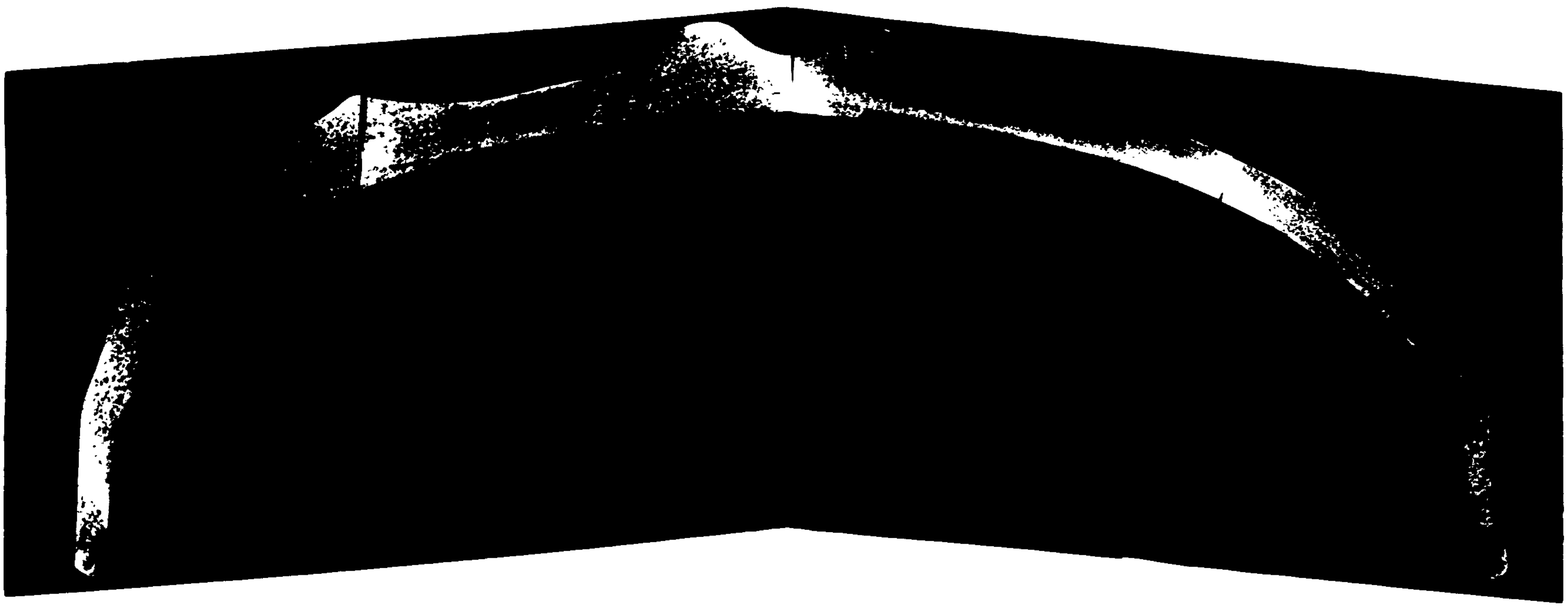

ETCHANT: 5% HF, 35% HNO_3 MAG: 1/4X

MACROSTRUCTURE OF RADIAL SECTION THROUGH FULL SCALE 40-INCH DIAMETER FRONT DOME ELA-3 PRESS-FORGED AT 1850F BY THE PANCAKE AND PREFORM METHOD. NOTE RELATIVELY FINE GRAIN STRUCTURE THROUGHOUT

Figure 54

ETCHATNT 5% HF, 35% HNO_3 MAG: 1/4X

MACROSTRUCTURE OF RADIAL SECTION THROUGH FULL SCALE 40-INCH DIAMETER REAR DOME ELA-2 PRESS-FORGED AT 1850F BY THE DOGBONE TECHNIQUE. NOTE COARSER GRAIN STRUCTURE IN MID-RADIAL LOCATIONS CORRESPONDING TO APPROXIMATE LOCATION OF DOGBONE PREFORM (BRACKETS)

Figure 55

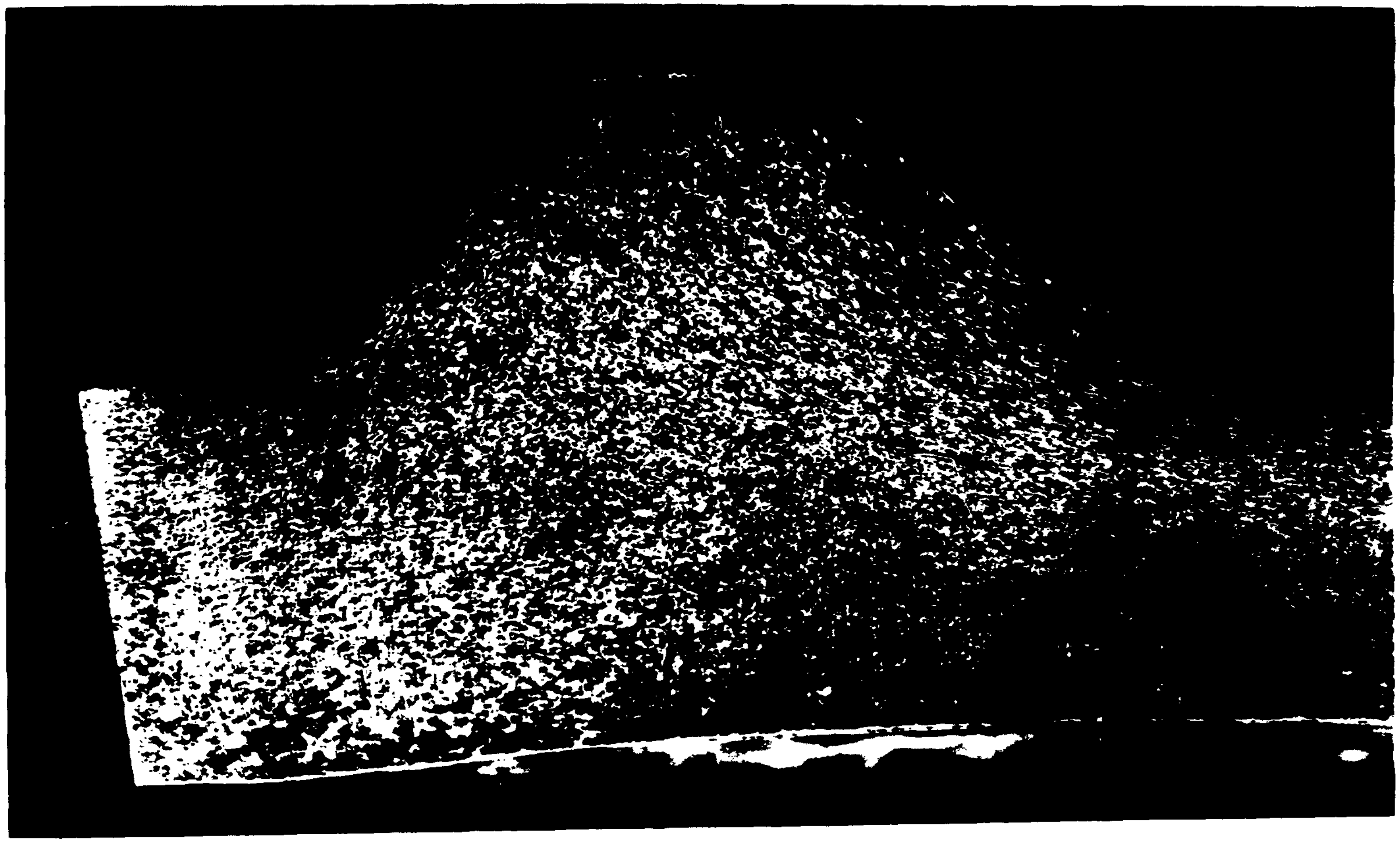

ETCHANT: 5% HF, 35% HNO_3 MAG: 2X

MACROSTRUCTURE OF RADIAL SECTION THROUGH HALF SECTION OF POLAR BOSS FROM FULL SCALE 40-INCH DIAMETER FRONT DOME ELA-3 PRESS-FORGED AT 1850F BY THE PANCAKE AND PREFORM METHOD. NOTE RELATIVELY FINE BUT EQUI-AXED GRAIN STRUCTURE WITH SOME COARSENING TOWARD INSIDE SURFACE (BOTTOM)

H-25656

Figure 56

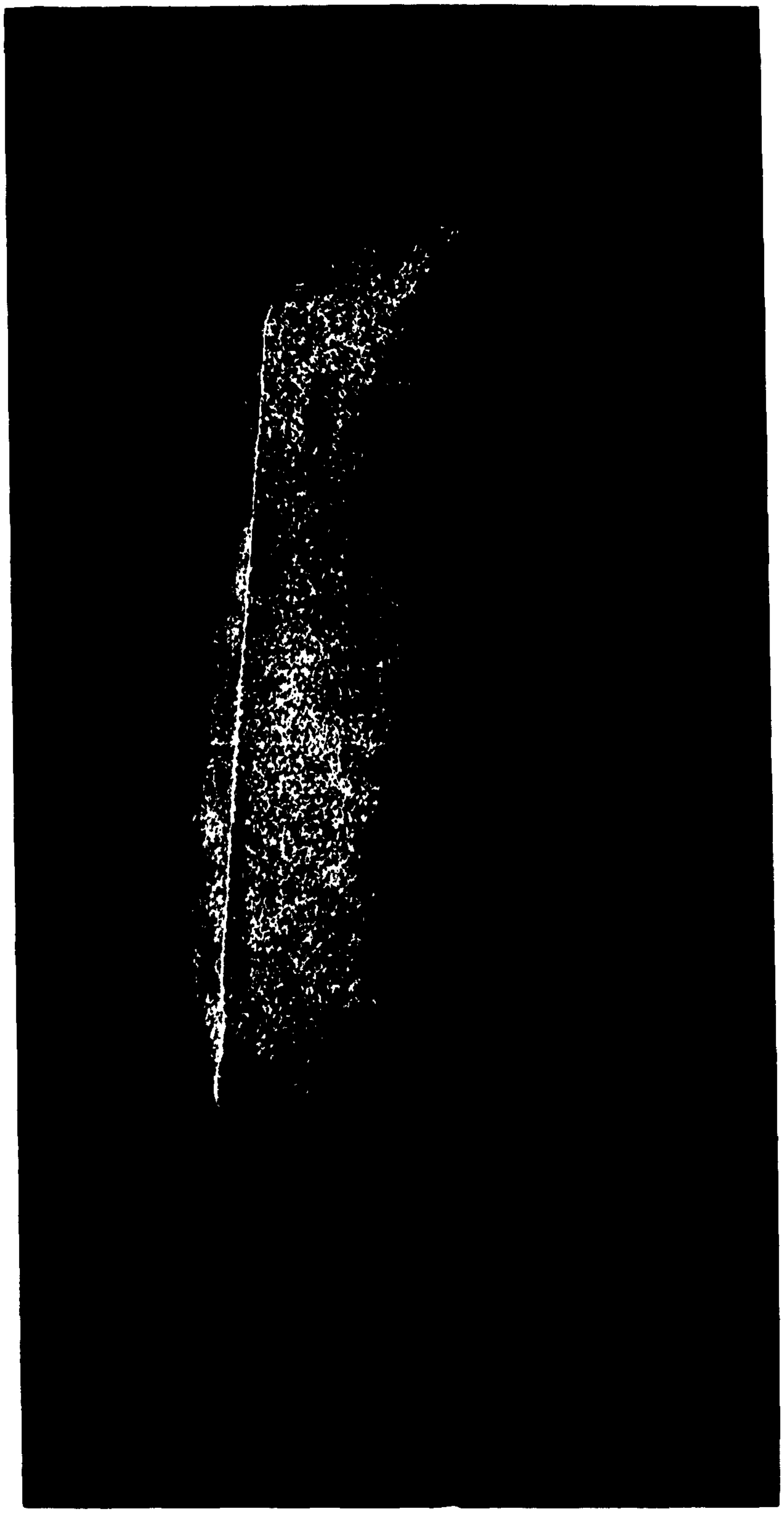

MAG: 7/8X

ETCHANT: 5% HF, 35% HNO3

MACROSTRUCTURE OF RADIAL SECTION THROUGH OFFSET (THRUST REVERSER) BOSS FROM FULL SCALE 40-INCH DIAMETER FRONT DOME ELA-3 PRESS-FORGED AT 1850F BY THE PANCAKE AND PREFORM TECHNIQUE. NOTE RELATIVELY FINE BUT EQUI-AXED GRAIN STRUCTURE

H-25655

Figure 57

AGING CURVES FOR FULL SCALE 40 - INCH DIAMETER REAR DOME ELA - 2 PRESS - FORGED AT 1850 F BY THE DOGBONE METHOD

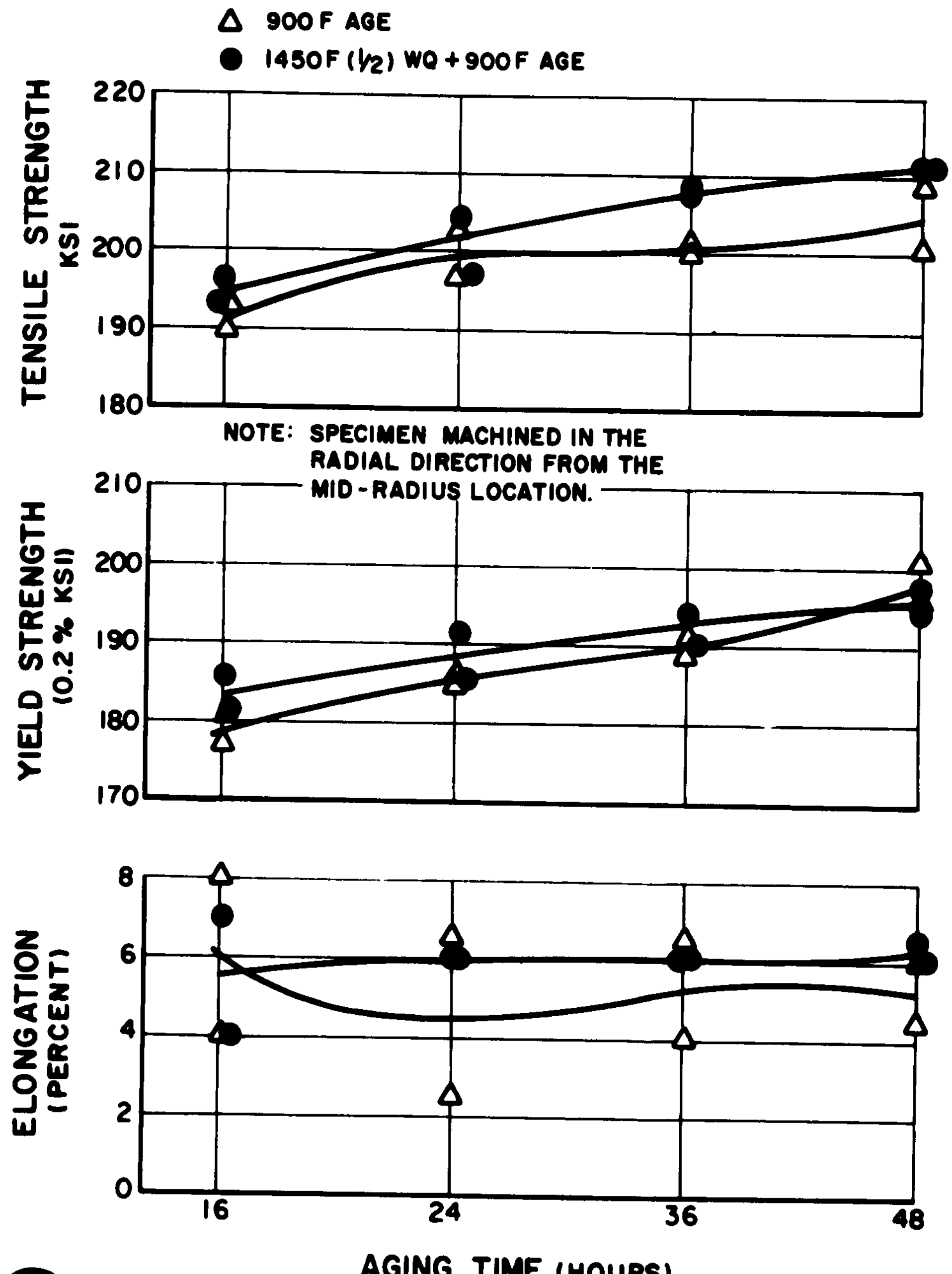

PRATT & WHITNEY AIRCRAFT
DIVISION OF
UNITED AIRCRAFT CORPORATION

621101

AGING CURVES FOR FULL SCALE 40 - INCH DIAMETER FRONT DOME ELA - 3 PRESS - FORGED AT 1850 F BY THE PANCAKE AND PREFORM METHOD

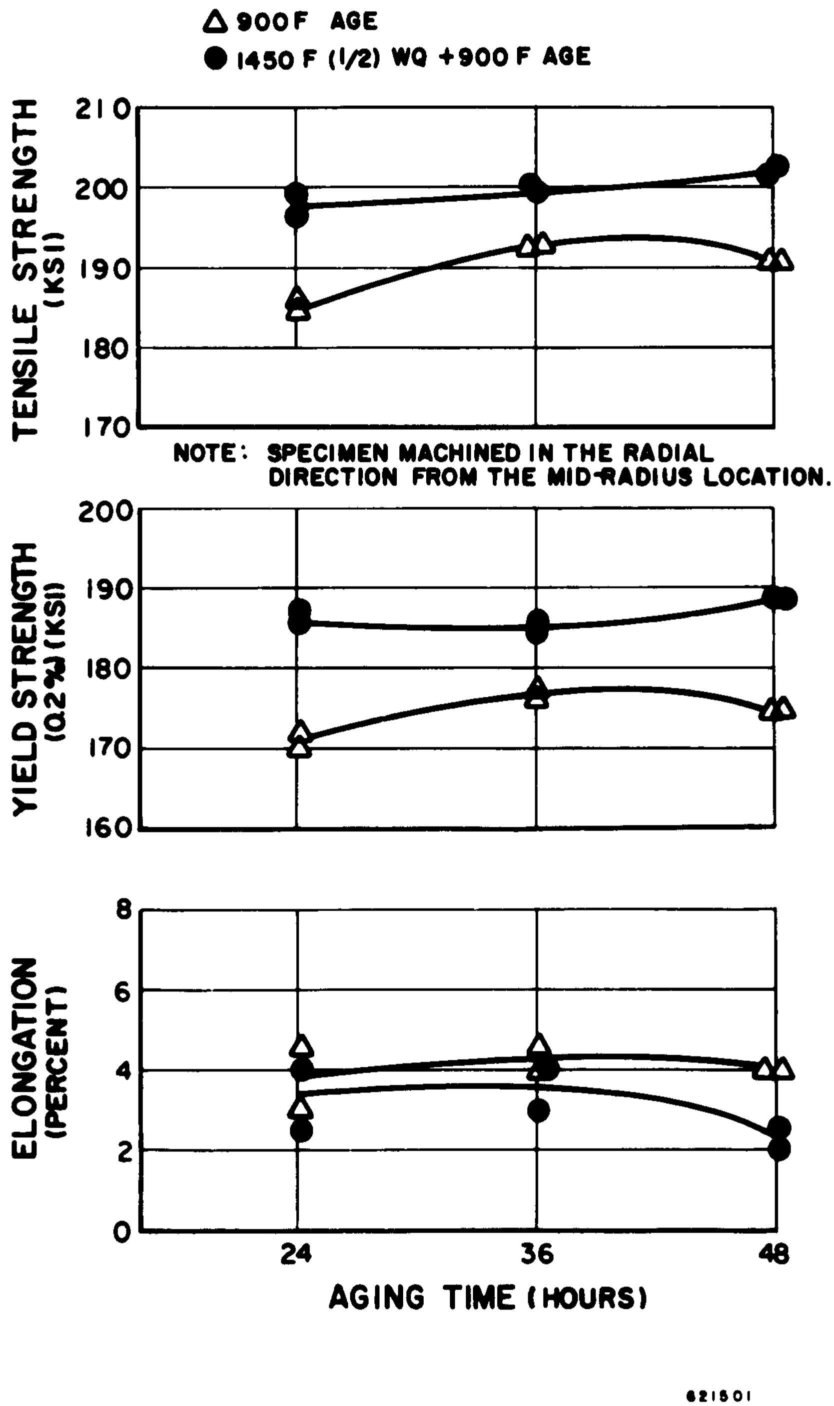

TENSILE PROPERTY UNIFORMITY OF FULL SCALE 40 - INCH DIAMETER REAR DOME ELA -2 PRESS - FORGED AT 1850F BY THE DOGBONE METHOD

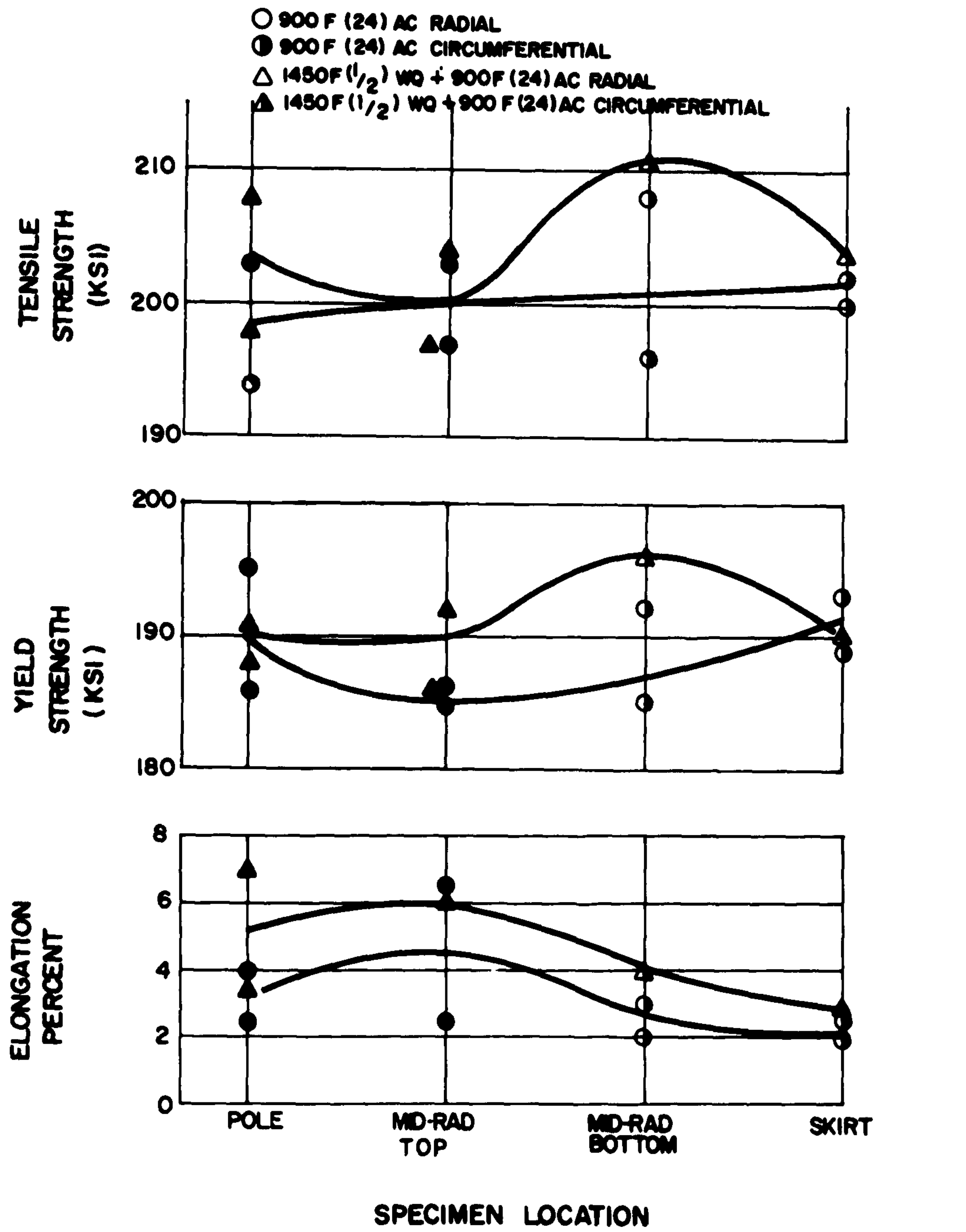

PRATT & WHITNEY AIRCRAFT
DIVISION OF
UNITED AIRCRAFT CORPORATION

621201

TENSILE PROPERTY UNIFORMITY OF FULL SCALE 40 - INCH DIAMETER FRONT DOME ELA - 3 PRESS - FORGED AT 1850 F BY THE PANCAKE AND PREFORM METHOD

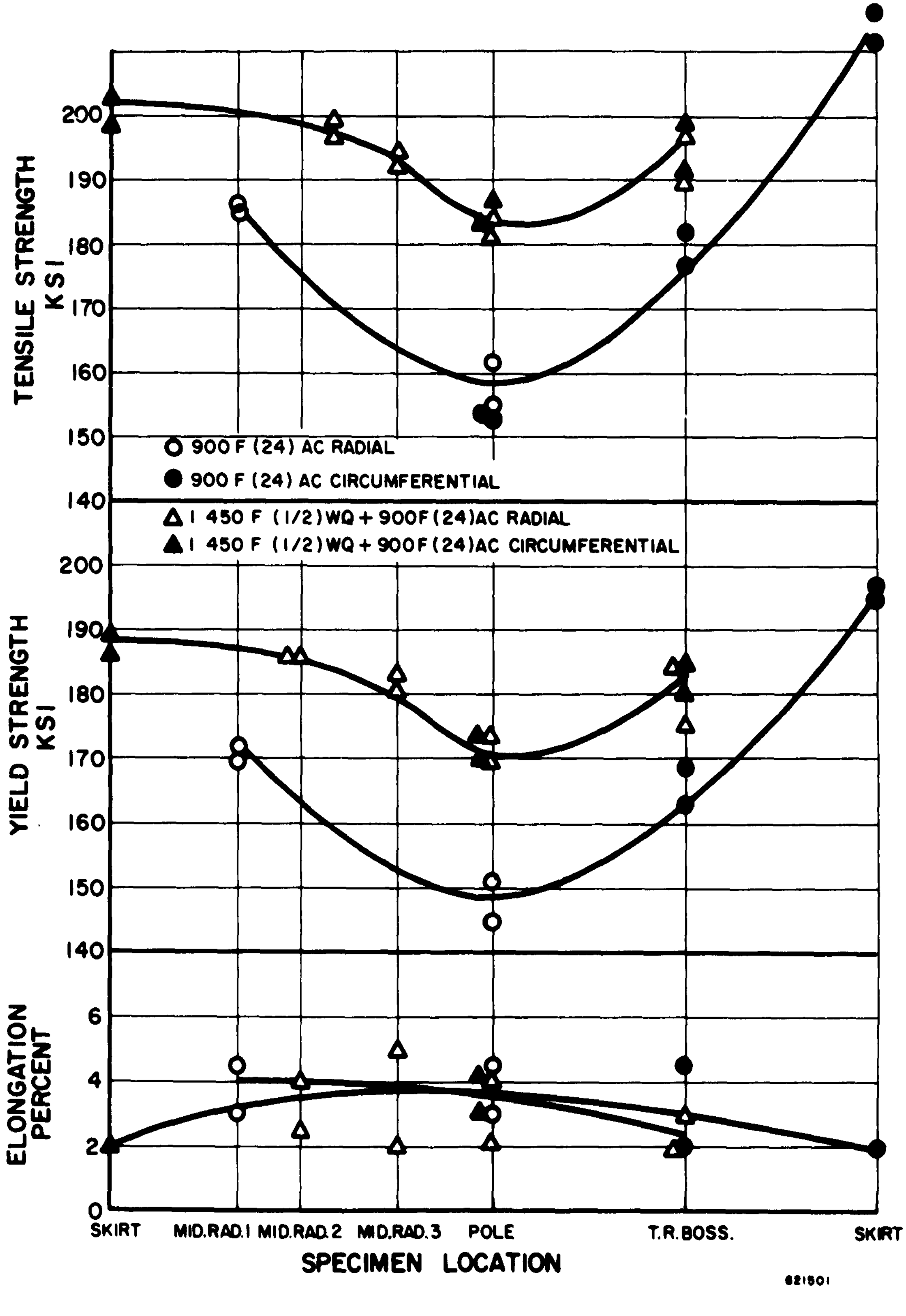

Figure 61

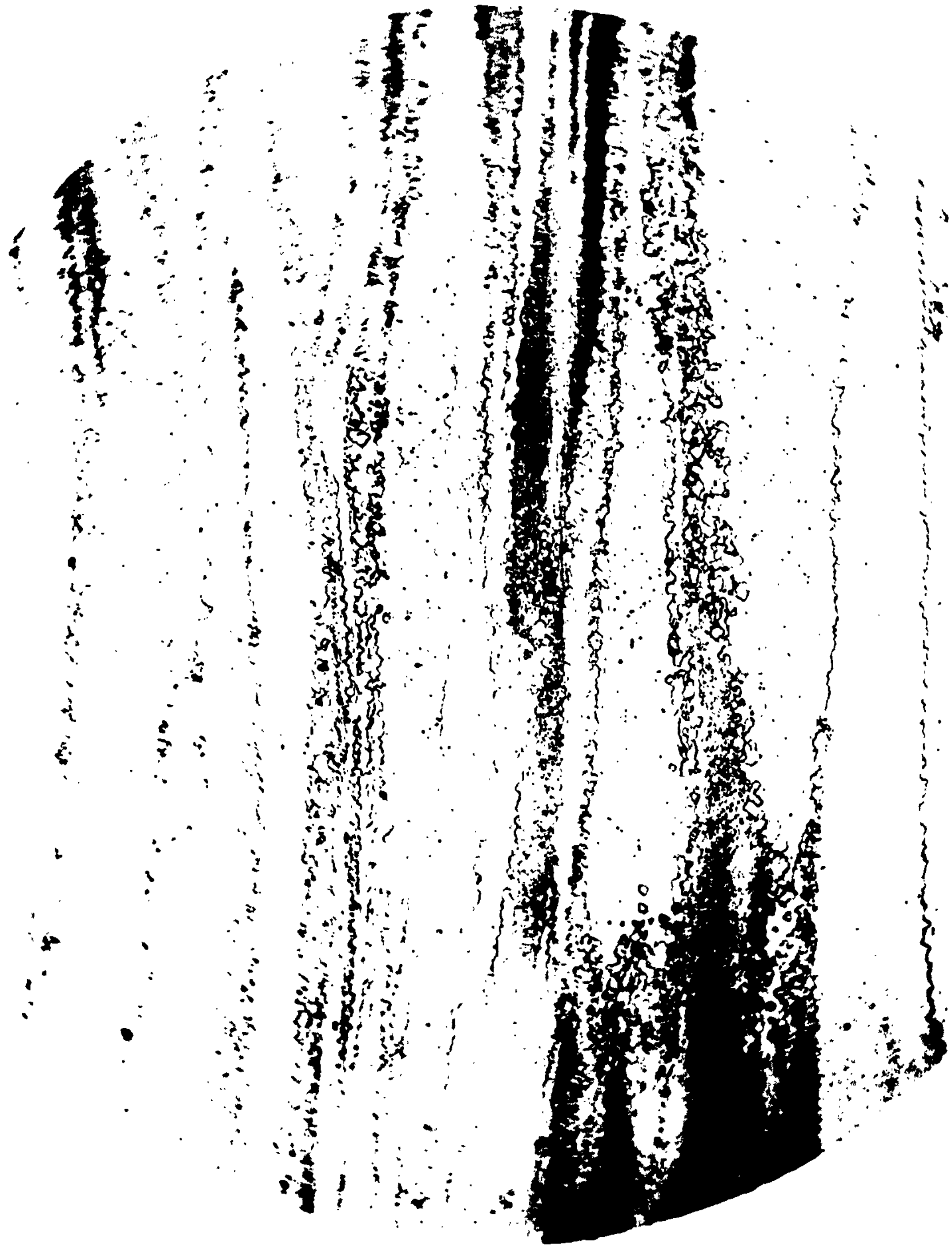

ETCHANT: 5% HF, 35% HNO_3 MAG: 100X
TYPICAL AS-FORGED MICROSTRUCTURE (RADIAL SECTION) OF FULL
SCALE FRONT (ELA-3) AND REAR (ELA-2) DOMES PRESS-FORGED AT
1850F SHOWING WORKED AND PARTIALLY RECRYSTALLIZED STRUCTURE
H-25672-4

Figure 62

TENSILE PROPERTY UNIFORMITY FOR HAMMER-FORGED PANCAKE NO. 4 AGED AT 900 F FOR 60 HOURS

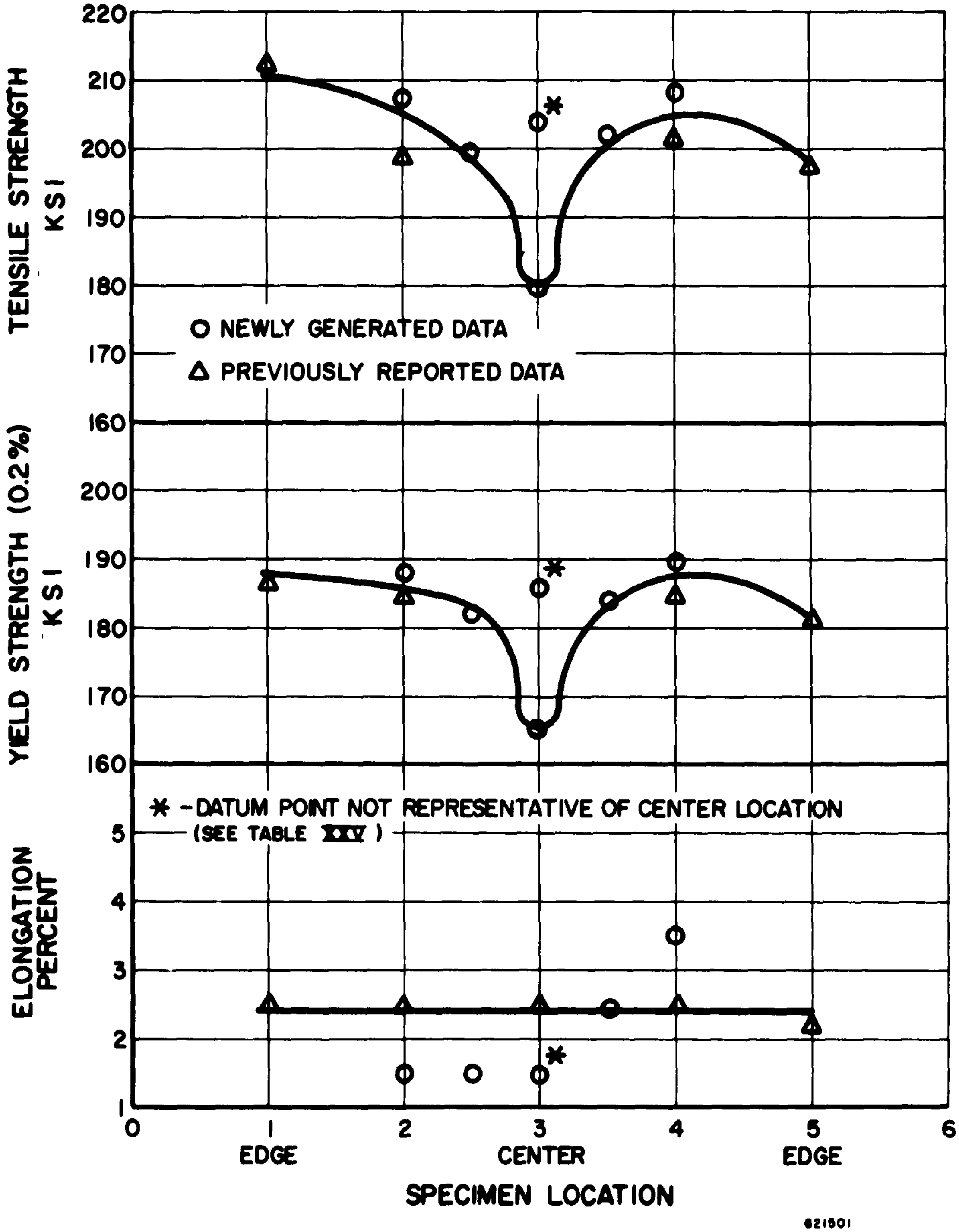

Figure 63

AGING CURVES (AXIAL DIRECTION) FOR SUBSCALE 14 - INCH DIAMETER FLOW - TURNED CYLINDERS NO'S 1 - 3 AFTER STRESS RELIEF AT 900 F FOR ONE HOUR

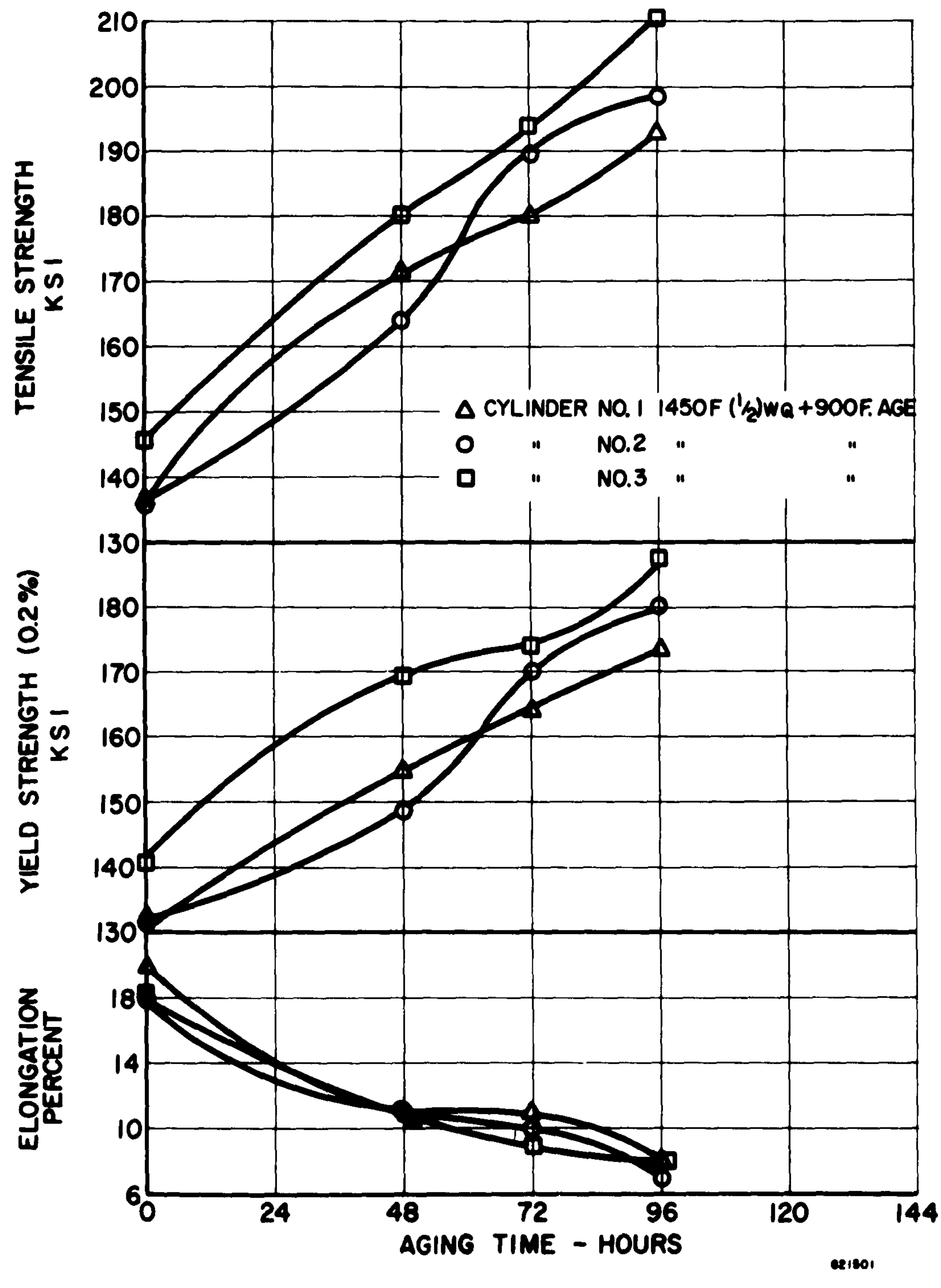

Figure 64

ETCHANT: HF, HNO_3, LACTIC ACID MAG: 17,500X
MICROSTRUCTURE NEAR OUTSIDE SURFACE OF FULL SCALE 40-INCH DIAMETER CYLINDER WHICH BEHAVED SATISFACTORILY DURING FLOW-TURNING. NOTE PRECIPITATE PARTICLES AT GRAIN BOUNDARY (ARROWS)

Figure 65

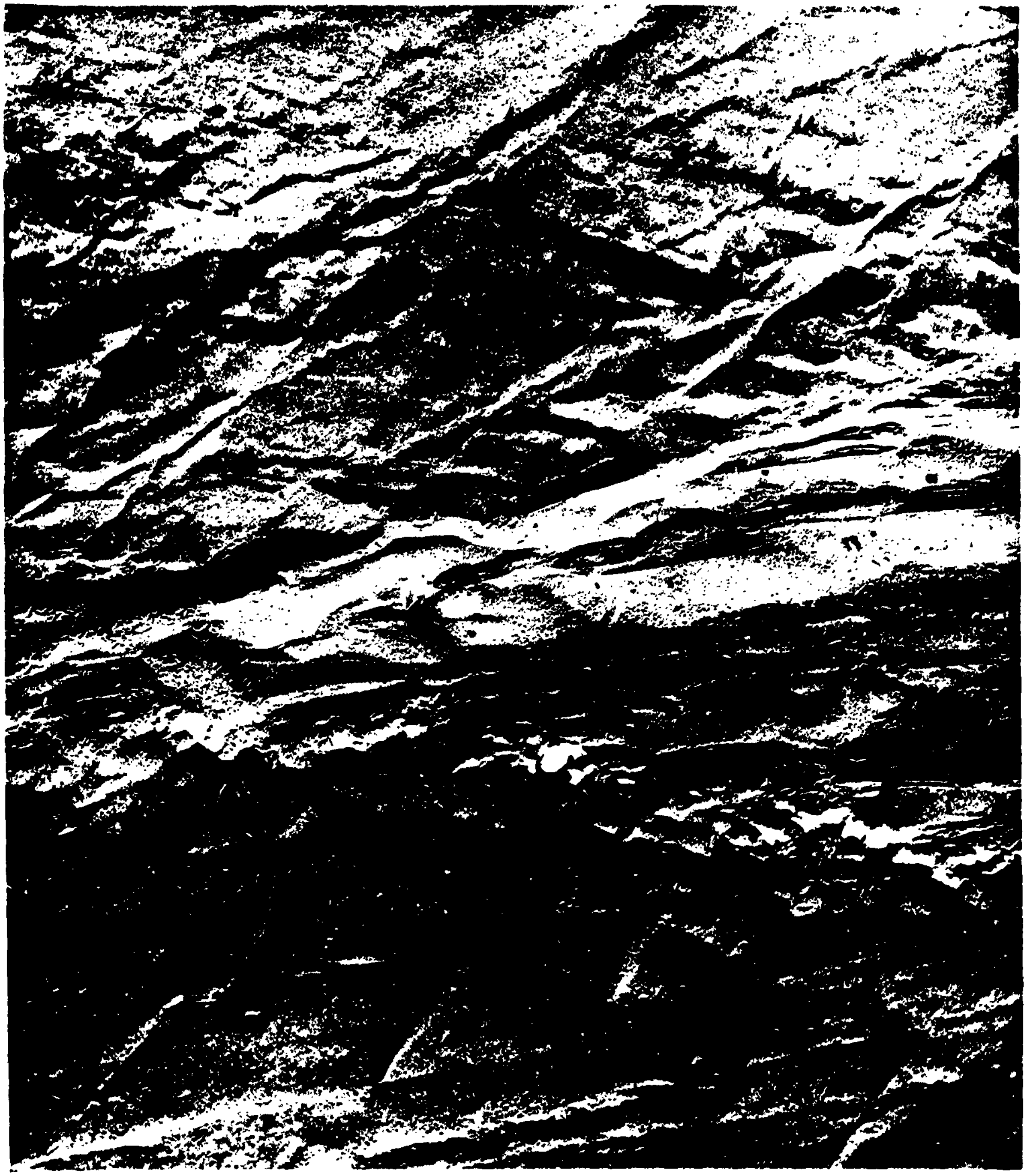

ETCHANT: HF, HNO_3, LACTIC ACID MAG: 17,500X
MICROSTRUCTURE NEAR INSIDE SURFACE OF FULL SCALE 40-INCH DIAMETER CYLINDER WHICH BEHAVED SATISFACTORILY DURING FLOW-TURNING. NOTE PRECIPITATE PARTICLES AT GRAIN BOUNDARY (ARROWS)

Figure 66

ETCHANT: HF, HNO_3, LACTIC ACID MAG: 17,500X
MICROSTRUCTURE OF FULL SCALE 40-INCH DIAMETER CYLINDER WHICH RUPTURED DURING FLOW-TURNING. NOTE PRECIPITATE PARTICLES (ARROWS) AND ETCH PITTING (BRACKETS) AT GRAIN BOUNDARY. COMPARE WITH FIGURES 65 AND 66

Figure 67

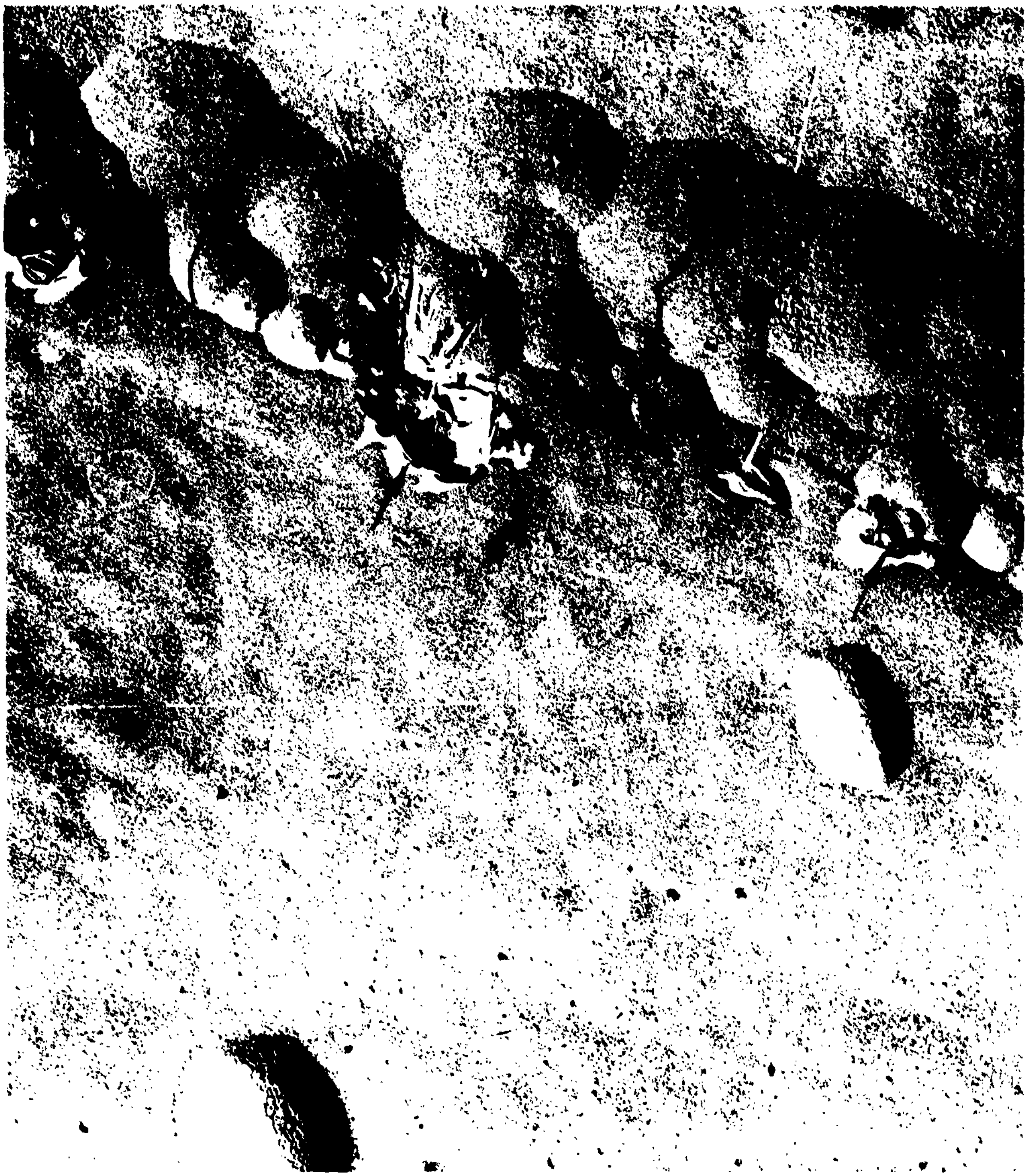

ETCHANT: HF, HNO_3, LACTIC ACID MAG: 17,500X
MICROSTRUCTURE OF FULL SCALE 40-INCH DIAMETER CYLINDER WHICH RUPTURED DURING FLOW-TURNING. NOTE PRECIPITATE PARTICLES (ARROWS) AND ETCH PITTING (BRACKETS) AT GRAIN BOUNDARY. COMPARE WITH FIGURE 65 AND 66.

Figure 68

ELECTRON MICROPROBE ANALYSES OF PRESS - FORGED SAMPLE (LOCATION A) WHICH SHOWED LOW YIELD STRENGTH (175.5 KSI) AND LOW ELONGATION (2.5 PERCENT) AFTER AGING AT 900 F FOR 96 HRS

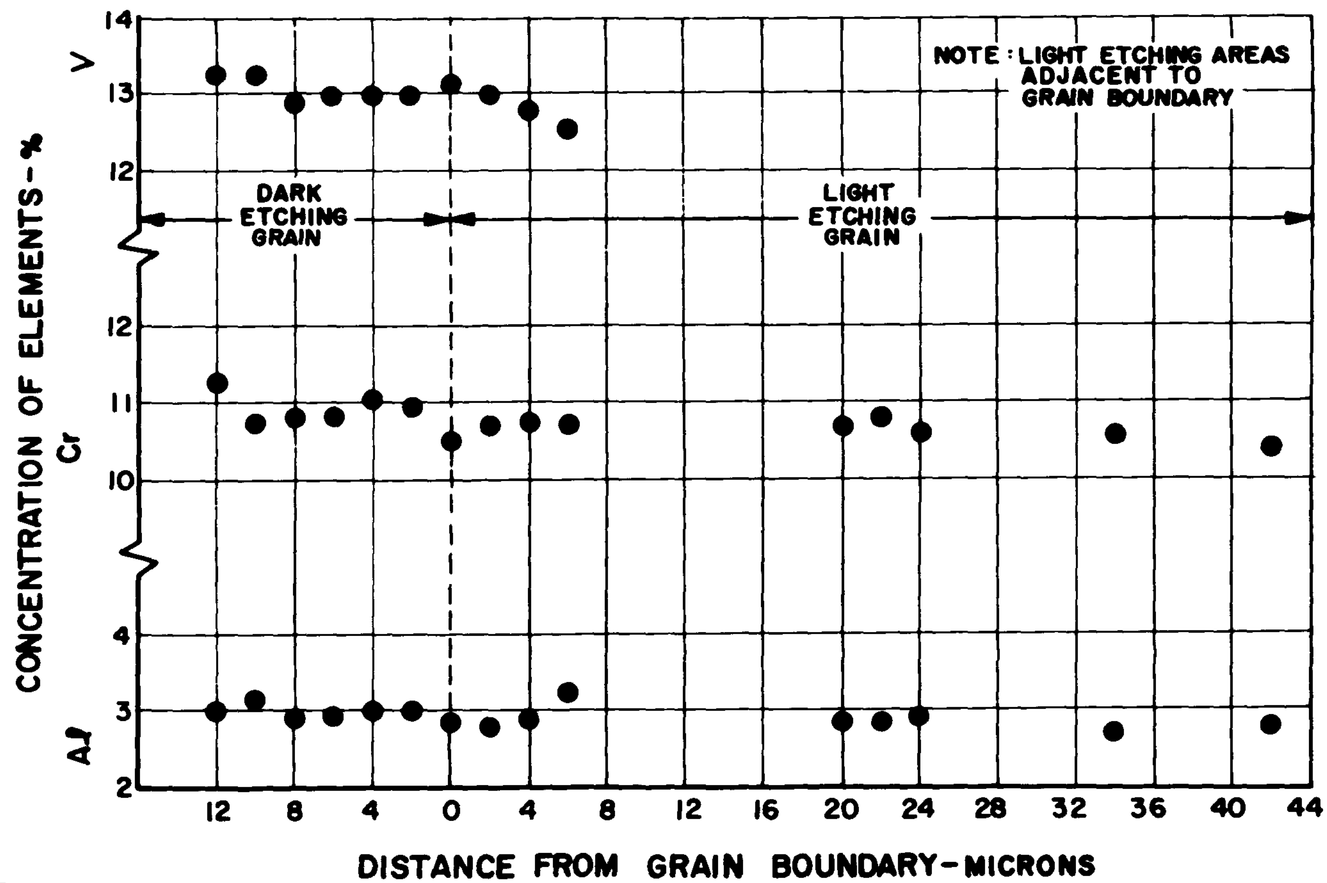

PRATT & WHITNEY AIRCRAFT
DIVISION OF
UNITED AIRCRAFT CORPORATION

621201

ELECTRON MICROPROBE ANALYSES OF PRESS - FORGED SAMPLE (LOCATION A - 1) WHICH SHOWED LOW YIELD STRENGTH (177.0 KSI) AND HIGH ELONGATION (8.0 PERCENT) AFTER AGING AT 900 F FOR 96 HOURS

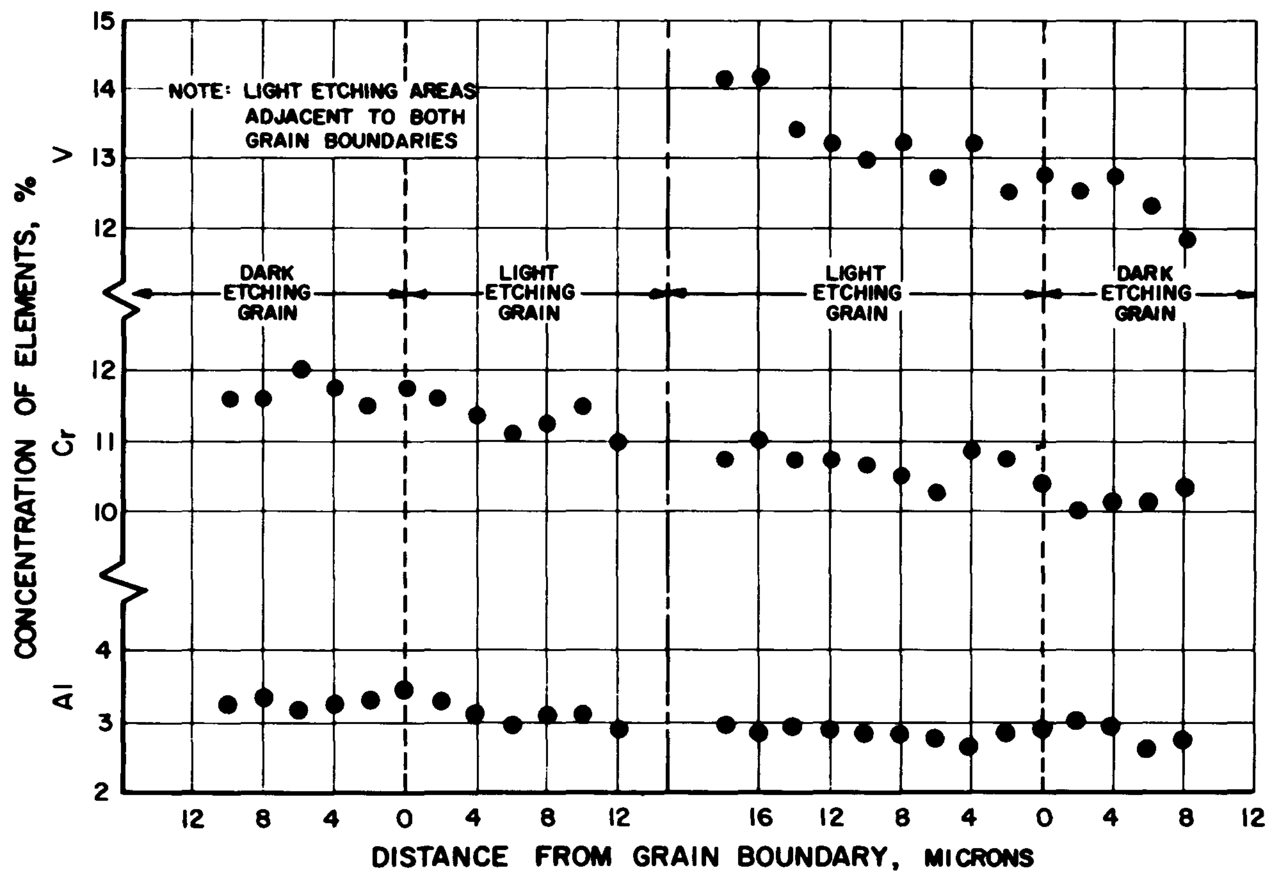

PRATT & WHITNEY AIRCRAFT
DIVISION OF
UNITED AIRCRAFT CORPORATION

621201

ELECTRON MICROPROBE ANALYSES OF PRESS - FORGED SAMPLE (LOCATION A - 1) WHICH SHOWED LOW YIELD STRENGTH (177.0 KSI) AND HIGH ELONGATION (8.0 PERCENT) AFTER AGING AT 900 F FOR 96 HOURS

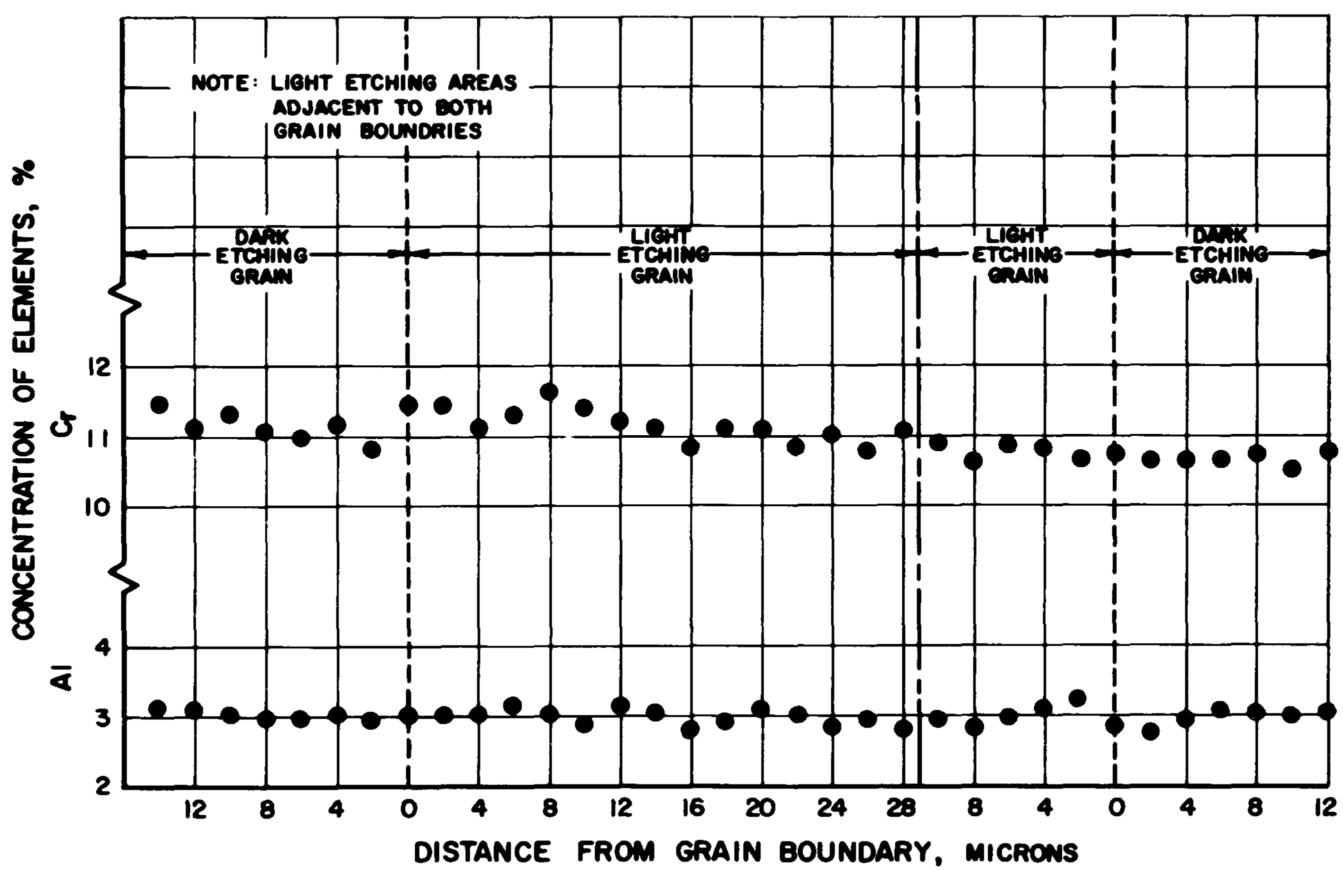

PRATT & WHITNEY AIRCRAFT
DIVISION OF
UNITED AIRCRAFT CORPORATION

62160I

AGING CURVES FOR SUBSCALE 14-INCH DIAMETER FLOW-TURNED CYLINDER NO. 4 (AXIAL DIRECTION) AFTER STRESS-RELIEVING AT 850F FOR 30 MINUTES

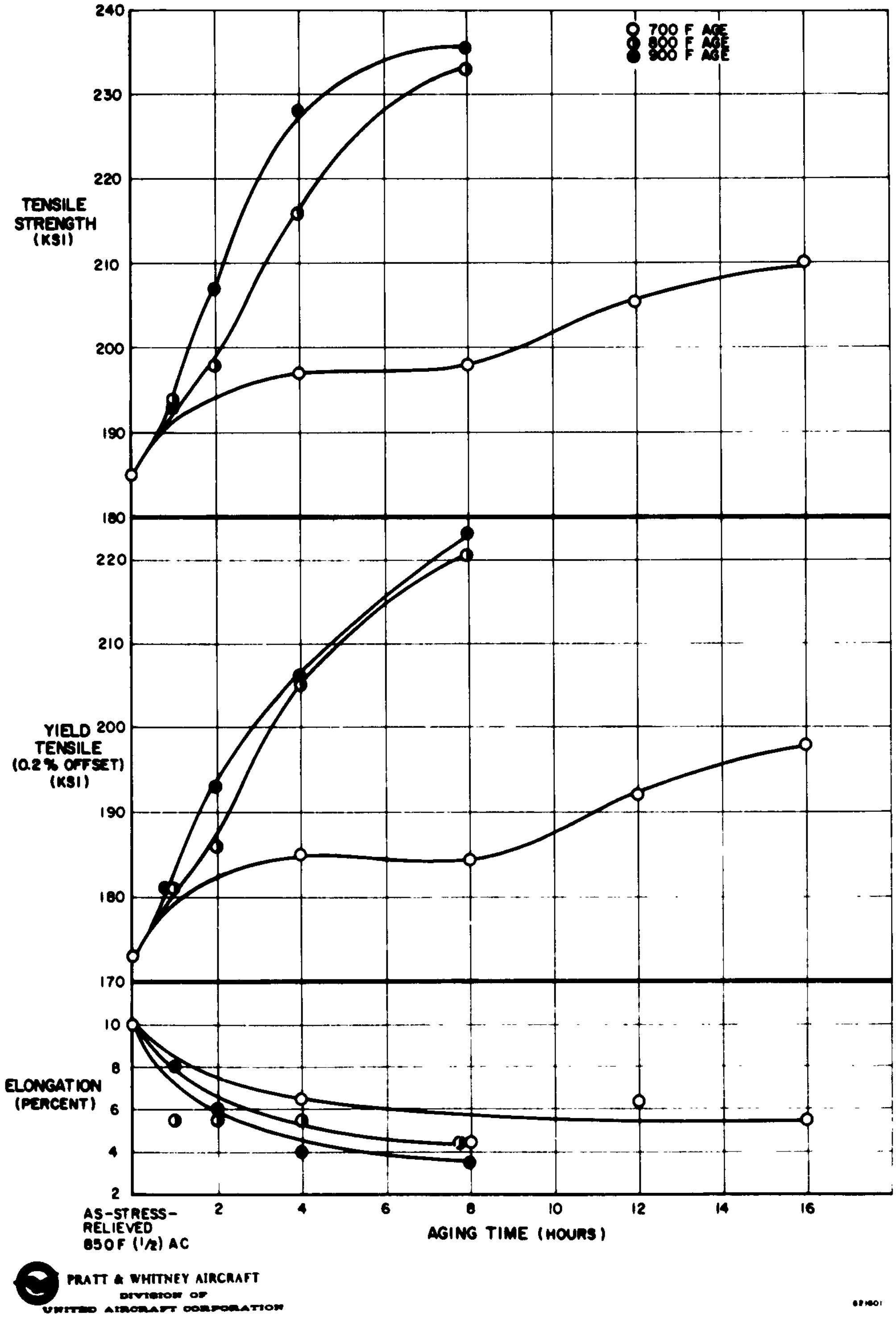

Figure 72

AGING CURVES FOR SUBSCALE 14 - INCH DIAMETER FLOW - TURNED CYLINDER NO. 4 (AXIAL DIRECTION) AFTER STRESS RELIEVING AT 850 F FOR ONE HOUR

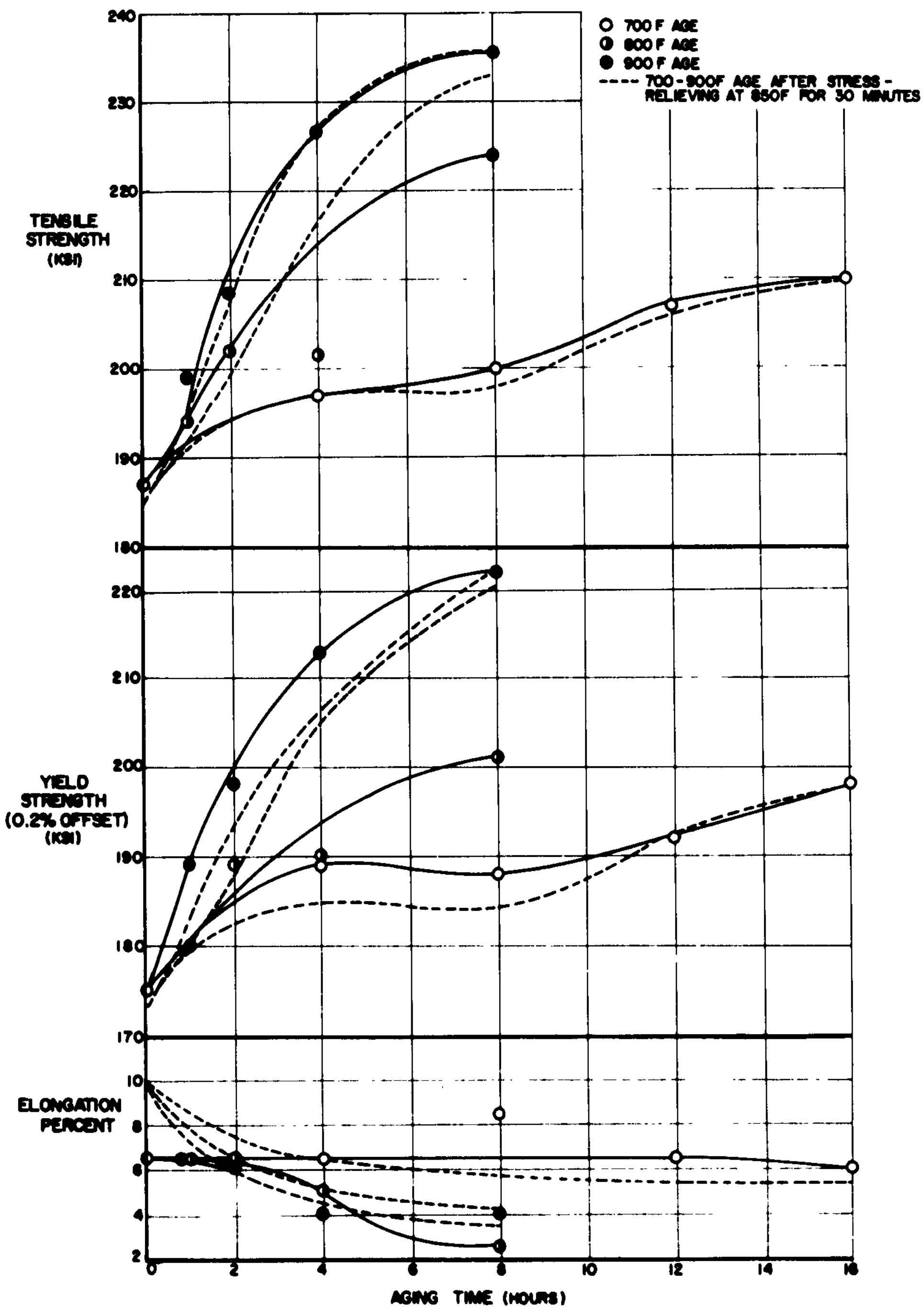

PRATT & WHITNEY AIRCRAFT
DIVISION OF
UNITED AIRCRAFT CORPORATION

Figure 73

AGING CURVES FOR SUBSCALE 14 - INCH DIAMETER FLOW - TURNED CYLINDER NO. 4 (AXIAL DIRECTION) AFTER STRESS - RELIEVING AT 900 F FOR ONE HOUR.

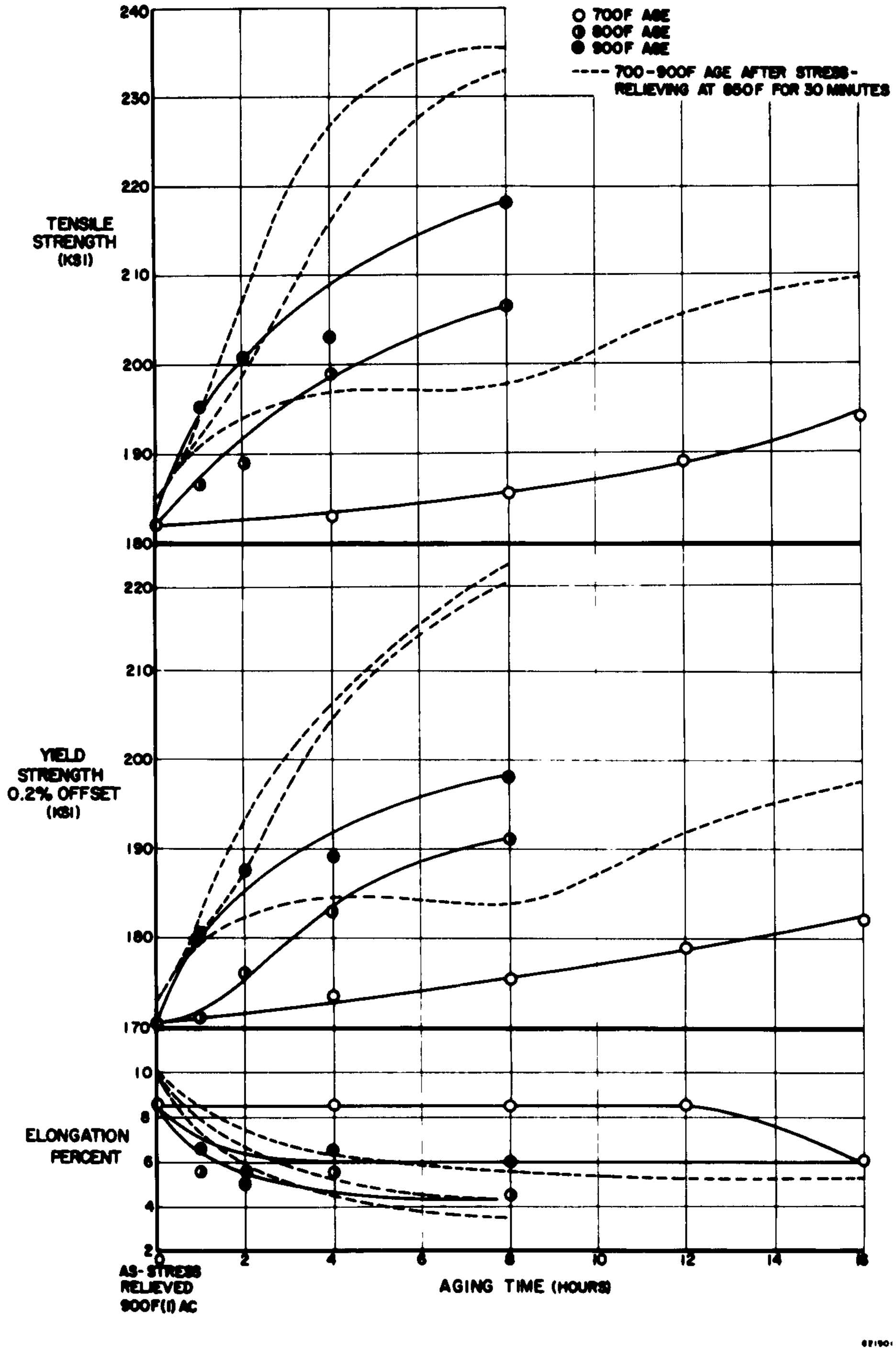

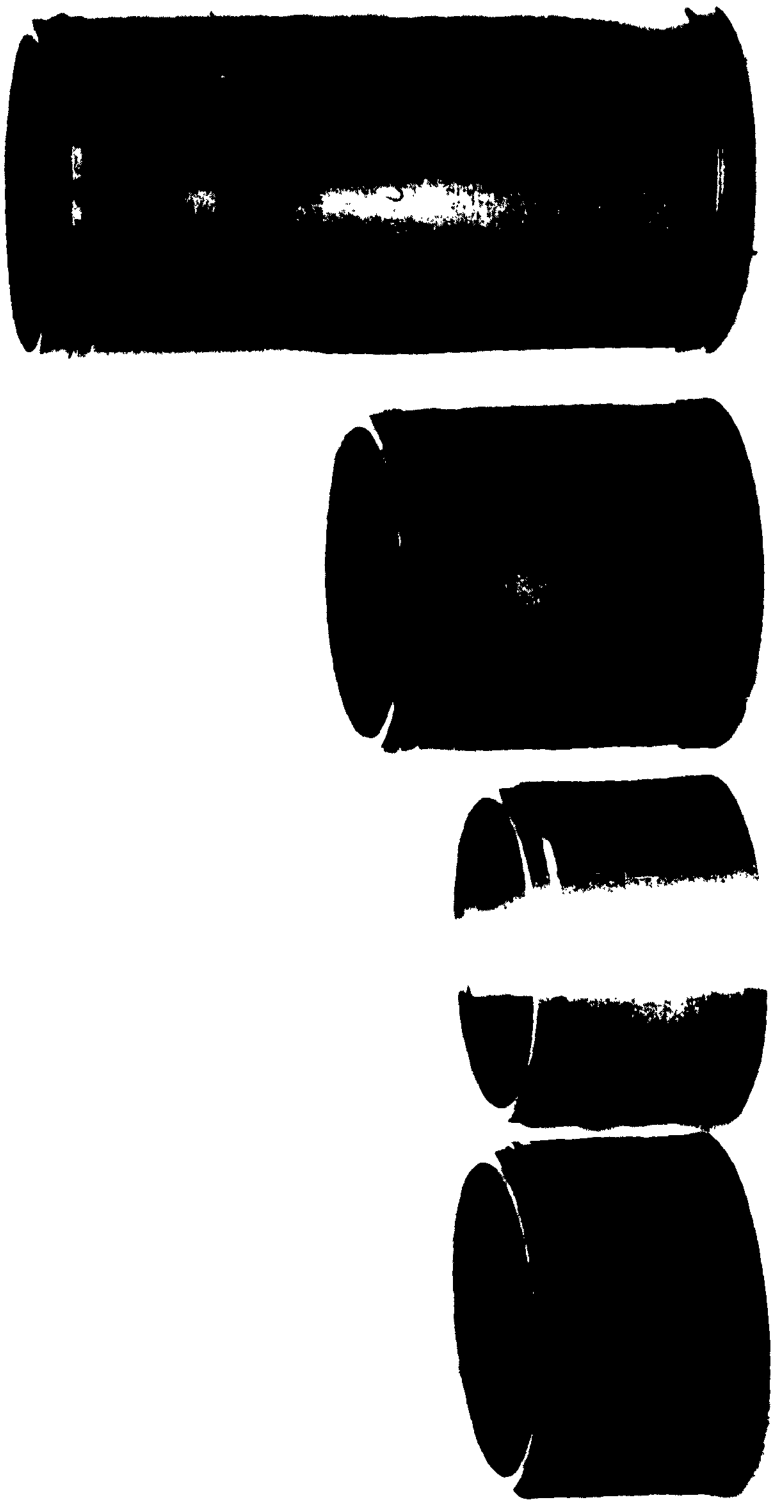

9.4 INCH DIAMETER FLOW-TURN BLANKS FABRICATED FROM ROLLED AND WELDED 0.375-INCH PLATE STOCK. AS-WELDED, MACHINED, AND AFTER FIRST AND SECOND FLOW-TURN PASSES

XP-10764

Figure 75

using titanium filler wire, 3) cyclic loading test results on TIG and electron beam-welded material, 4) tensile properties of subscale 14-inch diameter domes press-forged by the dogbone and the pancake and preform techniques, 5) tensile properties of a hammer-forged pancake, 6) tensile properties of full scale 40-inch diameter domes press-forged by the dogbone and the pancake and preform techniques, 7) tensile properties of subscale 14-inch diameter rolled rings before and after flow-turning, 8) flow-turning results on subscale 9.4-inch diameter rolled and welded blanks, and 9) electron microscope and microprobe results on press-forged, TIG and electron beam-welded, and flow-turned material.

using titanium filler wire, 3) cyclic loading test results on TIG and electron beam-welded material, 4) tensile properties of subscale 14-inch diameter domes press-forged by the dogbone and the pancake and preform techniques, 5) tensile properties of a hammer-forged pancake, 6) tensile properties of full scale 40-inch diameter domes press-forged by the dogbone and the pancake and preform techniques, 7) tensile properties of subscale 14-inch diameter rolled rings before and after flow-turning, 8) flow-turning results on subscale 9.4-inch diameter rolled and welded blanks, and 9) electron microscope and microprobe results on press-forged, TIG and electron beam-welded, and flow-turned material.

using titanium filler wire, 3) cyclic loading test results on TIG and electron beam-welded material, 4) tensile properties of subscale 14-inch diameter domes press-forged by the dogbone and the pancake and preform techniques, 5) tensile properties of a hammer-forged pancake, 6) tensile properties of full scale 40-inch diameter domes press-forged by the dogbone and the pancake and preform techniques, 7) tensile properties of subscale 14-inch diameter rolled rings before and after flow-turning, 8) flow-turning results on subscale 9.4-inch diameter rolled and welded blanks, and 9) electron microscope and microprobe results on press-forged, TIG and electron beam-welded, and flow-turned material.

using titanium filler wire, 3) cyclic loading test results on TIG and electron beam-welded material, 4) tensile properties of subscale 14-inch diameter domes press-forged by the dogbone and the pancake and preform techniques, 5) tensile properties of a hammer-forged pancake, 6) tensile properties of full scale 40-inch diameter domes press-forged by the dogbone and the pancake and preform techniques, 7) tensile properties of subscale 14-inch diameter rolled rings before and after flow-turning, 8) flow-turning results on subscale 9.4-inch diameter rolled and welded blanks, and 9) electron microscope and microprobe results on press-forged, TIG and electron beam-welded, and flow-turned material.

Pratt & Whitney Aircraft Division of United Aircraft Corporation, East Hartford 8, Connecticut
SIXTH QUARTERLY REPORT ON RESEARCH AND DEVELOPMENT OF TITANIUM ROCKET MOTOR CASES, by R. P. Brody and W. E. Helfrich, December 31, 1961. 162 p. incl. illus. Project No. TB4-004, Contract No. DA-19-020-ORD-5230.

Unclassified Report

The results of work performed during the quarter October 1 through December 31, 1961 on the development of a high strength, lightweight titanium alloy rocket case are reported. These results include 1) tensile and sustained-load properties of a full scale 40-inch diameter flow-turned cylinder with 240 ppm of hydrogen, 2) tensile, bend and fracture toughness test results on material TIG-welded using an improved copper-fixturing technique and TIG-welded
(over)

UNCLASSIFIED

1. Rockets, Motor Cases
2. Titanium Fabrication
3. Titanium Alloys

I. Brody, R. P. and Helfrich, W. E.
II. U. S. Army Ordnance Corps, Watertown Arsenal
III. Contract DA-19-020-ORD-5230

Pratt & Whitney Aircraft Division of United Aircraft Corporation, East Hartford, Connecticut
SIXTH QUARTERLY REPORT ON RESEARCH AND DEVELOPMENT OF TITANIUM ROCKET MOTOR CASES, by R. P. Brody and W. E. Helfrich, December 31, 1961. 162 p. incl. illus. Project No. TB4-004, Contract No. DA-19-020-ORD-5230.

Unclassified Report

The results of work performed during the quarter October 1 through December 31, 1961 on the development of a high strength, lightweight titanium alloy rocket case are reported. These results include 1) tensile and sustained-load properties of a full scale 40-inch diameter flow-turned cylinder with 240 ppm of hydrogen, 2) tensile, bend and fracture toughness test results on material TIG-welded using an improved copper-fixturing technique and TIG-welded
(over)

UNCLASSIFIED

1. Rockets, Motor Cases
2. Titanium Fabrication
3. Titanium Alloys

I. Brody, R. P. and Helfrich, W. E.
II. U. S. Army Ordnance Corps, Watertown Arsenal
III. Contract DA-19-020-ORD-5230

Pratt & Whitney Aircraft Division of United Aircraft Corporation, East Hartford 8, Connecticut
SIXTH QUARTERLY REPORT ON RESEARCH AND DEVELOPMENT OF TITANIUM ROCKET MOTOR CASES, by R. P. Brody and W. E. Helfrich, December 31, 1961. 162 p. incl. illus. Project No. TB4-004, Contract No. DA-19-020-ORD-5230.

Unclassified Report

The results of work performed during the quarter October 1 through December 31, 1961 on the development of a high strength, lightweight titanium alloy rocket case are reported. These results include 1) tensile and sustained-load properties of a full scale 40-inch diameter flow-turned cylinder with 240 ppm of hydrogen, 2) tensile, bend and fracture toughness test results on material TIG-welded using an improved copper-fixturing technique and TIG-welded
(over)

UNCLASSIFIED

1. Rockets, Motor Cases
2. Titanium Fabrication
3. Titanium Alloys

I. Brody, R. P. and Helfrich, W. E.
II. U. S. Army Ordnance Corps, Watertown Arsenal
III. Contract DA-19-020-ORD-5230

Pratt & Whitney Aircraft Division of United Aircraft Corporation, East Hartford, Connecticut
SIXTH QUARTERLY REPORT ON RESEARCH AND DEVELOPMENT OF TITANIUM ROCKET MOTOR CASES, by R. P. Brody and W. E. Helfrich, December 31, 1961. 162 p. incl. illus. Project No. TB4-004, Contract No. DA-19-020-ORD-5230.

Unclassified Report

The results of work performed during the quarter October 1 through December 31, 1961 on the development of a high strength, lightweight titanium alloy rocket case are reported. These results include 1) tensile and sustained-load properties of a full scale 40-inch diameter flow-turned cylinder with 240 ppm of hydrogen, 2) tensile, bend and fracture toughness test results on material TIG-welded using an improved copper-fixturing technique and TIG-welded
(over)

DISTRIBUTION LIST

To:	No. of Copies
Office of the Director of Defense Research & Engineering Room 3D-1067, The Pentagon Washington 25, D. C. ATTN: Mr. J. C. Barrett	1
Advanced Research Project Agency The Pentagon Washington 25, D. C. ATTN: Dr. G. Mock	1
Commander Army Research Office Arlington Hall Station Arlington 12, Virginia	1
Office Chief of Ordnance Department of the Army Washington 25, D. C. ATTN: ORDTB-Materials	1
Commanding General Aberdeen Proving Ground Aberdeen Proving Ground, Maryland ATTN: Dr. C. Pickett, C&CL	1
Commanding General Army Ballistic Missile Agency Redstone Arsenal, Alabama ATTN: Dr. G. H. Reisig Mr. P. B. Wallace, ORDAB-RPEM Documentation & Technical Information Branch ORDAB-IEE	 1 1 2 1
Commanding General Ordnance Tank-Automotive Command Detroit 9, Michigan ATTN: Mr. S. Sobak, ORDMC-IF-2	1
Commanding General Ordnance Weapons Command Rock Island, Illinois ATTN: Mr. B. Gerke, ORDOW-IA	1
Commanding General U.S. Army Rocket & Guided Missile Agency Redstone Arsenal, Alabama ATTN: Mr. Robert Fink, ORDXR-RGS Mr. W. H. Thomas, ORDXR-IQI	 1 1
Commanding Officer Frankford Arsenal Philadelphia 37, Pa. ATTN: Dr. H. Gisser, ORDBA-1330 Mr. H. Markus, ORDBA-1320	 1 1
Commanding Officer Ordnance Materials Research Office Watertown Arsenal Watertown 72, Mass. ATTN: RPD	1
Commanding Officer Picatinny Arsenal Dover, N. J. ATTN: Mr. J. J. Scavuzzo, Plastics & Packaging Lab. Mr. D. Stein, ORDBB-DE3	 3 1
Commanding Officer PLASTEC Picatinny Arsenal Dover, N. J.	1
Commanding Officer Rock Island Arsenal Rock Island, Illinois ATTN: Materials Section, Laboratory	1
Commanding Officer Springfield Armory Springfield 1, Mass. ATTN: Mr. R. Korytoski, Research Materials Lab	1
Commanding Officer Watertown Arsenal Watertown 72, Mass. ATTN: ORDBE-LX	3
Commanding Officer Watervliet Arsenal Watervliet, New York ATTN: Mr. F. Dashnaw, ORDBF-RR	1
Commander Armed Services Technical Information Agency Arlington Hall Station Arlington 12, Virginia ATTN: TIPDR	10
Chief, Bureau of Naval Weapons Department of the Navy Room 2225, Munitions Building Washington 25, D. C. ATTN: RMMP	1
Commander U. S. Naval Ordnance Laboratory White Oak Silver Spring, Maryland ATTN: Code WM	1
Commander U.S. Naval Ordnance Test Station China Lake, California ATTN; Technical Library Branch	1
Commander U.S Naval Research Laboratory Anacostia Station Washington 25, D C ATTN; Mr. J. E. Srawley	1

To:	No. of Copies
Department of the Navy Office of Naval Research Washington 25, D. C. ATTN: Code 423	1
Department of the Navy Special Projects Office Washington 25, D. C. ATTN: SP 271	1
U.S. Air Force Directorate of Research & Development Room 4D-313, The Pentagon Washington 25, D. C. ATTN: Lt Col J. B. Shipp, Jr.	1
Wright Air Development Division Wright Patterson Air Force Base Ohio ATTN: H. Zoeller, ASRCEE-1	2
ARDC Flight Test Center Edwards Air Force Base California ATTN: Solid Systems Division, FTRSC	5
AMC Aeronautical Systems Center Wright Patterson Air Force Base Ohio ATTN: Manufacturing & Materials Technology Div., LMBMO	2
National Aeronautics and Space Administration Washington, D. C. ATTN: Mr. R. V. Rhode Mr. G. C. Deutsch	1 1
Dr. W. Lucas George C. Marshall Space Flight Center National Aeronautics and Space Administration Huntsville, Alabama ATTN: M-S&M-M	1
Mr. William A. Wilson George C. Marshall Space Flight Center Huntsville, Alabama ATTN: M-F&AE-M	1
Defense Metals Information Center Battelle Memorial Institute Columbus, Ohio	1
Solid Propellant Information Agency Applied Physics Laboratory The Johns Hopkins University Silver Spring, Maryland	3
Aerojet-General Corporation Post Office Box 1168 Sacramento, California ATTN: Librarian	1
Aerojet-General Corporation Post Office Box 296 Azusa, California ATTN: Librarian Mr. C. A. Fournier	1 1

To:	No. of Copies
Allison Division General Motors Corporation Indianapolis 6, Indiana ATTN: D. K. Hanink	1
ARDE-Portland, Inc. 100 Century Road Paramus, N. J. ATTN: Mr. R. Alper	1
Atlantic Research Corporation Shirley Highway and Edsall Road Alexandria, Virginia ATTN: Mr. E. A. Olcott	1
Curtiss-Wright Corporation Wright Aeronautical Division Wood-Ridge, N. J. ATTN: R. S. Shuris A. M. Kettle, Technical Library	1 1
Hercules Powder Company Allegheny Ballistics Laboratory Post Office Box 210 Cumberland, Maryland ATTN: Dr. R. Steinberger	1
Hughes Aircraft Company Culver City California ATTN: Librarian	1
Dr. L. Jaffe Jet Propulsion Laboratory California Institute of Technology 4800 Oak Grove Drive Pasadena, California	1
Tapco Group 23555 Euclid Avenue Cleveland 17, Ohio ATTN: W. J. Piper	1
Chief of Research and Development U.S. Army Research and Development Liaison Group APO 757, New York, N. Y. ATTN: Dr. B. Stein	1
Allegheny Ludlum Steel Corporation Research Center Brackenridge, Pennsylvania ATTN: Mr. R. A. Lula	1
Alloyd Electronics Corporation 35 Cambridge Parkway Cambridge, Mass. ATTN: Dr. S. S. White	1
Armco Steel Corporation General Offices Middletown, Ohio ATTN: Mr. J. Barnett	1

To:	No. of Copies
Battelle Memorial Institute 505 King Avenue Columbus 1, Ohio ATTN: Mr. R. Monroe Mr. G. Faulkner	 1 1
Borg-Warner Corporation Ingersoll Kalamazoo Division 1810 N. Pitcher St. Kalamazoo, Michigan ATTN: Mr. L. E. Hershey	 1
The Budd Company Defense Division Philadelphia 32, Pennsylvania ATTN: R. C. Dethloff Mr. Ohman	 1 1
General Electric Company Rocket Engine Section Flight Propulsion Laboratory Department Cincinnati 15, Ohio	 1
Jones and Laughlin Steel Corporation 45 South Montgomery Avenue Youngstown 1, Ohio ATTN: Mr. H. Steinbrenner	 1
Arthur D. Little, Inc. Acorn Park Cambridge 40, Mass. ATTN: Dr. R. Davis	 1
Lyon, Inc. 13881 W. Chicago Boulevard Detroit, Michigan ATTN: W. Martin	 1
Manufacturing Laboratories 21-35 Erie Street Cambridge 42, Mass. ATTN: Dr. P. Fopiano Dr. V. Radcliffe	 1 1
Massachusetts Institute of Technology Cambridge, Massachusetts ATTN: Prof. W. A. Backofen Prof. M. C. Flemings	 1 1
Mellon Institute 4400 Fifth Avenue Pittsburgh 13, Pa. ATTN: C. J. Owen Dr. H. L. Anthony	 1 1
Norris-Thermador Corporation 5215 South Boyle Avenue Los Angeles 58, California ATTN: Mr. L. Shiller	 1
Ohio State University Research Foundation Columbus, Ohio ATTN: Dr. McMaster	 1

To:	No. of Copies
The Perkin-Elmer Corporation Main Avenue Norwalk, Connecticut ATTN: H. L. Sachs	 1
Commanding Officer Boston Ordnance District Army Base Boston, Massachusetts ATTN: R & D Branch	 1
Reactive Metals Corporation Niles, Ohio ATTN: Mr. H. Lundstrom	 1
Republic Steel Corporation Research Center Independence, Ohio ATTN: Mr. H. P. Manger	 1
Space Technology Laboratories, Inc. Post Office Box 95001 Los Angeles 45, California ATTN: Technical Information Center Document Procurement	 1
Titanium Metals Corporation 233 Broadway New York, N. Y. ATTN: Mr. G. Erbin	 1
United States Rubber Company Research Center Wayne, N. J. ATTN: Dr. E. J. Joss	 1
Library Rohm & Haas Company Redstone Arsenal Research Division Huntsville, Alabama	 1
Douglas Aircraft Company Inc. Santa Monica Division Santa Monica, California ATTN: Mr. J. L. Waisman	 1
Chief, Bureau of Naval Weapons Department of the Navy Washington 25, D. C. Attn: Mr. P. Goodwin	 1
Headquarters Aeronautical Systems Division Wright-Patterson Air Force Base, Ohio Attn: Dr. Tamborski, ASRCNP	 1
Headquarters U. S. Army Signal R&D Laboratory Fort Monmouth, N.J. Attn: Mr. H. H. Kedesky, SIGRA/SL-XE	 1

To:	No. of Copies
Wright Air Development Division Wright-Patterson Air Force Base, Ohio Attn: Mr. G. Peterson, ASRCNC-1	1
The Boeing Company Aero Space Division P. O. Box 3707 Seattle 24, Washington	1
Climax Molybdenum Company 1270 Avenue of the Americas New York 20, N.Y. Attn: Mr. R. R. Freeman	1
Minneapolis-Honeywell Regulator Company 1230 Soldiers Field Road Boston 35, Mass.	1
Thiokol Chemical Corporation Utah Division Brigham City, Utah	1
Universal-Cyclops Steel Corp. Stewart Street Bridgeville, Pennsylvania	1
U. S. Borax Research Corp. 412 Crescent Way Anaheim, California Attn: Mr. R. J. Brotherton	1
Michigan State University Department of Chemistry East Lansing, Michigan Attn: Mr. R. N. Hammer	1
Ohio State University Research Foundation Columbus, Ohio Attn: R. R. McMaster	1
Wyman-Gordon Company Grafton, Massachusetts Attn: Mr. Arnold Rustay	1
Ladish Company Cudahy, Wisconsin Attn: Mr. Robert P. Daykin	1